SYNTHESIS, PROPERTIES, AND FUNCTIONS OF NOVEL POLY(DIPHENYLACETYLENES) AND RELATED POLYMERS

MASAHIRO TERAGUCHI

2000

Table of Contents

General Introduction

Research Background

Nowadays, the importance of polymer materials has been recognized along with ceramics and metals, and a variety of polymers contribute to the convenience and enrichment of our daily life. For example, commodity polymers are consumed in large amounts as fibers and plastics thanks to their good moldability, light weight, variety, low cost, and so forth. High-performance polymers such as engineering plastics are now extensively used in place of metal materials due to their excellent heat resistance and high mechanical strength. Functional polymers, which exhibit not only intrinsic molding property but also particular functions such as separation of substances, optoelectronic functions (e.g., conductivity, magnetism), and biomedical functions, are also currently employed in many fields.

As mentioned above, various polymer materials with high performance and unique functions are used at present. However, an even higher degree of performance and functionality will be demanded in the future. Further development of new polymer materials will proceed in line with the following four strategies: (i) fabrication of composites from known polymeric and other materials; (ii) treatments such as orientation and drawing; (iii) precise synthesis of tailor-made polymers (e.g., stereoregular polymers, monodisperse polymers, and block copolymers); (iv) synthesis of polymers with novel molecular structure. In (iv), polymers with novel structure will be designed so as to provide unique properties and specific functions. Such novel polymers may be further modified by means of the treatments of (i) and (ii) and the controlled polymerization of (iii). Thus, creation of novel polymers is essential for the development of new materials.

At present, vinyl polymers such as polyolefins, the backbone of which is composed of carbon-carbon single bonds, are industrially manufactured on a large scale. In contrast, polyacetylenes possess a main-chain structure consisting of alternating carbon-carbon double bonds. This structure endows polyacetylenes with unique properties such as stiffness and π-conjugation.

The unsubstituted polyacetylene was first synthesized as a black powder in 1958 by Natta and coworkers using a transition-metal catalyst.[1] In 1974, the synthesis of a uniform polyacetylene film was achieved by Shirakawa by the polymerization of acetylene with a $Ti(O\text{-}n\text{-}Bu)_4$–$Et_3Al$ catalyst (eq. 1).[2] This finding subsequently led to discovery of the metallic conductivity of polyacetylene doped with halogen, AsF_5, and Na.[3] This series of research opened the door to the field of synthetic metals. Polyacetylene, however, is insoluble, infusible, and unstable in air, which hampers its practical application.

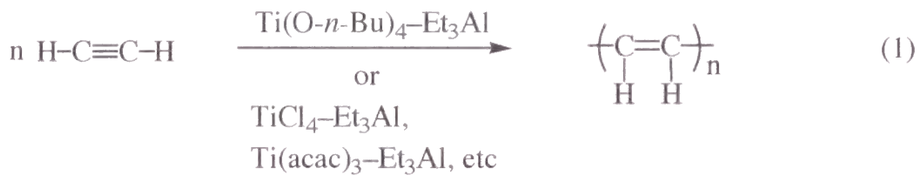

(1)

Polyacetylenes with appropriate substituents are expected to be soluble and stable unlike the unsubstituted polyacetylene. Thus, the polymerization of substituted acetylenes was attempted for a long time by use of Ziegler-Natta catalysts as for the unsubstituted acetylene. The Ziegler-Natta catalysts consist of a group 4–8 transition-metal compound and a group 1–3 main-group metal organometallic. In most of these attempts, however, only linear oligomers with molecular weight of a few thousand and/or insoluble polymers were formed; only sterically unhindered acetylenes such as aliphatic linear 1-alkynes could afford high molecular weight polymers.

In 1974, Masuda and coworkers found that $MoCl_5$ and WCl_6 (group 6 transition metal chlorides) are specifically effective in the polymerization of phenylacetylene. Further, polymerization of various mono- and disubstituted acetylenes, especially sterically crowded ones, was achieved with $MoCl_5$- and WCl_6-based catalysts (eq. 2).[4] It was also revealed that sterically demanding disubstituted acetylenes such as 1-phenyl-1-alkyne[5] and diphenylacetylene[6] can be polymerized by group 5 transition metal chlorides (i.e., $TaCl_5$ and $NbCl_5$).

(2)

Niki *et al.* reported the synthesis of poly(diphenylacetylene) using a $TaCl_5$-based catalyst in 1982.[6] Poly(diphenylacetylene) was thermally very stable as demonstrated by no weight loss in air below 500 °C. However, it was infusible and insoluble in any solvent, which prevented its detailed characterization.

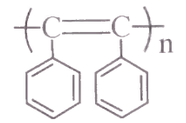

Poly(diphenylacetylene)

In 1991, Tsuchihara *et al.* accomplished the synthesis of a poly(diphenylacetylene) derivative in high yields by using $TaCl_5$-based catalysts.[7] The monomer employed is 1-phenyl-2-[*p*-(trimethylsilyl)phenyl]acetylene, which has a trimethylsilyl group on one phenyl ring, and the formed polymer was completely soluble in common organic solvents. Poly[1-phenyl-2-[*p*-(trimethylsilyl)phenyl]acetylene] had high thermal stability similar to poly(diphenylacetylene) and, interestingly, the polymer showed high oxygen permeability. In general, the introduction of bulky ring-substituents proved effective in obtaining soluble poly(diphenylacetylenes).

Other typical examples of the polymerization of substituted acetylenes include Schrock's studies using group 5 and 6 transition-metal carbene complexes. He accomplished the living polymerization of several monosubstituted acetylenes[8] with Mo and W alkylidenes developed by themselves as well as the living polymerization of 2-butyne[9] with a Ta alkylidene. The acetylene monomers that can be polymerized by these metal carbene catalysts, however, are still limited.

In recent years, some Rh catalysts such as $[(nbd)RhCl]_2$ have been found to induce the polymerization of monosubstituted acetylenes (e.g., phenylacetylenes[10] and

alkyl propiolates[11]), and the formed polymers have a stereoregular structure (cis-transoidal configuration) in the main chain. The Rh-catalyzed polymerization proceeds not by the metathesis mechanism but by an insertion mechanism. There have been no disubstituted acetylenes that polymerize with Rh catalysts.

Polyacetylene with suitable substituents is soluble and stable in air, which should facilitate their practical applications. Polyacetylenes with bulky substituents possess many molecular-scale voids owing to both the stiff main chain and the steric repulsion of substituents, and consequently they readily permeate gases and liquids. Further, substituted polyacetylenes can provide various extents of conjugation based on the conjugated main-chain structure and various sizes of side groups. Hence, these polymers are interesting as new optoelectronic materials as well. Thus, the following properties and functions are expected of substituted polyacetylenes: (i) high gas permeability; (ii) pervaporation of ethanol/water mixtures; (iii) photoconductivity; (iv) electrochromism; (v) non-linear optical property; (vi) electroluminescence.

In 1983, Masuda *et al.* synthesized poly[(1-trimethylsilyl)-1-propyne] with $TaCl_5$-based catalysts and found that the polymer shows extremely high oxygen permeability.[12] Its oxygen permeability coefficient (P_{O2}) is about 10 times larger than that of poly(dimethylsiloxane), which had previously been known as the most gas-permeable polymer.[13] Synthesis of poly[1-phenyl-2-[*p*-(trimethylsilyl)phenyl]-acetylene], which has both high gas permeability and excellent thermal stability, was reported in 1991.[7] In recent years, substituted polyacetylene membranes for gas and vapor separation have been intensively studied from both fundamental and applied viewpoints. Studies on both synthesis and modification of polyacetylenes are also extensively performed in the search for more permeable polymers and to elucidate the permeation mechanism.[13]

Recently, there have been a few studies on the optoelectronic functions of polyacetylenes, e.g., photoconductivity of ring-substituted poly(phenylacetylenes).[14] Photoluminescence and electroluminescence have been intensively studied with

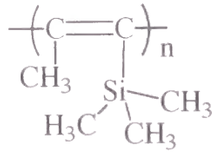

Poly[1-(trimethylsilyl)-1-propyne]

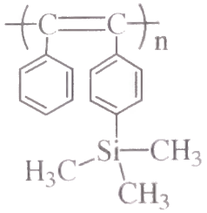

Poly[1-phenyl-2-[*p*-(trimethylsilyl)-phenyl]acetylene]

poly(phenylene vinylene)[15], but substituted polyacetylenes have hardly been examined except for Yoshino's work.[16]

Objectives of This Thesis

As mentioned above, the development of functional polymers is a very important subject in the advanced materials science and technology. To this end, fundamental studies on the design and synthesis of novel polymers that are expected to show excellent functions are essential.

The gas-separation membranes and optoelectronic materials are under intensive research, and substituted polyacetylenes are used more and more frequently. On the other hand, studies on the synthesis of novel substituted polyacetylenes are still rather restricted despite their importance. In this thesis, the author aimed at the synthesis of novel substituted polyacetylenes and the development of unique functions based on them. Specifically, the author examined the following three points in detail: (i) molecular design of novel acetylenic monomers and establishment of the methodology of the synthesis of high molecular weight polymers from them; (ii) characterization of the product polymers with respect to thermal stability, solubility, film-forming ability, and so forth; (iii) examination of polymer functions such as gas permeability and optoelectronic properties (e.g., electroluminescence and photoluminescence) and elucidation of the relationship between polymer structure and functions.

Outline of This Thesis

This thesis consists of three parts: **Part I** (Chapters 1–3) and **Part II** (Chapters 4–6) deal with the synthesis of novel ring-substituted poly(diphenylacetylenes) and related acetylene polymers and their properties. **Part I** describes mainly poly(diphenylacetylenes) with silicon-containing substituents, and **Part II** concerns poly(arylacetylenes) having bulky ring substituents and conjugating substituents. **Part III** (Chapters 7–10) deals with functions of the formed polymers such as gas permeation and electroluminescence.

In **Part I** are discussed the synthesis and properties of poly(diphenylacetylenes) with bulky silyl groups as ring substituents.

Chapter 1 deals with the polymerization of diphenylacetylenes having very bulky triphenylsilyl and triisopropylsilyl groups (**1** and **2**, respectively) and properties of the formed polymers. Both monomers polymerized with $TaCl_5$-based catalysts to yield polymers in good yields. The weight-average molecular weights (M_w) of poly(**1**) and poly(**2**) reached around $1x10^6$ and $4x10^6$, respectively. Both polymers were soluble in toluene, $CHCl_3$, etc, and gave tough free-standing films on solution casting. These polymers were thermally fairly stable, as seen from their onset temperatures of weight loss in TGA in air (T_0) of 430 and 270 °C, respectively. The P_{O2} values of poly(**1**) and poly(**2**) were 3.8 and 20 barrers (25 °C), respectively, and relatively low.

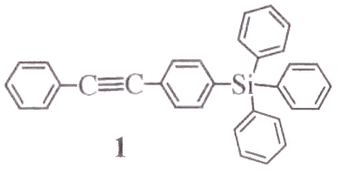

1

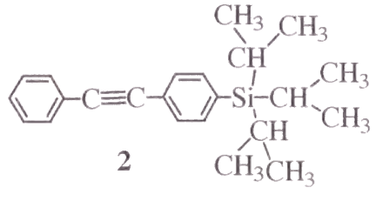

2

Chapter 2 concerns the copolymerization of diphenylacetylene having two trimethylsilyl groups on one phenyl ring (**3**). No polymer was obtained by homopolymerization of this monomer catalyzed by $TaCl_5$–*n*-Bu_4Sn, which was attributed to steric hindrance. On the other hand, copolymerization of **3** with

diphenylacetylene derivatives (**4a–c**) at various feed ratios gave soluble copolymers in relatively good yields. The formed copolymers had relatively high molecular weights (the highest M_w ca. $6x10^5$) and film-forming ability. All the copolymers were thermally very stable and their T_0 values were as high as around 400 °C. The P_{O2} values of copoly(**3/4a**) (feed mole ratio 1:1) and copoly(**3/4b**) (feed mole ratio 1:2) were 21 and 100 barrers, respectively.

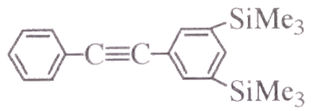

3

4a: R = *p*-H
4b: R = *p*-Me_3Si
4c: R = *m*-Me_3Si

Chapter 3 deals with the polymerization of disubstituted acetylenes having a chiral silyl group derived from *β*-pinene (**5–8**). All the monomers polymerized with Mo- or Ta-based catalysts into high molecular weight polymers in good yields. Poly(**5**) and poly(**6**) possessed very large optical rotations compared with the starting monomers and showed intense circular dichroism (CD) effects in the UV-vis region, which suggests that these polymers exist in helical conformation with an excess of one-handed screw sense. Further, poly(**5**), poly(**6**), and poly(**7**) had good film-forming ability, and exhibited enantioselectivity in the permeation of racemic tryptophan, to permeate the (R)-enantiomer faster than (S)-isomer.

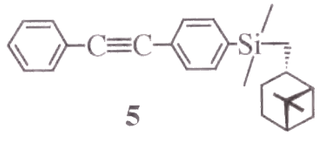

5

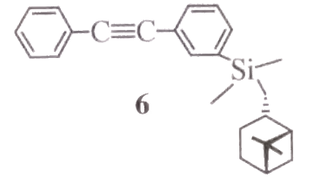

6

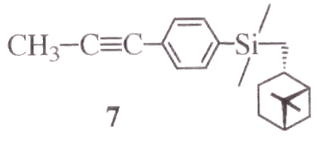

7

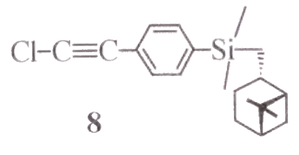

8

Part II describes the synthesis of polyacetylenes having widely conjugating substituents or functional groups.

In **Chapter 4** are discussed the copolymerization of a diphenylacetylene having a hexaphenylbenzene moiety (**9**) with other diphenylacetylene derivatives (**10a–c**) and the properties of the formed copolymers. No polymer was obtained by

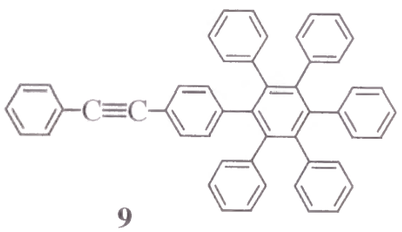

9

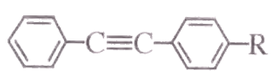

10a: R = *p*-H
10b: R = *p*-Me_3Si
10c: R = *n*-Oct

homopolymerization of **9** with a $TaCl_5$–*n*-Bu_4Sn catalyst because of steric hindrance. In contrast, **9** copolymerized with other diphenylacetylenes to give the corresponding copolymers in moderate yields. Copoly(**9/10a**), which is soluble in $CHCl_3$, was obtained when **9** was 25 mol% in the feed. This copolymer had an M_w up to $1.1x10^6$, and gave a free-standing film on solution casting. Transformation of the hexaphenylbenzene moiety in copoly(**9/10a**) to a more widely conjugated group was attempted (Scheme 1).

Scheme 1

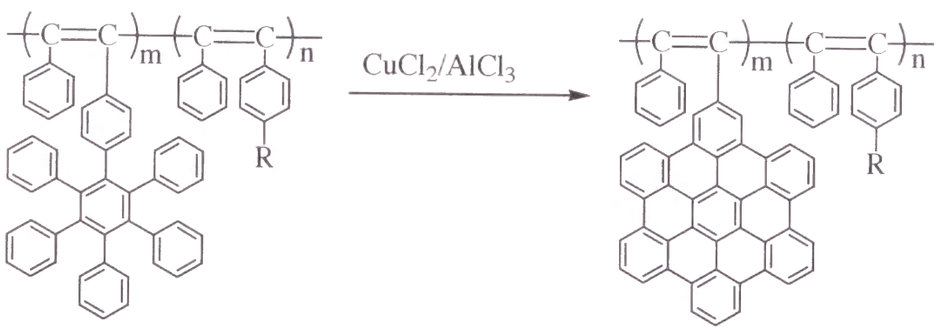

Chapter 5 delineates the polymerization of three disubstituted acetylenes (**11–13**) containing an adamantyl group, a very bulky cage compound. Each monomer polymerized in the presence of suitable Mo- or Ta-based catalysts into a polymer with high molecular weight in good yield. The highest M_w values of poly(**11**), poly(**12**), and poly(**13**) reached $3.6x10^5$, $1.1x10^6$, and $6.0x10^6$, respectively. These polymers were white to yellow solids and all of them completely dissolved in toluene, $CHCl_3$, etc. They were fairly thermally stable, as demonstrated by their T_0 values over 360 °C. Poly(**12**) and poly(**13**) afforded free-standing films, and their P_{O2} values were 8.6 and 55 barrers (25 °C), respectively.

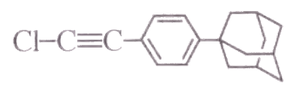

11

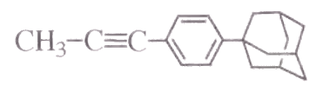

12

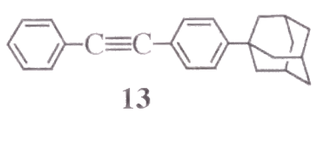

13

Chapter 6 deals with the polymerization of acetylenes having an azobenzene moiety at the para or meta position (**14** and **15**) as well as the characterization and properties of the formed polymers. It is well known that azobenzene derivatives exhibit reversible photoisomerization. Both monomers polymerized with $[(nbd)RhCl]_2$–Et_3N to give polymers in quantitative yields. Whereas poly(**14**) was insoluble in any solvent, poly(**15**) was soluble in common organic solvents and its M_w reached about $5x10^5$. It was found that the azobenzene moieties in poly(**15**) undergo trans-cis photoisomerization on UV irradiation.

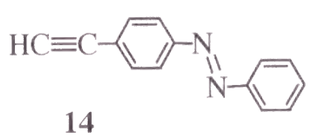

14

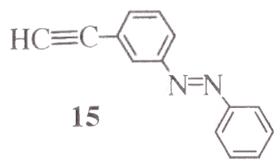

15

Part III is focused on the development and the evaluation of functions of the substituted polyacetylenes synthesized in Parts I and II and related polymers.

Chapter 7 describes the gas permeability and hydrocarbon solubility of poly[1-phenyl-2-[*p*-(triisopropylsilyl)phenyl]acetylene] synthesized in Chapter 1 and further the effects of film thickness, physical aging, and methanol conditioning on solubility. In general, this polymer had high gas permeability coefficients and was more permeable to larger hydrocarbons (e.g., propane, *n*-butane) than to light gases such as hydrogen. The permeability coefficients of this polymer strongly depended on film preparation history, physical aging, and methanol conditioning.

In **Chapter 8**, the dynamics of substituted polyacetylenes was investigated by means of quasielastic neutron scattering technique, aiming at elucidation of the relationship between the local mobility of substituents in the polymer and the gas permeability. Although all of the three disubstituted acetylene polymers **16**–**18** have bulky trialkylsilyl groups, their P_{O2} values were quite different. It was found that the local flux, which is defined as the product of the relaxation rate (Γ) and mobile fraction (f_m) increased with the gas permeability coefficient. This result indicates that local flux is one of the important factors to control gas permeability.

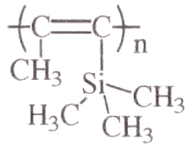

16

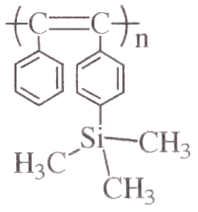

17

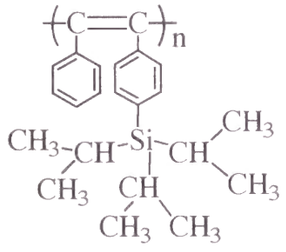

18

In **Chapter 9**, free volume and free volume distribution in several substituted polyacetylenes were examined by the spin probe technique. That is, ESR measurement of TEMPO in glassy polyacetylenes was carried out and the rotation correlation time (τ_c) or frequencies ($\nu = 1/\tau_c$) of TEMPO were measured. For highly

gas-permeable polymers, large rotational mobility was indicated, which evidences the existence of high free volume in the glassy polyacetylenes. Correlations between frequencies (ν) and gas permeability and diffusion coefficients were usually observed.

Chapter 10 deals with the photoluminescence and electroluminescence of various substituted polyacetylenes. Disubstituted acetylene polymers usually showed stronger photoluminescence than monosubstituted acetylene polymers. Poly(diphenylacetylene) derivatives emitted intense green photoluminescence and electroluminescence among disubstituted acetylene polymers.

In conclusion, this thesis has delineated the synthesis of novel substituted polyacetylenes and their properties and functions. The author clarified the polymerization behavior of various aromatic acetylenes having bulky ring substituents, polymer molecular weight, and polymer properties such as solubility and thermal stability. Regarding polymer functions, the gas permeability of polyacetylenes with bulky substituents was examined and a correlation between gas permeability and local mobility was proposed. It was found that various substituted polyacetylenes, especially poly(diphenylacetylene) derivatives, showed intense photoluminescence and electroluminescence. In the future, polymeric functional materials will become more and more important as separation membranes and electroluminescence materials. The author hopes that the present thesis will contribute to the design and synthesis of novel functional conjugated polymers and the development of their functions.

References

1) Natta, G.; Mazzati, G.; Corradini, P. *Atti. Accad. Naz. Lincei, Rend., Cl. Sci. Fis. Mat. Nat.* **1958**, *25*, 3.

2) Ito, T.; Shirakawa, H.; Ikeda, S. *J. Polym. Sci., Polym. Chem. Ed.* **1974**, *12* 11.

3) a) Shirakawa, H.; Louis, E. J.; MacDiarmid, A. G.; Chiang, C. K.; Heeger, A. J. *J. Chem. Soc., Chem. Commun.* **1977**, 578. b) Chien, J. C. W. *Polyacetylenes*; Academic Press: New York, 1984. c) Curran, S.; Stark-hauser, A.; Roth, S. In

Handbook of Organic Conductive Molecules and Polymers: Conductive Polymers: Spectroscopy and Physical Properties; Nalwa, H. S., Ed.; Wiley: Chichester, 1997; Vol. 2, Chapter 1.

4) Masuda, T.; Hasegawa, K.; Higashimura, T. *Macromolecules* **1974**, *7*, 728.

5) a) Masuda, T.; Takahashi, T.; Higashimura, T. *Macromolecules* **1985**, *18*, 311. b) Masuda, T.; Niki, A.; Isobe, E.; Higashimura, T. *Macromolecules* **1985**, *18*, 2109.

6) Niki, A.; Masuda, T.; Higashimura, T. *J. Polym. Soc., Part A: Polym. Chem.* **1987**, *25*, 1553.

7) a) Tsuchihara, K.; Masuda, T.; Higashimura, T. *J. Am. Chem. Soc.* **1991**, *113*, 8548. b) Tsuchihara, K.; Masuda, T.; Higashimura, T. *Macromolecules* **1992**, *25*, 5816.

8) a) Buchmeiser, M.; Schrock, R. R. *Macromolecules* **1995**, *28*, 6642. b) Schrock, R. R.; Luo, S.; Lee, J. C.; Zanneti, N.; Davis, W. M. *J. Am. Chem. Soc.* **1996**, *118*, 3883.

9) Wallace, K. C.; Liu, A. H.; Davis, W. M.; Schrock, R. R. *Organometallics* **1989**, *8*, 644.

10) a) Furlani, A.; Napoletano, C.; Russo, M. V.; *J. Polym. Sci., Part A*: *Polym. Chem.* **1989**, *27*, 75. b) Kishimoto, Y.; Eckerle, P.; Miyatake, T.; Ikariya, T.; Noyori, R. *J. Am. Chem. Soc.* **1994**, *116*, 12131.

11) a) Tabata, M.; Inaba, Y.; Yokota, K.; Nozaki, Y. *J. Macromol. Sci., Pure Appl. Chem.* **1994**, *A31*, 465. b) Minakawa, H.; Tabata, M.; Yokota, K. *J. Macromol. Sci., Pure Appl. Chem.* **1996**, *A33*, 291.

12) Masuda, T.; Isobe, E.; Higashimura, T. *J. Am. Chem. Soc.* **1983**, *105*, 7473.

13) a) *Polymer Membranes for Gas and Vapor Separation: Chemistry and Materials Science*; Freeman, B. D., Pinnau, I., Eds.; ACS Symp. Ser. 733; Am. Chem. Soc.: Washington, DC, 1999. b) Kesting, R. E.; Fritzsche, A. K. *Polymeric Gas Separation Membranes*; Wiley: New York, 1993. c) Stern, S. A. *J. Membr. Sci.* **1994**, *94*, 1.

14) a) Kang, E. T.; Neoh, K. G.; Masuda, T.; Higashimura, T.; Yamamoto, M. *Polymer* **1989**, *30*, 1328. b) Zhou, S.; Hong, H.; He, Y.; Yang, D.; Jin, X.; Qian, R.; Masuda, T.; Higashimura, T. *Polymer* **1992**, *33*, 2189.

15) a) Kraft, A.; Grimsdale, A. C.; Holmes, A. B. *Angew. Chem., Int. Ed.* **1998**, *37*, 403. b) Friend, R. H.; Greeham, N. C. In *Handbook of Conducting Polymer*, 2nd ed.; Marcel Dekker: New York, 1998; p 823. c) Burroughes, J. H.; Bradley, D. D. C.; Brown, A. R.; Marks, R. N.; Mackay, K.; Friend, R. H.; Burns, P. L.; Holmes, A. B. *Nature* **1990**, *347*, 539.

16) Tada, K.; Sawada, H.; Kyokane, J.; Yoshino, K. *Jpn. J. Appl. Phys.* **1995**, *34*, L1083.

Part I

Synthesis and Properties of Novel Silicon-Containing Poly(diphenylacetylenes)

Chapter 1

Polymerization and Polymer Properties of Diphenylacetylenes with Very Bulky Silyl Substituents

Abstract

Polymerization and polymer properties of 1-phenyl-2-[*p*-(triphenylsilyl)-phenyl]acetylene (*p*Ph_3SiDPA) and 1-phenyl-2-[*p*-(triisopropylsilyl)phenyl]acetylene (*pi*Pr_3SiDPA), which have very bulky silyl groups, were examined. These monomers polymerized in good yields in the presence of $TaCl_5$-based catalysts. The highest weight-average molecular weights of poly(*p*Ph_3SiDPA) and poly(*pi*Pr_3SiDPA) reached about $1x10^6$ and $4.8x10^6$, respectively. The polymers were yellow to orange-colored solids which were soluble in toluene, $CHCl_3$, etc. and provided free-standing films by solution casting. The onset temperatures of weight loss of poly(*p*Ph_3SiDPA) and poly(*pi*Pr_3SiDPA) in TGA in air were 430 and 270 °C, respectively. The oxygen permeability coefficients of poly(*p*Ph_3SiDPA) and poly(*pi*Pr_3SiDPA) at 25 °C were 3.8 and 20 barrers, respectively, and relatively small.

Introduction

It is known that various substituted acetylenes can be polymerized by group 5 and 6 transition-metal catalysts.[1] Among the acetylenic monomers, 1-(trimethylsilyl)-1-propyne (TMSP)[2] and 1-phenyl-2-[*p*-(trimethylsilyl)phenyl]-acetylene (*p*Me_3SiDPA)[3,4] polymerize with $TaCl_5$ alone or its mixture with organometallic cocatalysts to provide high molecular weight polymers ($M_w > 1x10^6$) in quantitative yield. Both of these Si-containing polymers show high gas permeability and their gas permeation behavior has recently been under intensive research.[5-9] Thus, one can assume that bulky substituents like trimethylsilyl group are effective to enhance the gas permeability of substituted polyacetylenes. Further, poly(*p*Me_3Si-DPA) is thermally fairly stable, as is seen from its onset temperature of the weight loss in air (T_0) as high as 430 °C.[3,4]

Hence, it is of interest to study the polymerization behavior and polymer properties of diphenylacetylenes that have substituents bulkier than the trimethylsilyl group. In this chapter, the author investigated the polymerization of 1-phenyl-2-[*p*-(triphenylsilyl)phenyl]acetylene (*p*Ph_3SiDPA) and 1-phenyl-2-[*p*-(triisopropylsilyl)-phenyl]acetylene (*pi*Pr_3SiDPA), both of which possess very bulky silyl groups. $TaCl_5$-based catalysts were employed, and suitable polymerization conditions were established. The structure and properties of the polymers formed are also discussed.

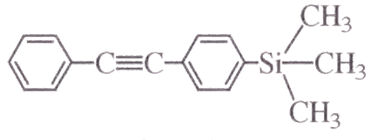

pMe_3SiDPA

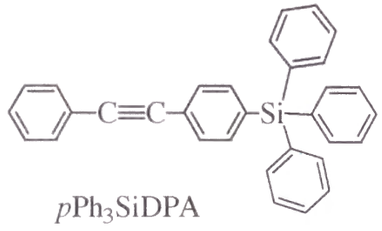

pPh_3SiDPA

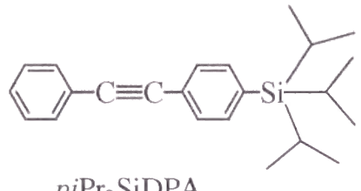

piPr_3SiDPA

Results and Discussion

Polymerization. Polymerization of *p*Ph_3SiDPA was examined by using various catalysts based on tantalum pentachloride ($TaCl_5$). When $TaCl_5$ alone was used as catalyst, no methanol-insoluble polymer was obtained; the products were linear oligomers (Table 1).

By contrast, polymers were obtained in over 60% yields when suitable organometallic cocatalysts such as Me_4Sn, *n*-Bu_4Sn, and Et_3SiH were used in a twofold excess over $TaCl_5$. The weight-average molecular weights (M_w) of the polymers were as high as $1.1x10^6$–$1.4x10^6$. The polymers were yellow solid and completely soluble in toluene and $CHCl_3$.

Table 2 shows the results for the polymerization of *pi*Pr_3SiDPA using various Ta catalysts. This monomer behaved in a similar way to *p*Ph_3SiDPA. Thus, no methanol-insoluble polymer was obtained with $TaCl_5$ alone, while the use of suitable organometallic cocatalysts led to the formation of methanol-insoluble polymers in good yield (ca. 80%). The M_w values of the polymers were $4.8x10^6$–$5.3x10^6$ and extremely high.

Table 1. Polymerization of *p*Ph_3SiDPA by Various Catalysts[a]

catalyst	polymer[b]		
	yield, %	$M_w/10^3$[c]	$M_n/10^3$[c]
$TaCl_5$	0	–	–
$TaCl_5$–Me_4Sn	83	1100	400
$TaCl_5$–*n*-Bu_4Sn	61	1400	510
$TaCl_5$–Et_3SiH	75	1200	330
$TaCl_5$–Ph_4Sn	20	1000	430
$TaCl_5$–Ph_3SiH	11	–	–

[a] Polymerized in toluene at 80 °C for 3 h; $[M]_0$ = 0.10 M, [Cat] = 20 mM, [Cocat] = 40 mM. [b] Methanol-insoluble product. [c] Measured by GPC.

Table 2. Polymerization of *pi*Pr$_3$SiDPA by Various Catalysts[a]

catalyst	polymer[b]		
	yield, %	$M_w/10^3$[c]	$M_n/10^3$[c]
$TaCl_5$	0	–	–
$TaCl_5$–Me_4Sn	84	5100	2200
$TaCl_5$–n-Bu_4Sn	77	4800	1900
$TaCl_5$–Et_3SiH	79	5300	2000
$TaCl_5$–Ph_4Sn	39	7300	4300
$TaCl_5$–Ph_3SiH	0	–	–

[a] Polymerized in toluene at 80 °C for 3 h; $[M]_0$ = 0.10 M, [Cat] = 20 mM, [Cocat] = 40 mM. [b] Methanol-insoluble product. [c] Measured by GPC.

The time profile of the polymerizations was examined by using the $TaCl_5$–Et_3SiH catalyst at 80 °C (Figure 1). With *p*Ph$_3$SiDPA, the polymer yield immediately reached about 75%. The M_w of the polymer was hardly dependent on polymerization time and about 1.2x10^6. In the case of *pi*Pr$_3$SiDPA, the polymer yield increased with the polymerization time to reach about 80% after 3 h, and the M_w became as large as 5.3x10^6 after 24 h. The molecular weights of polymers did not decrease even though the polymerization systems were left over 24 h.

Polymer Structure. The IR spectra of both polymers exhibited no absorption at 2220 cm^{-1} ($\nu_{C\equiv C}$) that is seen in the monomers. Otherwise, similar bands were observed in both the polymers and the starting monomers. The NMR data of the polymers also supported the absence of the carbon-carbon triple bond. Hence, the main chain of the polymers is considered to consist of alternating double bonds.

Figure 2 illustrates UV-visible spectra of the present polymers. Both polymers show a broad absorption band due to the main chain in the visible region; poly(*p*Ph$_3$SiDPA) has an absorption maximum (ε_{max} 4400 M^{-1} cm^{-1}) at 420 nm, and

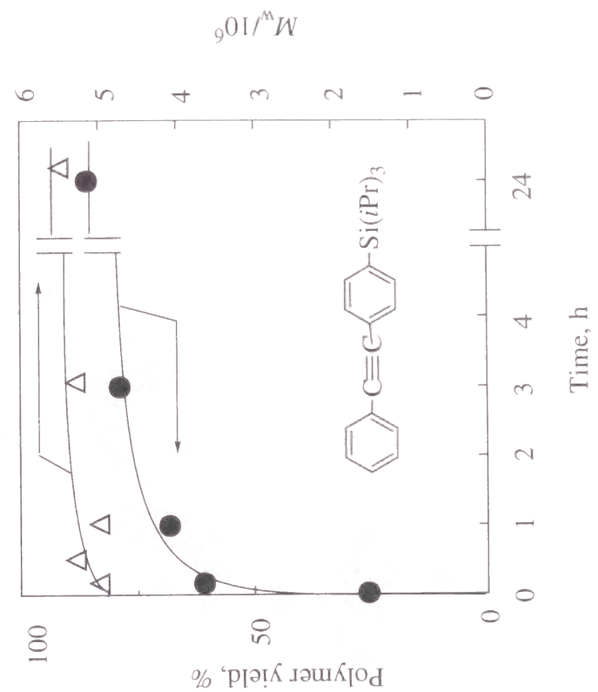

Figure 1. Time profiles for the polymerization of *p*Ph$_3$SiDPA and *pi*Pr$_3$SiDPA by $TaCl_5$-Et_3SiH (in toluene, 80 °C, $[M]_0$ = 0.10 M, $[TaCl_5]$ = 20 mM, $[Et_3SiH]$ = 40 mM).

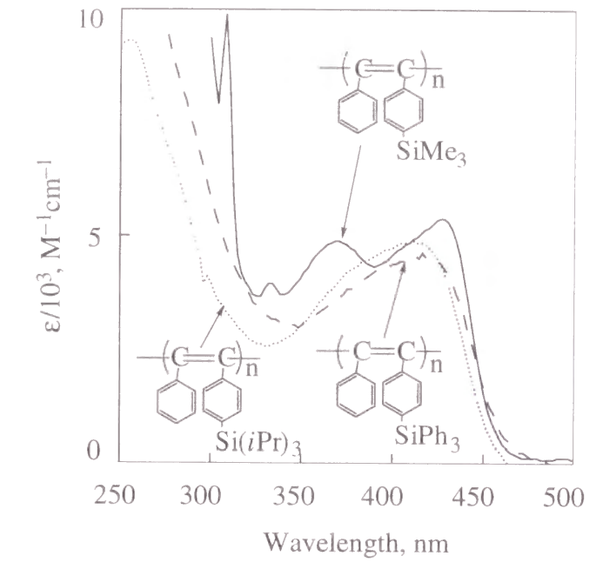

Figure 2. UV-visible spectra of poly(diphenylacetylene)s with bulky silyl groups (in THF).

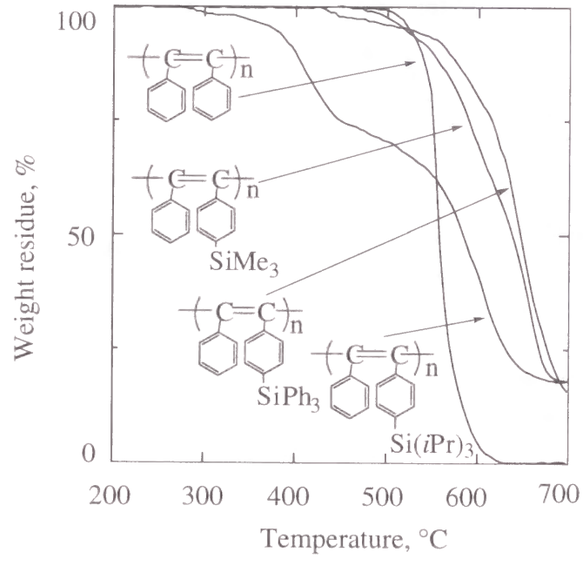

Figure 3. TGA curves of poly(diphenylacetylene)s with bulky silyl groups (in air, heating rate 10 °C/min).

the cutoff wavelength is ca. 480 nm. Poly($p i$Pr$_3$SiDPA) has a similar maximum (ε_{max} 4800 M^{-1} cm^{-1}) at 410 nm, and the cutoff wavelength is ca. 460 nm. These spectral data correspond to the color of the polymer (yellow).

Polymer Properties. Polymer properties were examined by using the samples obtained using $TaCl_5$–Et_3SiH as catalyst in Tables 1 and 2.

Both poly(pPh$_3$SiDPA) and poly($p i$Pr$_3$SiDPA) completely dissolved in common solvents such as toluene, $CHCl_3$, THF, carbon tetrachloride, etc., but exhibited no solubility in polar solvents such as DMF, DMSO, and lower alcohols. Poly($p i$Pr$_3$SiDPA) was soluble in hexane and cyclohexane, whereas poly(pPh$_3$SiDPA) was partly insoluble in them.

Thermogravimetric analyses (TGA) of the present and related polymers were conducted in air (Figure 3). The onset temperature of the weight loss in air (T_0) for poly(pPh$_3$SiDPA) was 430 °C, indicating the high thermal stability of the polymer though somewhat inferior to poly(DPA). Thus, the introduction of a triphenylsilyl group on the phenyl ring exhibits no significant adverse effect on the thermal stability. On the other hand, poly($p i$Pr$_3$SiDPA) began to lose weight at 270 °C, and hence the triisopropylsilyl group, which contains *sec*-alkyl groups, proves to considerably decrease the thermal stability.

The oxygen permeability coefficients (P_{O_2}) of poly(pPh$_3$SiDPA) and

Table 3. Gas Permeability Coefficients of Silicon-Containing Poly(diphenylacetylene)s

–(CPh=CC$_6$H$_4$X)–	P^a					
X	He	H_2	O_2	N_2	CO_2	CH_4
p-SiMe$_3$	1000	2100	1100	520	4700	1500
p-SiiPr$_3$	50	72	20	4.9	112	11
p-SiPh$_3$	15	22	3.8	0.94	21	0.84

[a] Oxygen permeability coefficient at 25 °C in the units of 1×10^{-10} cm^3(STP)cm/(cm^2·s·cmHg).

poly(piPr$_3$SiDPA) at 25 °C were 3.8 and 20 barrers, respectively, which are relatively small against expectation (Figure 4). Freeman and coworkers carried out the gas permeation measurements of poly(piPr$_3$SiDPA) to obtain its P_{O_2} value of 39.2 barrers (film thickness: 20 μm), which roughly agrees with our result.[10] The separation factors between oxygen and nitrogen (P_{O_2}/P_{N_2}) of poly(pPh$_3$SiDPA) and poly(piPr$_3$SiDPA) were 4.0 and 4.1, respectively, higher than that of natural rubber. The permeability coefficients of the present polymers to various gasses are shown in Table 3. It is noted that the small He and H_2 molecules permeate easier than the larger ones through the present polymers.

The observed P_{O_2} values are about 1/200–1/1000 that of poly(TMSP), 1/50–1/300 that of poly(pMe$_3$SiDPA), close to that of natural rubber (23 barrers), and appreciably small among those of various substituted polyacetylenes.[11] Other bulky silyl substituents (e.g., Et$_3$Si and iPrMe$_2$Si) also drastically reduce the gas permeability (P_{O_2} = 95 and 200 barrers, respectively).[12] Thus, the gas permeability of substituted

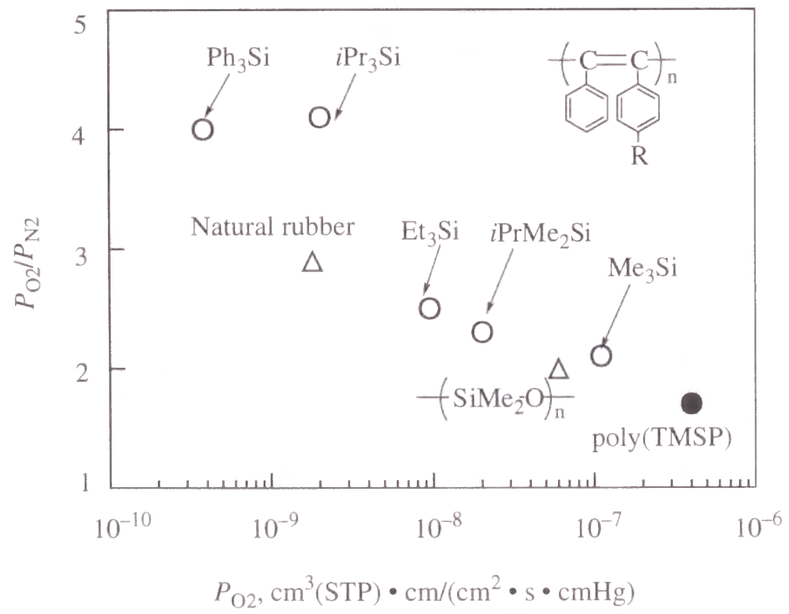

Figure 4. Oxygen permeability coefficients (P_{O2}) of poly(diphenylacetylene)s with bulky silyl groups (25 °C) (data from this chapter and ref. (3), (4), (12)).

polyacetylenes greatly depends on the kind of substituents, and not only the bulkiness of substituents but also their shape and rigidity are very important for gas permeability.

Two explanations are possible for the unexpectedly small P_{O_2} values for the present polymers; i.e., one is that these polymers undergo relaxation so quickly that the gas permeability decreases sharply, and the other is that too bulky, round-shaped substituents such as present ones lack mobility, leading to the low gas permeability. More detailed studies on the gas permeation mechanism is necessary to conclude this problem.

Experimental

Materials. The two monomers were prepared with reference to the method of preparing other Si-containing DPAs[3,4,13] according to Scheme 1:

Scheme 1

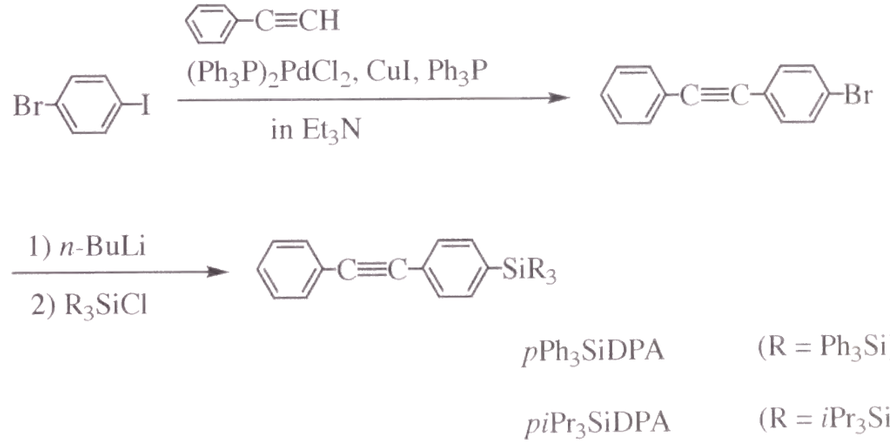

pPh$_3$SiDPA (R = Ph$_3$Si)

piPr$_3$SiDPA (R = iPr$_3$Si)

1-(p-Bromophenyl)-2-phenylacetylene: A 1-L round-bottomed flask was equipped with a reflux condenser, a three-way stopcock, and a magnetic stirring bar, and flushed with dry nitrogen. Triethylamine (200 mL), (Ph$_3$P)$_2$PdCl$_2$ (246 mg, 0.35 mmol), CuI (400 mg, 2.1 mmol), Ph$_3$P (367 mg, 1.4 mmol), and phenylacetylene (11.6 mL, 106 mmol) were placed in the flask, and the mixture was stirred for 1 h at 60 °C. Then, p-bromoiodobenzene (30.0 g, 106 mmol) in triethylamine (100 mL) was added

dropwise, and stirring was continued for an additional 2 h. After the completion of the reaction had been confirmed by thin layer chromatography (TLC), triethylamine was evaporated. Diethyl ether (ca. 400 mL) was added, and insoluble salts were removed by filtration. The solution was washed with 2 N hydrochloric acid and then water. The organic phase was dried over anhydrous sodium sulfate, and diethyl ether was evaporated. The crude product was purified by flash column chromatography (Nakarai Tesque Co., silica gel 60; eluent: hexane) to give the desired product (yield 24.5 g, 90%) as a white solid, mp 84.0–85.5 °C, purity > 99% (by ^{1}H NMR).

pPh$_3$SiDPA: A 500-mL round-bottomed flask was equipped with a three-way stopcock, a dropping funnel, and a magnetic stirring bar. After the flask was flushed with nitrogen, a hexane solution of *n*-butyllithium (18.8 mL, 1.6 M, 30 mmol) was placed in the flask at –20 °C. At the same temperature, a solution of 1-(*p*-bromophenyl)-2-phenylacetylene (7.8 g, 30 mmol) in diethyl ether (70 mL) was added dropwise, and the reaction mixture was left for 30 min at –78 °C. A solution of triphenylchlorosilane (8.9 g, 30 mmol) in diethyl ether (80 mL) was added dropwise, and stirring was continued for an additional 1 h at room temperature. After the completion of the reaction had been confirmed by TLC, ice-water (20 mL) was added. The product was extracted with diethyl ether, washed with water, and dried over anhydrous sodium sulfate. Diethyl ether was evaporated, and the crude product was purified by flash column chromatography (eluent: hexane) to give a white solid (10.0 g, 77%), mp 158.0–159.8 °C, purity > 99% (by ^{1}H NMR); IR (KBr) 2998, 2220 (C≡C), 1428, 1110, 830, 702, 594 cm^{-1}; ^{1}H NMR ($CDCl_3$) δ 7.8–7.2 (m, 24H, aromatic); ^{13}C NMR ($CDCl_3$) δ 136.3, 136.2, 134.7, 133.7, 131.6, 130.7, 129.7, 128.3, 127.9, 124.4, 123.1, 90.4, 89.3. Anal. Calcd for $C_{32}H_{24}Si$: C, 88.02; H, 5.55; Si, 6.43. Found: C, 87.87; H, 5.47; Si, 6.66.

piPr$_3$SiDPA: This monomer was prepared in the same way using triisopropylchlorosilane: overall yield 14.0%, mp 151.0–152.7 °C, purity > 99% (by ^{1}H NMR); IR (KBr) 2953, 2221(C≡C), 1595, 1096, 826, 758 cm^{-1}; ^{1}H NMR ($CDCl_3$) δ 7.6–7.3 (9H, aromatic), 1.5–1.3 (3H), 1.1–1.0 (18H); ^{13}C NMR ($CDCl_3$) δ 135.7, 135.1,

131.6, 130.4, 128.3, 128.1, 123.3, 123.2, 89.8, 89.5, 18.4, 10.7. Anal. Calcd for $C_{23}H_{30}Si$: C, 82.55; H, 9.06; Si, 8.39. Found: C, 82.58; H, 9.08; Si, 8.34.

$TaCl_5$ and organometallic cocatalysts were all commercially obtained and used without further purification. Polymerization solvents were purified by the standard methods.[14]

Polymerization. Polymerizations were carried out in a Schlenk tube equipped with a three-way stopcock under dry nitrogen. Unless otherwise specified, the reaction conditions are: in toluene, 80 °C, 3 h, $[M]_0$ = 0.10 M, [Cat] = 20 mM, [Cocat] = 40 mM. A detailed procedure of polymerization has been described elsewhere.[4] Polymers were isolated by precipitation into a large amount of methanol, and polymer yields were determined by gravimetry.

Characterization. The molecular weights of polymers were determined by GPC with use of a polystyrene calibration. GPC curves were observed with a Shimadzu LC-9A liquid chromatograph [eluent, $CHCl_3$; columns, Shodex K-805, K-806, and K-807 polystyrene gels (Showa Denko, Co., Japan)].

IR, UV, and NMR spectra were measured on a Shimadzu FTIR-8100 spectrophotometer, a Shimadzu UV-2200 spectrophotometer, and a JEOL GSX-270 spectrometer, respectively. TGA was conducted with a Perkin Elmer TGA-7 (in air, heating rate 10 °C/min). The gas permeability coefficients were measured with a Rikaseiki K-315-N gas permeability apparatus.

References

1) Shirakawa, H.; Masuda, T.; Takeda, K. In *The Chemistry of Triple-Bonded Functional Groups (supplement C2)*; Patai, S., Ed.; Wiley: Chichester, 1994; Chapter 17.
2) Masuda, T.; Isobe, E.; Higashimura, T.; Takada, K. *J. Am. Chem. Soc.* **1983**, *105*, 7473.
3) Tsuchihara, K.; Masuda, T.; Higashimura, T. *J. Am. Chem. Soc.* **1991**, *113*, 8548.

4) Tsuchihara, K.; Masuda, T.; Higashimura, T. *Macromolecules* **1992**, *25*, 5816.
5) Kesting, R. E.; Fritzsche, A. K. In *Polymeric Gas Separation Membranes;* Wiley: New York, 1993; pp 109–114.
6) Ichiraku, Y.; Stern, S. A.; Nakagawa, T. *J. Membr. Sci.* **1987**, *34*, 5.
7) Lin, X.; Qiu, X.; Zheng, G.; Xu, J. *J. Appl. Polym. Sci.* **1995**, *58*, 2137.
8) Pinnau, I.; Casillas, C. G.; Morisato, A.; Freeman, B. D. *J. Polym. Sci., Part B: Polym. Phys.* **1996**, *34*, 2613.
9) Toy, L. G.; Freeman, B. D.; Spontak, R. J.; Morisato, A.; Pinnau, I. *Macromolecules* **1997**, *30*, 4766.
10) Freeman, B. D. private communication.
11) Masuda, T.; Iguchi, Y.; Tang, B.-Z.; Higashimura, T. *Polymer* **1988**, *29*, 2041.
12) Tsuchihara, K.; Masuda, T.; Higashimura, T. *J. Polym. Sci., Part A: Polym. Chem.* **1993**, *31*, 547.
13) Häbich, D.; Effenberger, F. *Synthesis* **1979**, 841.
14) Perrin, D. D.; Armarego, W. L. F.; Perrin, D. R. *Purification of Laboratory Chemicals,* 2nd ed.; Pergamon Press: Oxford, 1980.

Chapter 2

Copolymerization and Copolymer Properties of 1-[3,5-Bis(trimethylsilyl)phenyl]-2-phenylacetylene

Abstract

Copolymerization of 1-[3,5-bis(trimethylsilyl)phenyl]-2-phenylacetylene (*m,m*(Me_3Si)$_2$DPA) with other diphenylacetylene derivatives and their copolymer properties were investigated. Homopolymerization of *m,m*(Me_3Si)$_2$DPA by $TaCl_5$–*n*-Bu_4Sn (1:2) did not give the polymer owing to steric hindrance. However, *m,m*(Me_3Si)$_2$DPA copolymerized with diphenylacetylene (DPA), 1-phenyl-2-[*p*-(trimethylsilyl)phenyl]acetylene (*p*Me_3SiDPA), and 1-phenyl-2-[*m*-(trimethylsilyl)-phenyl]acetylene (*m*Me_3SiDPA) in the presence of $TaCl_5$–*n*-Bu_4Sn at various feed ratios to give copolymers in moderate yields. The formed copolymers were yellow to orange solids, which were soluble in common organic solvents such as toluene and $CHCl_3$. The highest weight-average molecular weights (M_w) of these copolymers reached ca. $6x10^5$ and tough films could be obtained by solution casting. Their onset temperatures of weight loss in air were observed around 400 °C, indicating high thermal stability. The oxygen permeability coefficients at 25 °C of copoly [*m,m*(Me_3Si)$_2$DPA/DPA] (feed ratio 1:1) and copoly[*m,m*(Me_3Si)$_2$DPA/*p*Me_3SiDPA] (feed ratio 1:2) were 21 and 100 barrers, respectively, medium in magnitude among polymers from substituted acetylenes.

Introduction

Whereas silicon is a group 14 element like carbon and shows properties close to those of carbon, it has vacant *d*-orbitals and hence is more electropositive and reactive than carbon.[1] The organosilicon polymers so far synthesized[2] can be roughly classified into two categories, i.e., polymers with Si atoms in the main chain[3-5] (e.g., polysilanes, polycarbosilanes, polycarbosiloxanes, polysiloxanes, etc.) and those with Si atoms in the side chain.[6] These polymers often show interesting features such as heat resistance, cold resistance, optoelectronic properties, and microlithographic functions.[2,3a,7,8]

It is known that Si-containing polyacetylenes often exhibit unique properties, especially high gas permeability.[9] For example, poly[1-(trimethylsilyl)-1-propyne] [poly(TMSP)][10] and poly[1-phenyl-2-[*p*-(trimethylsilyl)phenyl]acetylene] [poly-(*p*Me_3SiDPA)][11] show extremely high oxygen permeability coefficient (P_{O2}) up to 4000 and 1100 barrers, respectively; the former polymer is the most permeable to gases among all the synthetic polymers. In general, it can be said that the introduction of trimethylsilyl groups is effective to enhance the gas permeability of substituted polyacetylenes. Further, poly(*p*Me_3SiDPA) is thermally very stable, as is seen from its onset temperature of the weight loss in air (T_0) as high as 430 °C. These sterically crowded disubstituted acetylene polymers can be obtained by the polymerization of the corresponding acetylene monomers catalyzed by $TaCl_5$-based catalysts. The formed polymers have extremely high molecular weight over $1x10^6$ and good film-forming ability.

It is interesting to study the polymerization behavior and polymer properties of diphenylacetylenes having plural trimethylsilyl groups. In this chapter, the author used a diphenylacetylene having two trimethylsilyl groups at meta position, 1-[3,5-bis(trimethylsilyl)phenyl]-2-phenylacetylene [*m,m*($Me_3Si)_2$DPA] as monomer, and examined its homopolymerization and copolymerization with other diphenyl-acetylenes such as diphenylacetylene (DPA), *p*Me_3SiDPA, and 1-phenyl-2-[*m*-(trimethylsilyl)phenyl]acetylene (*m*Me_3SiDPA) by using $TaCl_5$–*n*-Bu_4Sn catalyst

(Scheme 1). The homopolymer was not obtained but copolymers were available. Properties of the formed copolymers such as solubility, thermal stability, and gas permeability were clarified.

Scheme 1

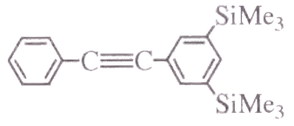

m,m($Me_3Si)_2$DPA

DPA

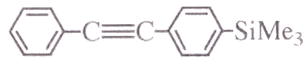

pMe_3SiDPA

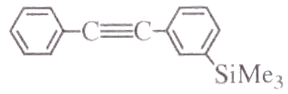

mMe_3SiDPA

Results and Discussion

Polymerization. Table 1 shows the results of homo- and copolymeri-zations of *m,m*($Me_3Si)_2$DPA. As the polymerization catalyst, a 1:1 mixture of $TaCl_5$ and *n*-Bu_4Sn was employed, which is the most effective in the polymerization of diphenylacetylenes. Unfortunately *m,m*($Me_3Si)_2$DPA gave no homopolymer. This result is attributable to the steric hindrance based on the two trimethylsilyl groups at both meta positions. On the other hand, its copolymerizations with DPA, *p*Me_3SiDPA and *m*Me_3SiDPA at a feed mole ratio 1:1 proceeded successfully to give the copolymers in moderate yields (runs 4, 9, 12). All the formed copolymers completely dissolved in toluene and $CHCl_3$, and their M_w values were ca. $1x10^5$–$4x10^5$ and relatively high.

In general, both molecular weight and yield of copolymers tended to increase when the content of the comonomers (DPA, *p*Me_3SiDPA and *m*Me_3SiDPA) in the feed were increased (see Table 1). Thus, the M_w values of copoly[*m,m*($Me_3Si)_2$DPA/*p*-

Table 1. Copolymerization of *m,m*(Me_3Si)$_2$DPA (M_1) with Various DPAs (M_2) by $TaCl_5$–*n*-Bu_4Sn at Various Feed Ratios[a]

run	feed ratio	monomer convn., %		polymer[b]		
	M_1 : M_2	M_1	M_2	yield, %	$M_w/10^3$[c]	$M_n/10^3$[c]
		comonomer: none				
1	1:0	34	–	0	–	–
		comonomer: DPA				
2	3:1	22	22	7	56	36
3	2:1	37	30	14	87	53
4	1:1	38	46	33	370	190
5	1:1[d]	19	23	11	230	140
6	1:1[e]	40	44	26	380	230
7	1:2	71	71	–	–	–
		comonomer: *p*Me_3SiDPA				
8	2:1	35	29	8	48	31
9	1:1	34	42	21	200	82
10	1:2	56	59	42	440	230
		comonomer: *m*Me_3SiDPA				
11	2:1	25	21	6	40	26
12	1:1	18	17	7	110	56
13	1:2	22	31	20	610	68

[a] Polymerized in toluene at 80 °C for 24 h; $[M]_{0,total}$ = 0.40 M, $[TaCl_5]$ = 20 mM, [*n*-Bu_4Sn] = 40 mM. [b] Methanol-insoluble product. [c] Measured by GPC. [d] $[M]_{0,total}$ = 0.20 M. [e] $[M]_{0,total}$ = 1.0 M.

Me_3SiDPA] (feed mole ratio 1:2, run 10), and copoly[*m,m*(Me_3Si)$_2$DPA/*m*Me_3SiDPA] (feed mole ratio 1:2, run 13) reached 4.4×10^5 and 6.1×10^5, respectively. Most of the copolymers obtained in Table 1 are soluble in common solvents. However copoly[*m,m*(Me_3Si)$_2$DPA/DPA] (feed ratio 1:2, run 7) was insoluble in toluene, $CHCl_3$,

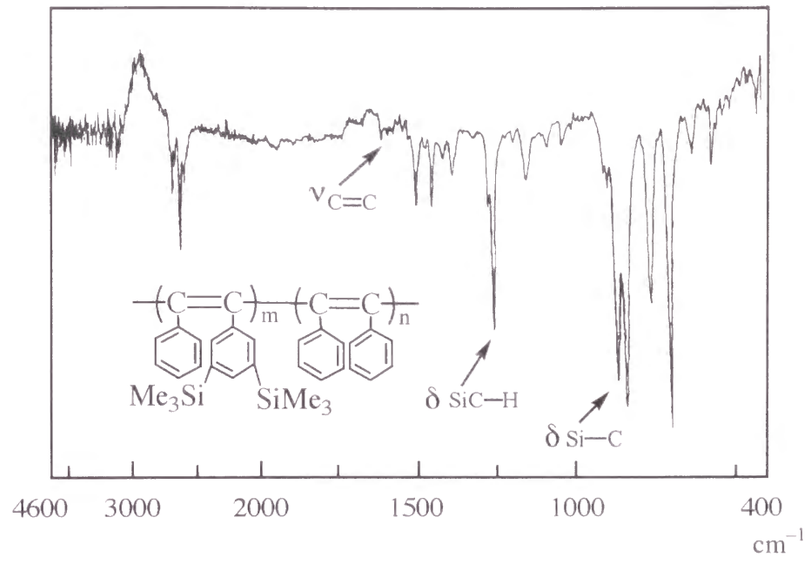

Figure 1. IR spectra of copoly[*m,m*(Me_3Si)$_2$DPA/DPA] produced at 1:1 feed ratio.

etc, which is consistent with the result that poly(DPA) is insoluble in any solvent.[12] The copolymers obtained in runs 4, 10, and 13 had enough high M_w to give free-standing films by solution casting.

Polymer Structure. Figure 1 illustrates the IR spectrum of copoly [*m,m*(Me_3Si)$_2$DPA/DPA] (feed mole ratio 1:1). A weak absorption band is observed around 1550 cm^{-1}, which is assignable to the stretching of the highly symmetrical tetrasubstituted ethylene structure in the main chain. Further, absorptions due to SiC–H deformation and Si–C stretching were seen around 1260 and 890–830 cm^{-1}, respectively. Figure 2 depicts the UV-visible spectrum of the copolymer. The copolymer is colored orange and has an absorption maximum at 430 nm whose cutoff wavelength is 500 nm. This absorption is due to the conjugated double bonds along the main chain. These spectral data support the alternating double bond structure of the main chain for this copolymer.

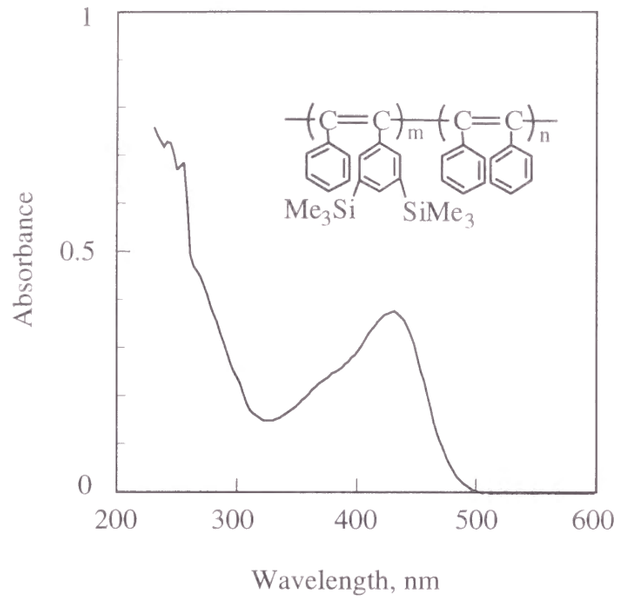

Figure 2. UV-visible spectra of copoly(*m,m*(Me_3Si)$_2$DPA/DPA) produced at 1:1 feed ratio (in THF).

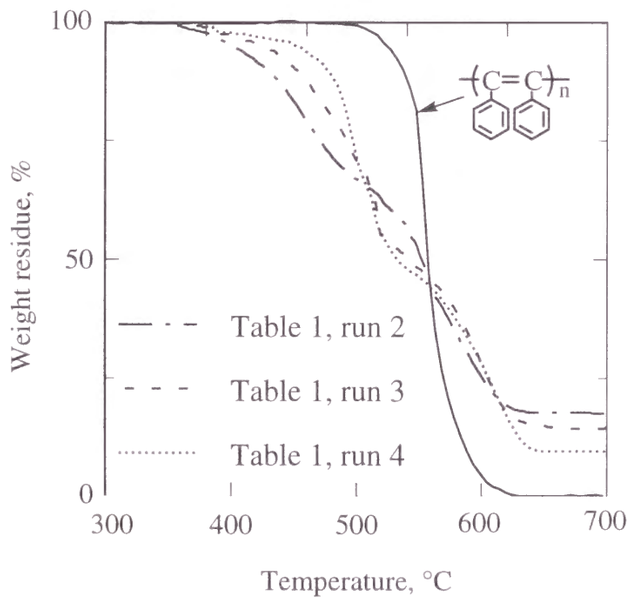

Figure 3. TGA curves of copoly[*m,m*(Me_3Si)$_2$DPA/DPA]s produced at various feed ratios (heating rate 10 °C/min, in air).

Polymer Properties. The present copolymers except the one of Table 1, run 7 were completely soluble in $CHCl_3$, dichloromethane, THF, toluene, benzene, and anisole, and insoluble in methanol, DMF, DMSO, diethyl ether, and hexane.

The thermal stability of copoly[*m,m*(Me_3Si)$_2$DPA/DPA]s was investigated (Figure 3). In TGA measured in air, these copolymers showed fairly high thermal stability (onset temperature of weight loss (T_0) ca. 400 °C), though inferior to poly(DPA) (T_0 = 500 °C).[12] The T_0 values of the copolymers hardly changed with the feed ratio, while the amount of weight residue around 700 °C was in the following order; run 4 > run 3 > run 2. This order corresponds to the Si-content in the copolymers, suggesting that the silicon in the copolymers is converted into SiO_2.

Figure 4 plots P_{O2} versus the separation factor (P_{O2}/P_{N2}) of copoly [*m,m*(Me_3Si)$_2$DPA/DPA] (Table 1, run 4) and copoly[*m,m*(Me_3Si)$_2$DPA/*p*Me_3SiDPA]

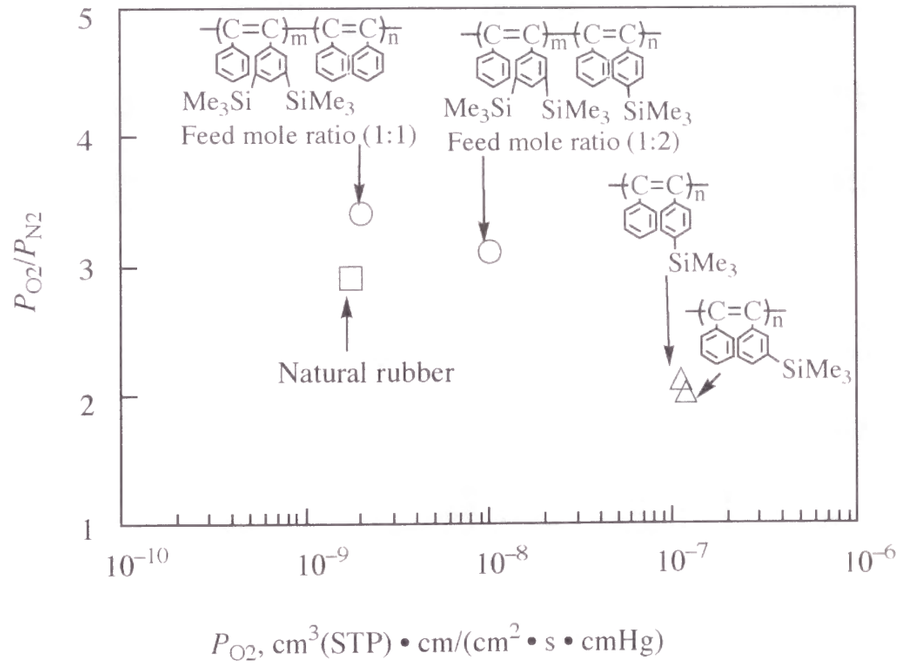

Figure 4. Oxygen permeability coefficients (P_{O2}) of copolymers from diphenylacetylenes having two trimethylsilyl groups (25 °C) [1barrer = 1x10^{-10} cm^3(STP) • cm/(cm^2 • s • cmHg)].

(Table 1, run 13). The P_{O2} values were 21 barrers (P_{O2}/P_{N2} = 3.4) and 100 barrers (P_{O2}/P_{N2} = 3.1), respectively. Rather opposite to expectation, these P_{O2} values are from one to two orders of magnitude smaller than that of poly(*p*Me_3SiDPA). A few explanations are possible for this finding: One is that the excess free volume is little due to stacking (packing) of substituents based on the symmetrical structure of the *m,m*-$(Me_3Si)_2C_6H_4$ moiety. The second is that, for some reason, the present copolymers undergo physical relaxation so quickly that the gas permeability that has already decreased is observed. The third is that the low mobility of the *m,m*-$(Me_3Si)_2C_6H_4$ group in the polymer may have brought about the low gas permeability; this idea has recently been proposed by Kanaya based on the finding that there is a correlation between the P_{O2} value and local mobility of the substituents in some polyacetylenes.[13] The oxygen permeability of copoly[*m,m*$(Me_3Si)_2$DPA/*p*-Me_3SiDPA] was also lower than that of poly(*p*Me_3SiDPA) against expectation. Probably one of the above reasons will apply, and the study on the gas permeation mechanism is needed to clarify the proper reason.

Experimental

Materials. Diphenylacetylene was commercially obtained and purified by sublimation. *m,m*$(Me_3Si)_2$DPA was synthesized with reference to the literature methods (Scheme 2).[14] The synthesis of other monomers was reported before.[15]

Scheme 2

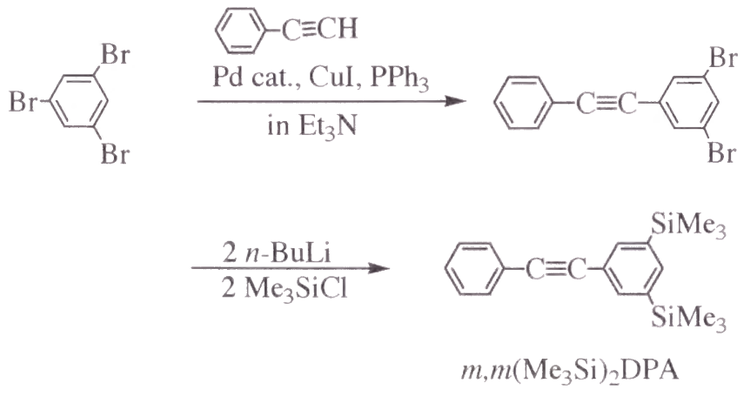

m,m$(Me_3Si)_2$DPA

1-(3,5-Dibromophenyl)-2-phenylacetylene: A 1-L three-necked flask was equipped with a reflux condenser, a magnetic stirrer, and a dropping funnel, and flushed with dry nitrogen. $(Ph_3P)_2PdCl_2$ (154 mg, 0.22 mmol), Ph_3P (233 mg, 0.89 mmol), CuI (248 mg, 1.3 mmol), Et_3N (200 mL) and 1,3,5-tribromobenzene (25 g, 81.4 mmol) were placed in the flask, and phenylacetylene (8.9 mL, 81.4 mmol) was added dropwise at room temperature with stirring. Then the reaction mixture was stirred at 60 °C for 6 h. Triethylamine was evaporated at reduced pressure. The residue was dissolved in diethyl ether and insoluble salts were filtered off. The filtrate was washed with 2N HCl aq. and water, and dried over anhydrous sodium sulfate. After evaporation of diethyl ether, the crude product was purified by flash column chromatography (Nakarai Tesque Co., silica gel 60; eluent: hexane) to afford a white solid (15.0 g, 55.0%), mp 108.0–108.9 °C.

1-[3,5-Bis(trimethylsilyl)phenyl]-2-phenylacetylene (m,m$(Me_3Si)_2$DPA): A 500-mL three-necked flask was equipped with a reflux condenser, a magnetic stirrer, and a dropping funnel, and flushed with dry nitrogen. 1-(3,5-Dibromophenyl)-2-phenylacetylene (5.0g, 14.9 mmol) and dry diethyl ether (50 mL) were placed in the flask and cooled down to –78 °C. *n*-BuLi (10.3 mL, 1.6 M, 16.4 mmol) was added slowly and the reaction mixture was stirred at –78 °C for 1 h. Then, a solution of trimethylchlorosilane (2.1 mL, 16.4 mmol) in diethyl ether (20 mL) was added dropwise. Subsequently the reaction mixture was recooled to –78 °C and monolithiation and monosilyation was repeated in the same way. The reaction mixture was warmed up to room temperature and stirred for 2 h. The reaction was quenched by addition of water. The organic phase was washed with water and dried over anhydrous sodium sulfate. Diethyl ether was evaporated and the crude product was purified by flash column chromatography (eluent: hexane) to give the desired product as a white solid (10 g, 69.1%), mp 66.0–67.0 °C, purity 99% (by ^{1}H NMR); IR (KBr) 2955, 1489, 1381, 1248, 918, 862, 837, 758, 693 cm^{-1}; ^{1}H NMR ($CDCl_3$) δ 7.3-7.7 (m, 9H, aromatic), 0.3 (s, 18H); ^{13}C NMR ($CDCl_3$) δ 139.6, 137.5, 136.8, 131.6, 128.3, 128.1, 123.4, 122.0, 90.0, 89.2, –1.2. Anal. Calcd for $C_{20}H_{27}Si_2$: C, 74.45; H, 8.14; Si, 17.41.

Found: C, 74.28; H, 8.14; Si, 17.58.

Procedures. Polymerizations were carried out as described in Chapter 1. Monomer conversions were determined by gas chromatography (GC) using docosane as the internal standard. Polymers were isolated by precipitation into a large amount of methanol, and polymer yields were determined by gravimetry. A detailed polymerization procedure has been described elsewhere.[16]

The molecular weights of polymers were evaluated by GPC (eluent, $CHCl_3$, polystyrene standard). UV-visible spectra was measured on a Jasco V-530 spectrometer. Measurements of IR, and NMR spectra, TGA, and gas permeabilities were carried out in the same manner as described in Chapter 1.

References

1) a) Lickiss, P. D. In *Encyclopedia of Inorganic Chemistry*; King, R. B., Ed.; Wiley: Chichester, 1994; Vol. 7, p 3771. b) Sakurai, H. In *Encyclopedia of Inorganic Chemistry*; King, R. B., Ed.; Wiley: Chichester, 1994; Vol. 7, p 3805. c) Rochow, E. G. *Chemistry of Silicones*; Wiley: New York, 1951.

2) a) *Silicon-Based Polymer Science: A Comprehensive Resource*; Zeigler, J. M., Fearon, F. W. G., Eds.; Adv. Chem. Ser. 224; Am. Chem. Soc.: Washington, DC, 1990. b) Yamashita, H.; Tanaka, M. *Bull. Chem. Soc. Jpn.* **1995**, *68*, 403.

3) a) West, R. In *Encyclopedia of Inorganic Chemistry*; King, R. B., Ed.; Wiley: Chichester, 1994; Vol. 6, p 3389. b) Miller, R. D.; Michl, J. *Chem. Rev.* **1989**, *89*, 1359.

4) a) Tsumura, M.; Iwahara, T. *Polym. J.* **1999**, *31*, 452. b) Kawakami, Y.; Takeyama, K.; Komuro, K.; Ooi, O. *Macromolecules* **1998**, *31*, 551.

5) Li, Y.; Kawakami, Y. *Macromolecules* **1999**, *32*, 548.

6) a) Hwang, D. H.; Kang, I. N.; Lee, J. I.; Do, L. M.; Hye, Y.; Zyung, T.; Shim, H. K. *Polym. Bull.* **1998**, *41*, 275. b) Pugh, C.; Bae, J. Y.; Dharia, J.; Ge, J.; Cheng, S. Z. D. *Macromolecules* **1998**, *31*, 5188. c) Gratt, J.; Cohen, R. E. *Macromolecules* **1997**, *30*, 3137.

7) a) Zhu, H. D.; Kantor, S. W.; MacKnight, W. J. *Macromolecules* **1998**, *31*, 850. b) Lauter, U.; Kantor, S. W.; Schmidt-Rohr, K.; MacKnight, W. J. *Macromolecules* **1999**, *32*, 3426. c) Itoh, M.; Inoue, K.; Iwata, K.; Mitsuzuka, M.; Kakigano, T. *Macromolecules* **1997**, *30*, 694.

8) a) Sohn, H.; Huddleston, R. R.; Powell, D. R.; West, R. *J. Am. Chem. Soc.* **1999**, *121*, 2935. b) Yamaguchi, S.; Jin, R.-Z.; Tamao, K. *J. Am. Chem. Soc.* **1999**, *121*, 2937. c) Ohshita, J.; Miura, N.; Arase, H.; Nodono, M.; Kunai, A.; Komaguchi, K.; Shiotani, M. *Macromolecules* **1998**, *31*, 7985. d) Yamaguchi, S.; Tamao, K. *J. Chem. Soc., Dalton Trans.* **1998**, 3693.

9) a) Aoki, T.; Kobayashi, Y.; Kaneko, T.; Oikawa, E.; Yamamura, Y.; Fujita, Y.; Teraguchi, M.; Nomura, R.; Masuda, T. *Macromolecules* **1999**, *32*, 79. b) Aoki, T.; Shinohara, K.; Kaneko, T.; Oikawa, E. *Macromolecules* **1996**, *29*, 4192. c) Masuda, T.; Teraguchi, M.; Nomura, R. In *Polymer Membranes for Gas and Vapor Separation: Chemistry and Materials Science*; Freeman, B. D., Pinnau, I., Eds.; ACS Symp. Ser. 733; Am. Chem. Soc.: Washigton, DC, 1999; Chapter 2.

10) Masuda, T.; Isobe, E.; Higashimura, T.; Takada, K. *J. Am. Chem. Soc.* **1983**, *105*, 7473.

11) Tsuchihara, K.; Masuda, T.; Higashimura, T. *J. Am. Chem. Soc.* **1991**, *113*, 8548.

12) Niki, A.; Masuda, T.; Higashimura, T. *J. Polym. Sci., Part A: Polym. Chem.* **1987**, *25*, 1553.

13) Kanaya, T.; Teraguchi, M.; Masuda, T.; Kaji, K. *Polymer* **1999**, *40*, 7157.

14) a) Armitage, J. B.; Jones, E. R. H.; Whiting, M. C. *J. Chem. Soc.* **1952**, 1993. b) Sonogashira, K.; Tohda, Y.; Hagihara, N. *Tetrahedron Lett.* **1975**, *50*, 4467.

15) Tsuchihara, K.; Masuda, T.; Higashimura, T. *Macromolecules* **1992**, *25*, 5816.

16) Ito, H.; Masuda, T.; Higashimura, T. *J. Polym. Sci., Part A: Polym. Chem.* **1996**, *34*, 2925.

Chapter 3

Polymerization and Polymer Properties of Disubstituted Acetylenes Having a Chiral Silyl Group

Abstract

Disubstituted acetylenes with chiral pinanyl groups, (–)-1-{4-[dimethyl(10-pinanyl)silyl]phenyl}-2-phenylacetylene (**1**), (–)-1-{3-[dimethyl(10-pinanyl)silyl]phenyl}-2-phenylacetylene (**2**), (–)-1-{4-[dimethyl(10-pinanyl)silyl]phenyl}-1-propyne (**3**) and (–)-1-chloro-2-{4-[dimethyl(10-pinanyl)silyl]phenyl}acetylene (**4**) polymerized with $NbCl_5$-, $TaCl_5$- or $MoCl_5$-based catalysts to give high molecular weight polymers in good yields. Poly(**1**) and poly(**2**) showed intense circular dichroism (CD) effects in the UV-visible region and large optical rotations, which suggests that these polymers exist in helical conformations with an excess of one-handed screw-sense. No significant decrease in the magnitude of CD effects of poly(**1**) and poly(**2**) with increasing temperature indicated the relatively high stability of their helical conformations. On the other hand, the intensities of CDs of poly(**3**) and poly(**4**) were approximately 1/10 those of poly(**1**) and poly(**2**), which means that introduction of two aromatic side groups into the repeating unit is favorable for the induction of helical conformation to disubstituted acetylene polymers. The free-standing membranes of poly(**1**), poly(**2**), and poly(**3**) exhibited characteristic properties as gas-permeable and optical resolution membranes.

Introduction

Synthesis of optically active polymers has been under intensive research because of their unique functions such as molecular recognition ability and catalytic activity for asymmetric synthesis.[1] Especially, chiral conjugated polymers are of great interest due to their potential benefits as asymmetric electrodes, polarization-sensitive electrooptical devices, nonlinear optical materials, and so on.[2] One of such conjugated polymers is represented by polyacetylenes with chiral substituents some of which are known to exhibit strong circular dichroism (CD) effects and large optical rotations based on the helical conformation.[3]

However, most of optically active polyacetylenes are limited to those from monosubstituted acetylenes. This is simply because almost perfect stereoregularity (*cis*) is readily obtained from monosubstituted acetylenes by Rh or Fe catalysts[4] and because stereoregular *cis*-configuration is favorable for the induction of one-handed screw-sense conformation.[4] In spite of these advantages, the chemical and thermal instability of polymers from monosubstituted acetylenes compared with those from disubstituted ones diminishes the utility of chiral polyacetylenes in the practical use. For example, the polymers from *n*- and *sec*-alkylacetylenes are readily oxidized in air leading to the degradation of the backbone.[5] The polymers from monosubstituted arylacetylenes without bulky *ortho*-substituents are more stable but still unstable in solution; a rapid decrease in molecular weight is often observed in solution.[6] In contrast, polymers from disubstituted acetylenes are thermally stable, and their excellent permeability of gases and liquids allow these polymers to be applied for separation membranes.[7] Therefore, synthesis of disubstituted acetylene polymers with optically active pendants is of great interest due to their potential utility as stable membranes for the resolution of racemic compounds.

It is unfortunate that the studies on the polymerization of disubstituted acetylenes with chiral substituents are quite few, and no systematic information is available on their polymerization behavior, structure, and characteristics of the formed polymers. An example has been reported by Aoki *et al.* for the polymerization of

(–)-1-[dimethyl(10-pinanyl)silyl]-1-propyne (**5**).[8] This monomer undergoes polymerization in the presence of $TaCl_5$–Ph_3Bi to give a high molecular weight polymer (M_w = 15x10^4). Small but clear Cotton effects in the absorption region of polymer backbone suggest that the polymer takes helical conformations with an excess of single-screw sense. The free-standing membrane of this polymer achieves the optical resolution of various racemates such as tryptophan, 1,3-butanediol, phenylalanine, and valine. This finding stimulated the author to study on the synthesis of a wide range of polymers from disubstituted acetylenes with chiral pendant groups and to clarify the relationship between the structure of the monomers and the conformation of the formed polymers.

This chapter deals with the polymerization of disubstituted acetylenes with chiral pinanyl groups by using various transition-metal catalysts. The monomers employed are (–)-1-{4-[dimethyl(10-pinanyl)silyl]phenyl}-2-phenylacetylene (**1**), (–)-1-{3-[dimethyl(10-pinanyl)silyl]phenyl}-2-phenylacetylene (**2**), (–)-1-{4-[dimethyl-(10-pinanyl)silyl]phenyl}-1-propyne (**3**) and (–)-1-chloro-2-{4-[dimethyl(10-pinanyl)silyl]phenyl}acetylene (**4**) (Chart). Both **1** and **2** were used for the examination of the effect of position of the chiral substituent on the conformation and permeability of the polymers. Monomers **3** and **4** were designed to investigate the influence of the

Chart

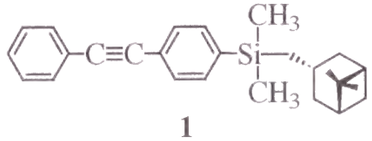

1

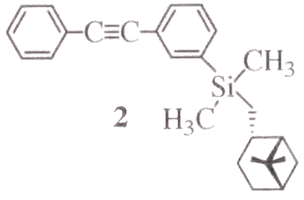

2

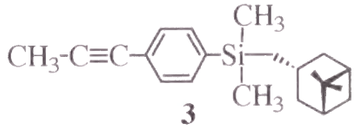

3

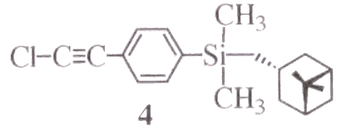

4

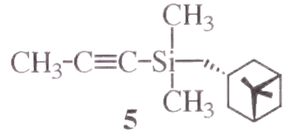

5

size of substituents on the conformation of the polymers. The characteristics of the polymers as gas-permeable and chiral resolution membranes were also examined.

Results and Discussion

Polymerization. In general, group 5 transition metals represented by Ta(V) and Nb(V) are active for the polymerization of diphenylacetylenes.[4,7a] Especially, formation of high molecular weight polymers of diphenylacetylenes is possible by the systems composed of $TaCl_5$ and organometallic cocatalysts. Both **1** and **2** polymerized with the $TaCl_5$- or $NbCl_5$-based catalysts, and the results are summarized in Table 1. Poly(**1**) with extremely high molecular weight was obtained in good yield with $TaCl_5$–*n*-Bu_4Sn catalyst. Increase in the monomer concentration improved both the yield and molecular weight of the polymer (runs 1 and 4). It was impossible to estimate the molecular weight of poly(**1**) by GPC measurement because its molecular weight exceeded the exclusion limit of the GPC-columns. However, poly(**1**) possessed very high molecular weight beyond one million. Though the use of $NbCl_5$ as main catalyst also gave the polymer, both the yield and molecular weight decreased (run 6). Such a tendency is often observed in the polymerization of disubstituted acetylenes by group 5 transition metals.[4b] The yield of poly(**1**) increased with increasing polymerization temperature and showed a maximum value at 80 °C (runs 2–5). Both the yield and molecular weight of poly(**2**) were lower than those of poly(**1**) (runs 7–9). These results are consistent with the general feature of acetylene polymerization where *meta*-substituted diphenylacetylenes usually provide lower molecular weight polymers in lower yield than do *para*-substituted ones.[9]

Disubstituted acetylenes **3** and **4** also well polymerized with group 5 or 6 metal catalysts, and the results are listed in Table 2. Ta and Nb catalysts were found to be effective for the polymerization of **3** giving the polymers in moderate to good yields (runs 1–4). The addition of Ph_3Bi as cocatalyst enabled the production of a polymer with molecular weight over one million (run 3). In contrast, a chlorine-containing monomer, **4**, polymerized with Mo catalysts (runs 5–10). Although the

Table 1. Polymerization of **1** and **2**[a]

					polymer		
run	monomer	$[M]_0$, M	catalyst	temp., °C	yield, %[b]	$M_w/10^4$ [b,c]	$[\alpha]_D$,°[d]
1	**1**[e]	0.10	$TaCl_5$–*n*-Bu_4Sn	80	63	>100	+2350
2		0.20	$TaCl_5$–*n*-Bu_4Sn	30	61	>190	+534
3		0.20	$TaCl_5$–*n*-Bu_4Sn	60	82	>110	+1750
4		0.20	$TaCl_5$–*n*-Bu_4Sn	80	90	>130	+2480
5[f]		0.20	$TaCl_5$–*n*-Bu_4Sn	120	69	>120	+2420
6		0.20	$NbCl_5$–*n*-Bu_4Sn	80	15	>160	+1970
7	**2**[g]	0.10	$TaCl_5$–*n*-Bu_4Sn	80	40	38	+1550
8		0.20	$TaCl_5$–*n*-Bu_4Sn	80	46	71	+1540
9[h]		0.10	$NbCl_5$–*n*-Bu_4Sn	80	5	42	+1860

[a] In toluene, 24 h, [Cat] = 10 mM, [*n*-Bu_4Sn] = 20 mM. [b] Methanol-insoluble part. [c] Estimated by GPC (PSt, $CHCl_3$). [d] $c = 4.0\times10^{-3}$g/dl, $CHCl_3$. [e] $[\alpha]_D = -2.39°$ (c = 1.0 g/dl, $CHCl_3$). [f] In *o*-xylene. [g] $[\alpha]_D = -1.21°$ (c = 1.0 g/dl, $CHCl_3$). [h] 6 days.

Table 2. Polymerization of **3** and **4**[a]

			polymer		
run	monomer	catalyst	yield, %[b]	$M_W/10^4$ [b,c]	$[\alpha]_D$, ° [d]
1	**3**[e]	$TaCl_5$	48	33	+10.7
2		$TaCl_5$–*n*-Bu_4Sn	54	84	+11.0
3		$TaCl_5$–Ph_3Bi	79	132	+14.4
4		$NbCl_5$–*n*-Bu_4Sn	87	41	+16.5
5	**4**[f]	$MoCl_5$	0	–	–
6		$MoCl_5$–*n*-Bu_4Sn	86	70	+6.7
7		$MoCl_5$–Ph_4Sn	84	61	+11.0
8		$MoCl_5$–Et_3SiH	96	71	+11.1
9		$MoCl_5$–Et_3SiH[g]	88	32	+8.3
10		$Mo(CO)_6$–CCl_4–*hν*	45	110	+9.8

[a] In toluene, 24 h, [Cat] = 10 mM, [Cocat] = 20 mM, 80 °C for **3**, 30 °C for **4**. [b] Acetone-insoluble part for poly(**3**) and methanol-insoluble part for poly(**4**). [c] Estimated by GPC (PSt, $CHCl_3$). [d] c = 0.1–0.13 g/dl, $CHCl_3$. [e] $[\alpha]_D$ = –2.85° (c = 1.0 g/dl, $CHCl_3$). [f] $[\alpha]_D$ = –2.50° (c = 1.0 g/dl, $CHCl_3$). [g] In anisole.

polymerization of **4** in the absence of any cocatalyst gave only oligomers (35%, run 5), combinations of $MoCl_5$ with organometallic cocatalysts such as *n*-Bu_4Sn, Ph_4Sn and Et_3SiH were quite active for the polymerization of **4** (runs 7–9). $Mo(CO)_6$–CCl_4–*hν* provided the polymer with the highest molecular weight (run 10).

All the polymers produced were soluble in various solvents including toluene, $CHCl_3$, heptane, cyclohexane, dichloromethane, THF etc., and partly soluble in ether. The difference in the catalysts, i.e., Ta or Nb, caused no difference in solubility among poly(**1**), poly(**2**) and poly(**3**), although a little difference in solubility is observed in the case of poly[1-(trimethylsilyl)-1-propyne] by changing the catalyst.[10] Reflected by the high molecular weights, poly(**1**), poly(**2**), and poly(**3**) exhibited excellent film-forming ability; free-standing films were readily obtained by casting the polymers from toluene. Thermogravimetric analyses (TGA) in air showed the onset

temperatures of weight loss (T_0) of poly(**1**) and poly(**2**) at 319 and 326 °C, respectively, which were about 70 °C higher than that of poly(phenylacetylene). Comparison of these T_0 values with that of poly[1-phenyl-2-[*p*-(trimethylsilyl)phenyl]acetylene] (430 °C) indicates that the introduction of the pinanyl group reduces the thermal stability. Indeed, TGA displayed two stages on weight loss of poly(**1**) and poly(**2**); the first weight loss left ca. 65% of weight residue below 450 °C, which agreed well with the predicted value assuming that pinanyl group was lost first upon heating.

Conformation of Polymers in Solution. The polymers derived from **1** and **2** displayed very large optical rotations. For example, polymerization of **1** by $TaCl_5$–*n*-Bu_4Sn gave a polymer with $[\alpha]_D$ of +2480° (c = 4.3x10^{-3} g/mL, $CHCl_3$), whereas the starting monomer, **1**, showed a much smaller $[\alpha]_D$ with opposite sign [–2.39° (c = 1.0 g/mL, $CHCl_3$)]. In a similar way, **2**, which has a quite small $[\alpha]_D$ [–1.21° (c = 1.0 g/mL, $CHCl_3$)], provided a polymer having a very large $[\alpha]_D$ [+1860° (c = 4.3x10^{-3} g/mL, $CHCl_3$)]. These values are approximately three orders larger than that of poly(**5**).[8] Both CD spectra of poly(**1**) and poly(**2**) also exhibited very large molar ellipticities [θ] in the UV-visible region in $CHCl_3$ (Figure 1). The magnitude of [θ] was comparable to that of poly(phenylacetylene) with chiral menthoxycarbonyl groups[3d] and about one order larger than that of poly(**5**).[9] Since the present Cotton effects are presumably attributable to the backbone π-π* transition, these results lead to the conclusions that the main chains of poly(**1**) and poly(**2**) exist in predominantly one screw-sense and that the large optical rotations arise from the twisted conformation with an excess of one sense of the backbones.[11]

Similarly to the cases of **1** and **2**, the signs of $[\alpha]_D$ reversed after the polymerizations of **3** and **4**. However, $[\alpha]_D$ values of poly(**3**) and poly(**4**) were quite small compared with those of poly(**1**) and poly(**2**) (Table 2). For instance, when the phenyl group of **1** was changed to a small substituent (methyl group), the value of $[\alpha]_D$ was drastically reduced from +2480° to +11.0°. In a similar way, the Cotton effects of poly(**3**) and poly(**4**) were quite weak (Figure 2). It is probable that there is

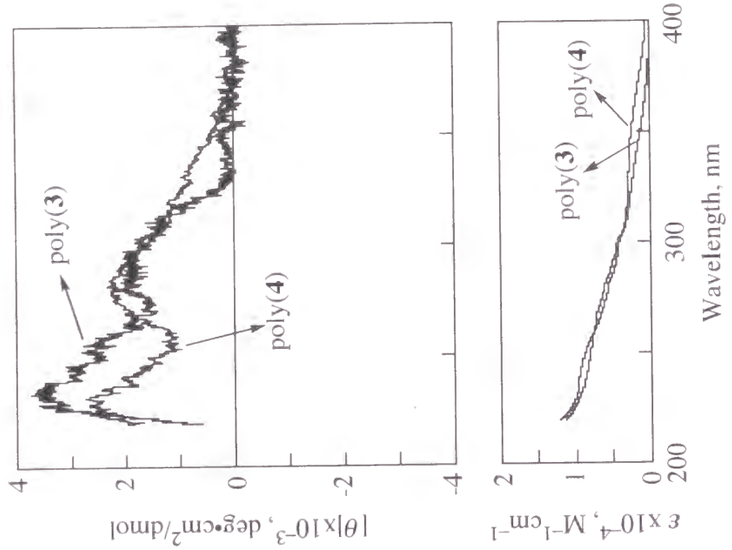

Figure 2. CD (top) and UV-visible (bottom) spectra of poly(**3**) prepared with $TaCl_5$–Ph_3Bi at 80 °C (in cyclohexane, 20 μg/mL, 25 °C) and poly(**4**) prepared with $MoCl_5$–Et_3SiH at 30 °C (in cyclohexane, 40 μg/mL, 25 °C).

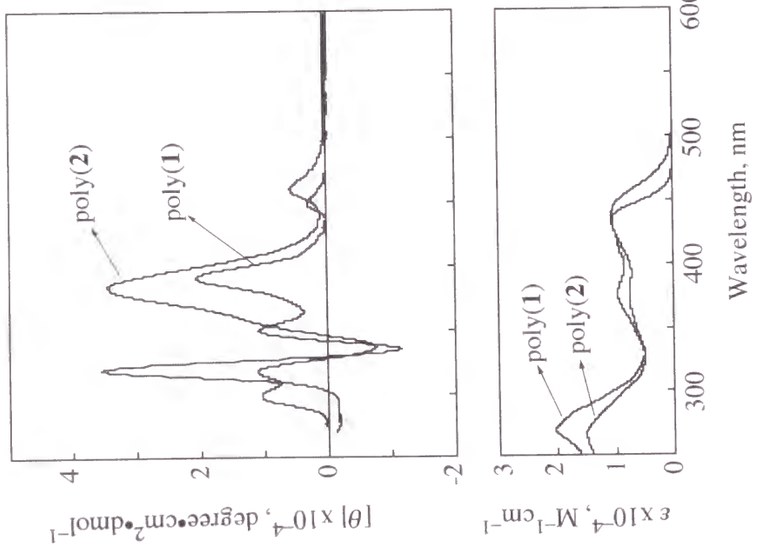

Figure 1. CD (top) and UV-visible (bottom) spectra of poly(**1**) and poly(**2**) prepared with $TaCl_5$–*n*-Bu_4Sn at 80 °C (in $CHCl_3$, 40 μg/mL, room temperature).

no significant difference in the geometrical structure among poly(**1**), poly(**2**), and poly(**3**) because they were prepared by the same catalyst. Therefore, the weak CD of poly(**3**) is not due to the difference in the geometrical structure of the polymer. Although the decrease in the conjugation between the main chain and the pendants for poly(**3**) and poly(**4**) may be a reason for the weak CD, the absence of clear Cotton effects as well as the extremely small optical rotations of poly(**3**) indicates that the helical conformation is not satisfactorily induced to poly(**3**) and poly(**4**). In other words, introduction of two aromatic side groups into the repeating unit is favorable for the induction of helical conformation to disubstituted acetylene polymers.

It is worthy to note that, as the polymerization temperature was raised, the $[\alpha]_D$ of poly(**1**) progressively increased (Table 1). A similar tendency was recognized in the CD spectra of poly(**1**); the molar ellipticities of *all* Cottons increased with increasing polymerization temperature (Figure 3). Though there is no evidence at present, this phenomenon is presumably due to the change in the steric structure of polymer backbone (cis to trans and/or head-to-head to head-to-tail) with polymerization temperature.

In general, the magnitude of the Cotton effects and the specific rotation of a helical polymer tend to decrease as the measuring temperature is raised, which is explicable by helix-to-coil transformation. Contrary to expectation, the intensity of the Cotton effects of poly(**1**) increased as its solution was heated (Figure 4). Namely, as the measuring temperature was raised from 20 to 50 °C, the signal at 390 nm gradually increased from (+) 1.7×10^4 to (+) 2.7×10^4. This enhancement of intensity was reversible, i.e., decreasing the temperature resulted in the recovery of the original value. It should be noted that the intensities of other Cottons at 320, 340, 350 and 450 nm did not change significantly over the temperature range of 20–50 °C. Such a phenomenon is unknown except the following case: in the poly(phenylacetylene) with chiral menthoxycarbonyl groups at the *para* position produced with a W catalyst, the specific rotation dramatically increased from –497° to –772° upon heating the $CHCl_3$-solution from 40 to 45 °C.[3d] On the other hand, the magnitudes of $[\theta]$ of poly(**3**) and

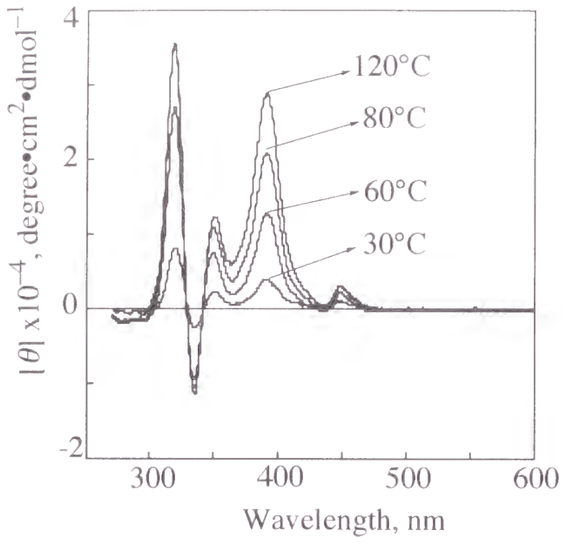

Figure 3. CD spectra of poly(**1**) prepared with $TaCl_5$–*n*-Bu_4Sn at various temperatures (in $CHCl_3$, 40 μg/mL).

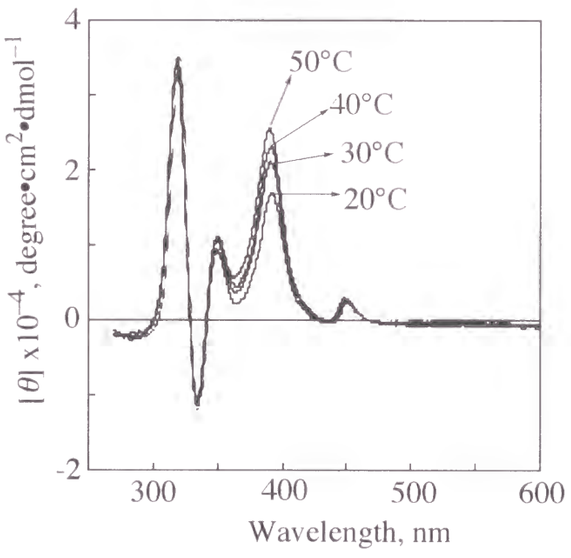

Figure 4. Various temperature CD spectra of poly(**1**) prepared with $TaCl_5$–*n*-Bu_4Sn at 80 °C (in $CHCl_3$, 40 μg/mL).

poly(**4**) slightly decreased with increasing temperature from 20 to 75 °C, similarly to the cases of chiral polyacetylenes previously reported.[3a-b] For example, the [θ] of poly(**4**) at 280 nm decreased from (+) 1900 at 20 °C to (+) 1450 at 75 °C.

These results suggest that the helical conformation of substituted poly(diphenylacetylenes) is appreciably stiff and stable in solution over the temperature range studied.

Permeability of the Polymers. Figure 5 plots the oxygen permeability coefficients (P_{O2}) versus separation factor against nitrogen (P_{O2}/P_{N2}) for poly(**1**), poly(**2**) and poly(**3**). Like most substituted polyacetylenes, the present polymers exhibited fairly large oxygen permeability. The P_{O2} of poly(**1**) is about 10 times larger than that of poly(**3**), which is consistent with the excellent gas permeability of poly(diphenylacetylene)s with round-shaped substituents. The *para*-substituted poly(**1**) exhibited a P_{O2} value 10 times larger than that of the *meta*-substituted counterpart, poly(**2**). The P_{O2} values of poly(**1**) and poly(**2**), however, were ca. one and two orders, respectively, lower than those of the corresponding poly-

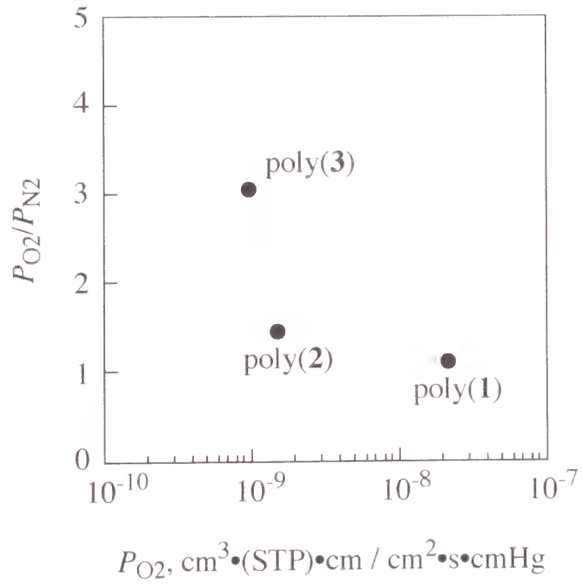

Figure 5. Plot of the separation factor against nitrogen (P_{O2}/P_{N2}) versus the oxygen permeability coefficients (P_{O2}) for poly(**1**), poly(**2**), and poly(**3**).

(diphenylacetylene)s with trimethylsilyl groups and comparable to those of poly(diphenylacetylene)s having dimethylisopropylsilyl groups.[9a]

Poly(**1**), poly(**2**), and poly(**3**) had enantioselectivities in the permeation of racemic tryptophan as shown in Figure 6. The decreasing order of P is Poly(**1**) > poly(**2**) > poly(**3**), while the decreasing order of α^R is poly(**3**) > poly(**2**) > poly(**1**). In other words, the selectivity increases with the decrease of the permeability in this enantiomer permeation. This behavior is the same as in the relationship between P_{O2} and P_{O2}/P_{N2} (Figure 5). Among the three disubstituted acetylene polymers, poly(**3**) displayed the highest selectivity (α^R= 3.16) which is comparable to that of poly(**5**).[8] The enantiomeric excess (%ee) increased from 0%ee to 51.9%ee after an initial period in the permeation of the racemic tryptophan solution through a poly(**3**) membrane (see the solid lines in the left graph and the right chromatogram (a) and (c) in Figure 7). Furthermore, a complete optical resolution was achieved at the initial period of the permeation (see the right chromatogram (b) in Figure 7).

Although poly(**3**) had much smaller $[\theta]$ and $[\alpha]_D$ values than poly(**1**) and poly(**2**), the former showed the best enantioselectivity. This is probably because poly(**1**) and poly(**2**) possess a stiffer structure than poly(**3**). Namely, compared with poly(**3**), both poly(**1**) and poly(**2**) are stiff owing to their bulky substituents and higher extents of helical conformation, so that the membranes of poly(**1**) and poly(**2**) may have more and larger molecular-scale voids. Indeed, the membranes of poly(**1**) and poly(**2**) were more brittle than that of poly(**3**). Hence high gas permeability and essentially no permselectivity were obtained when poly(**1**) and poly(**2**) were employed. Similarly, the presence of many molecular-scale voids in the membranes of poly(**1**) and poly(**2**) may achieve high permeation of the racemate and reduce the effect of the helical conformations. In other words, chiral environment originating from the helical conformations of polymers does not seem to improve the enantioselectivity if the polymer membranes have many molecular-scale voids.

In summary, a new example for the synthesis of disubstituted acetylene polymers having chiral pendant groups has been demonstrated. Satisfactorily high

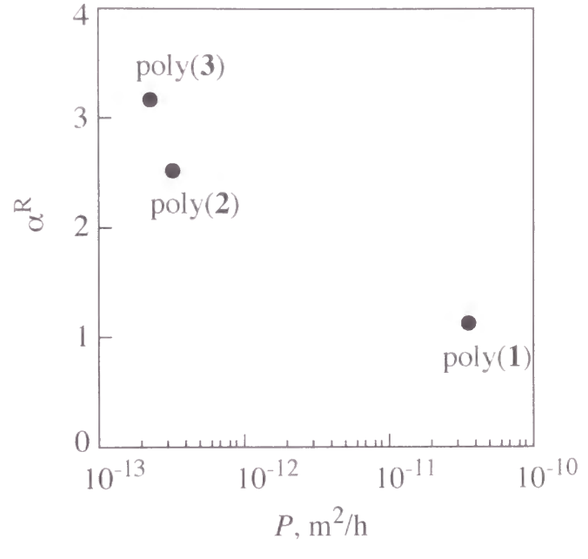

Figure 6. Plot of enantioselectivities (α^R) versus total permeability coefficients (P) in concentration-driven permeation of 0.5 wt% tryptophan (aqueous) for poly(**1**), poly(**2**), and poly(**3**).

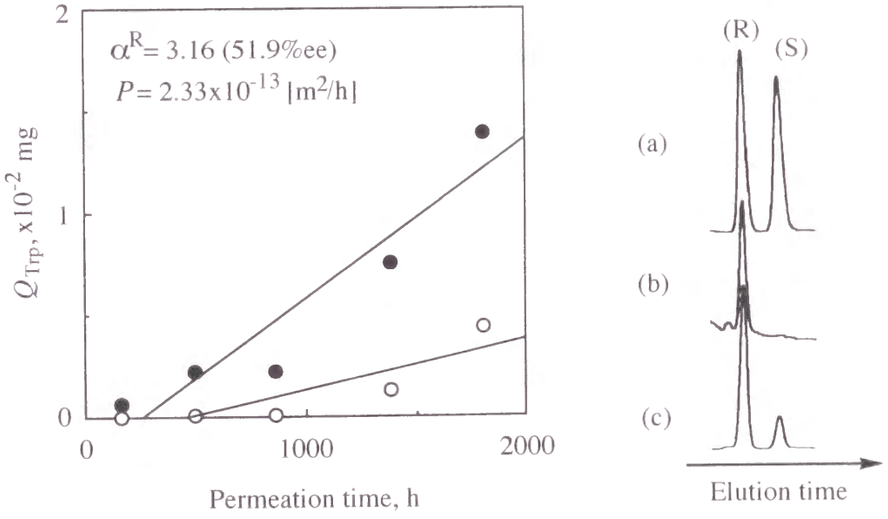

Figure 7. (Left) Plots of quantity (Q_{Trp}) of permeated R-(+)-(●)- and S-(–)-(○)-tryptophan (Trp) from 0.50 wt% racemic aq. solution *vs.* permeation time through a poly(**3**) membrane in concentration-driven permeation: (Right) HPLC chromatogram of Trp: (a) racemic Trp (feed); (b and c) Trp in the permeate at an initial period (160–497 h) and at a later (862–1385 h), respectively. Column, CROWNPAK-CR; eluent, $HClO_4$(aq).

molecular weight polymers with excellent solubility as well as good film-forming ability were readily accessible by the polymerization of diphenylacetylenes with chiral pinanyl groups. The polymers showed quite large optical rotations and intense CDs, which suggests helical conformations with an excess of one-handed screw-sense. Increase in the temperature caused no decrease in the intensity of the Cotton effects of poly(**1**) and poly(**2**), which means that the present poly(diphenylacetylene)s exist in fairly stable helical conformations. The produced polymers achieved enantio-selective permeation of racemic tryptophan. The author believes that appropriate design of chiral pendants of diphenylacetylenes offers advanced polymeric membranes for the separation of racemic compounds.

Experimental Section

Materials. All the solvents used were distilled by the standard procedures. $TaCl_5$, $NbCl_5$, $MoCl_5$, Ph_3Bi and $Mo(CO)_6$ were used as received. *n*-Bu_4Sn and Et_3SiH were distilled by the usual manners and used as toluene solutions (200 mmol/L). All the reagents in monomer synthesis were used as purchased without further purification unless specified. (–)-Chlorodimethyl(10-pinanyl)silane (**6**) was

Scheme 1

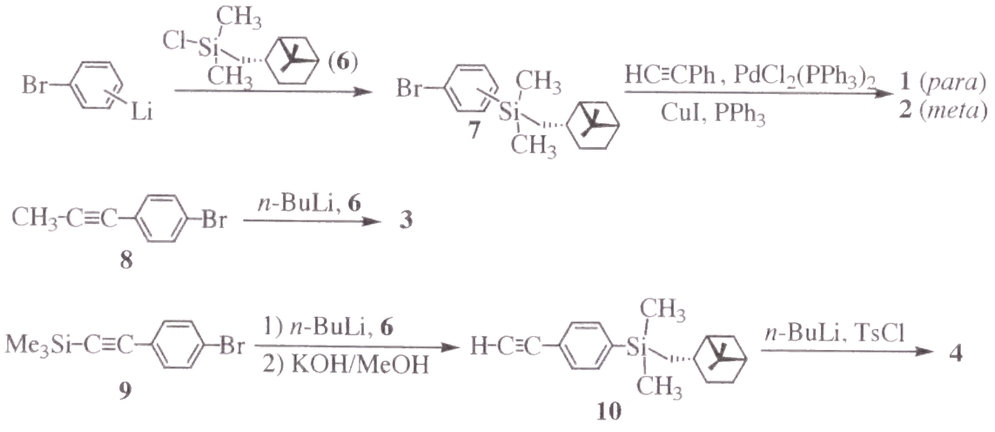

prepared by the reported manner.[8,12] 1-(4-Bromophenyl)-1-propyne (**8**)[13] and 1-(4-bromophenyl)-2-trimethylsilylacetylene (**9**)[14] were prepared by the Pd-catalyzed coupling of 4-iodo-1-bromobenzene with propyne and 1-trimethylsilylacetylene, respectively, with reference to the reported methods. Synthetic routes to these monomers are illustrated in Scheme 1.

Measurements. The molecular weights of the polymers were estimated by GPC ($CHCl_3$ as an eluent, polystyrene calibration). Measurements of IR and UV-visible spectra and TGA were carried out in the same way as in Chapter 1. NMR spectra were obtained by using JEOL GSX-270 and JNM-LA500 spectrometers. CD spectra were measured with a Jasco J-600 spectropolarimeter. Specific rotations were recorded with a Jasco DIP-1000 digital polarimeter.

Syntheses of 1 and 2: A hexane solution of *n*-BuLi (1.53 M, 58.8 mL) was added slowly to a solution of 1,4-dibromobenzene (21.2 g, 90.0 mmol) in dry Et_2O (60 mL) at 0 °C. After stirring for 1.5 h at 0 °C, **6** (20.8 g, 90.0 mmol) was added dropwise, and the solution was stirred for 3 h at 0 °C. The formed salt was removed by filtration and the filtrate was washed with water. The organic layer was dried over Na_2SO_4, concentrated, and distilled at 135–138 °C (0.5 mmHg) to yield (–)-1-[dimethyl(10-pinanyl)silyl]-4-bromobenzene (**7**, 16.8 g, 53.2%). A solution of **7** (4.42 g, 12.6 mmol) in dry Et_3N (20 mL) was added to a mixture of triphenylphosphine (77 mg, 0.29 mmol), dichlorobistriphenylphosphinepalladium (34 mg, 0.048 mmol), and cuprous iodide (46 mg, 0.24 mmol) in Et_3N (80 mL). To this mixture was added phenylacetylene (1.4 mL, 13 mmol). The mixture was heated at 90 °C and refluxed for 4 h. The resulting mixture was filtered and concentrated. The product was purified by a flash column chromatography (SiO_2, hexane) to give **1** as a white solid in a 42% yield based on **7**. All the above procedures concerning reactions were performed in nitrogen. mp 43–47 °C. ^{1}H NMR ($CDCl_3$) δ 7.60–7.28 (m, 5H), 7.49 (2d, 4H), 2.20–0.62 (m, 11H), 1.14 (s, 3H), 0.76 (s, 3H), 0.28 (s, 6H); ^{13}C NMR ($CDCl_3$) δ 140.9, 133.4, 131.6, 130.6, 128.3, 128.2, 123.3, 89.7, 89.6, 49.2, 40.6, 39.5, 31.1, 26.9, 25.5, 24.7, 23.9, 23.0, 20.0, 1.9, 2.0; IR (KBr)

3072, 3036, 2988, 2224, 1600, 1500, 1252, 1102 cm^{-1}. Anal. Calcd for $C_{26}H_{32}Si$: C, 83.81; H, 8.66. Found: C, 83.66; H, 8.76. **2** (viscous liquid) was prepared from 1,3-dibromobenzene instead of 1,4-dibromobenzene in a similar manner. Yields: 41% (based on the meta-isomer of **7**) and 15% (based on 1,3-dibromobenzene). ^1H NMR ($CDCl_3$) δ 7.68–7.28 (m, 9H), 2.20–0.65 (m, 11H), 1.15 (s, 3H), 0.77 (s, 3H), 0.29 (s, 6H); ^{13}C NMR ($CDCl_3$) δ 140.6, 136.6, 133.2, 131.73, 131.67, 131.6, 128.3, 128.2, 127.6, 127.5, 123.4, 122.6, 89.8, 89.2, 49.2, 40.6, 39.5, 31.1, 26.9, 25.6, 24.8, 23.8, 20.0, 1.8, 2.0; IR (neat) 3064, 2912, 2868, 2224, 1602, 1496, 1252, 1112 cm^{-1}. Anal. Calcd for $C_{26}H_{32}Si$: C, 83.81; H, 8.66. Found: C, 82.20; H, 8.79.

Synthesis of 3: 1-(4-Lithiophenyl)-1-propyne was prepared by adding 35.2 mmol of *n*-BuLi (22 mL of a 1.60 M solution in hexane) to a solution of 6.40 g of **8** (33.0 mmol) in dry Et_2O at –78 °C under nitrogen. After 1 h, a solution of **6** (7.65 mL, 32.5 mmol) in dry Et_2O (80 mL) was added dropwise to the solution of 1-(4-lithiophenyl)-1-propyne at –78 °C, and the solution was gradually warmed to room temperature. After stirring for 5 h, water was added to the reaction mixture. The organic layer was separated, and the aqueous layer was extracted with Et_2O. The combined ether layer was dried over $MgSO_4$, filtered and concentrated. The crude product was purified by a flash column chromatography (SiO_2, cyclohexane) to give **3** as a colorless liquid. Yield (based on **8**): 37%. ^1H NMR($CDCl_3$) δ 7.40 (d, 2H, J = 7.81 Hz), 7.34 (d, 2H, J = 7.81 Hz), 2.04 (s, 3H), 1.13 (s, 3H), 0.74 (s, 3H), 0.63–2.15 (m, 11H), 0.245 (s, 3H), 0.242 (S, 3H); ^{13}C NMR($CDCl_3$) δ 139.8, 133.3, 130.5, 124.1, 86.1, 79.8, 49.2, 40.6, 39.4, 31.1, 26.8, 25.5, 24.7, 23.8, 22.9, 19.9, 4.3, –1.9, –2.1; IR (neat) 3065, 2980, 2247, 1250, 1107, 837, 820 cm^{-1}. Anal. Calcd for $C_{21}H_{30}Si$: C, 81.21; H, 9.73. Found: C, 81.46; H, 9.84.

Synthesis of 4: **9** was lithiated by the slow addition of a 1.60 M solution of *n*-BuLi in hexane (25 mL, 40.0 mmol) into a dry Et_2O solution of **9** (9.2 g, 36 mmol) at –78 °C under nitrogen, which was followed by the additional stirring for 1 h. Into the solution was added dropwise **6** (8.6 mL, 36 mmol) in dry Et_2O (80 mL), and the reaction mixture was gradually warmed to room temperature over 2 h. Quenching

with water and ethereal working-up gave the crude product which was subjected to desilylation by treating with KOH (ca. 2 g) in methanol (10 mL) at room temperature for 30 min. This solution was concentrated with a rotary evaporator, and the residue was dissolved in Et_2O. The ether layer was washed with brine and then water, dried over $MgSO_4$, concentrated and purified by a flash column chromatography (SiO_2, hexane) to give (–)-4-[dimethyl-(10-pinanyl)silyl]-1-ethynylbenzene (**10**) as a colorless liquid (8.5 g, 94%). Into a dry Et_2O solution (70 mL) of **10** (8.5 g, 29 mmol) was added dropwise a 1.60 M solution of *n*-BuLi in hexane (18 mL, 29 mmol) at –78 °C, and the solution was stirred for an additional 1 h. Into this solution, *p*-toluenesulfonyl chloride (6.6 g, 35 mmol) in dry Et_2O (30 mL) was slowly added, and then the cooling bath was removed. After stirring for 4 h, the reaction was quenched by adding water. Ethereal working-up and purification by a flash column chromatography (SiO_2, hexane) gave **4** as a colorless liquid (3.3 g, 80%). ^1H NMR ($CDCl_3$) δ 7.38 (d, 2H, J = 7.35 Hz), 7.34 (d, 2H, J = 7.35 Hz), 1.13 (s, 3H), 0.74 (s, 3H), 0.63–2.14 (m, 11H), 0.252 (s, 3H), 0.249 (s, 3H); ^{13}C NMR ($CDCl_3$) δ 141.4, 133.4, 130.9, 122.2, 69.5, 68.2, 49.1, 40.5, 39.4, 31.0, 26.8, 25.5, 24.7, 23.7, 22.9, 19.9, –1.9, –2.2; IR (neat) 3067, 2980, 2220, 1250, 1103, 837, 818 cm^{-1}. Anal. Calcd for $C_{20}H_{27}SiCl$: C, 72.58; H, 8.22; Cl, 10.71. Found: C, 72.30; H, 8.25; Cl, 11.00.

Polymerization. Polymerizations were carried out as described in Chapter 1. The detailed polymerization conditions were indicated in the Tables. The polymers were isolated by reprecipitation into an excess of methanol or acetone, and the yields were determined by gravimetry.

Membrane Preparation. A 1–2 wt% (w/v) solution of a polymer in $CHCl_3$ was cast on a poly(tetrafluoroethylene) sheet, and the solvent was evaporated for 24 h at room temperature. The resulting solid membrane was detached from the sheet and dried in vacuo for 24 h. Thickness, 15.2–54.8 μm; area, $3.14x10^{-4}$ m^2 for air permeation, 5.72 or $6.15x10^{-4}$ m^2 for tryptophan solution permeation.

Measurements of Permeability of Gases and Amino Acid. Oxygen and nitrogen permeability coefficients (P_{O2} and P_{N2}: cm^3•(STP)•cm / cm•s•cmHg) were

measured by the gas chromatographic method using a YANAKO GTR-10 apparatus. Concentration-driven enantioselective permeations of aqueous tryptophan solution were measured by using a disproportionate two-chamber glass cell at 25 °C. To maintain constant the difference of the concentration (0.5 wt%) between the feed and permeate sides, the solution in the permeate-side chamber was exchanged by pure water before more than 1% of the solute in the feed had permeated. The permeated quantity was determined by analyzing aliquots on a HPLC equipped with a CROWNPAK CR column (diameter 4 mm, length 15 cm; Daicel Chemical Co). Enantiomer permeability coefficients (P_R and P_S) were estimated from the slope of the permeated quantity-permeation time. Enantioselectivities (α^R) and total permeability coefficients (P) were calculated from $\alpha^R = P_R / P_S$ and $P = P_R + P_S$, respectively.

References and Notes

1) For reviews of helical polymer syntheses, see: a) Okamoto, Y.; Nakano, T. *Chem. Rev.* **1994**, *94*, 349. b) Nolte, R. J. M. *Chem. Soc., Rev.* **1994**, 11. c) Qin, M.; Bartus, J.; Vogl, O. *Macromolecular Symposia* **1995**, *98*, 387.

2) a) Drenth, W.; Nolte, R. J. M. *Acc. Chem. Res.* **1979**, *12*, 30. b) Pu, L. *Acta Polym.* **1997**, *48*, 116.

3) For selected examples for chiral polyacetylenes, see: a) Ciardelli, F.; Lanzillo, S.; Pieroni, O. *Macromolecules* **1974**, *7*, 174. b) Moore, J. S.; Gorman, C. B.; Grubbs, R. H. *J. Am. Chem. Soc.* **1991**, *113*, 1704. c) Yamaguchi, M.; Omata, K.; Hirama, M. *Chem. Lett.* **1992**, 2261. d) Aoki, T.; Kokai, M.; Shinohara, K.; Oikawa, E. *Chem. Lett.* **1993**, 2009. e) Kishimoto, Y.; Itou, M.; Miyatake, T.; Ikariya, T.; Noyori, R. *Macromolecules* **1995**, *28*, 6662. f) Yashima, E.; Matsushima, T.; Okamoto, Y. *J. Am. Chem. Soc.* **1997**, *119*, 6345.

4) For reviews of polymerization of acetylenic monomers, see: a) Masuda, T. In *Catalysis in Precision Polymerization;* Kobayashi, S., Ed.; Wiley: Chichester, 1997; p 67. b) Masuda, T. In *The Polymeric Materials Encyclopedia*; Salamone, J. C., Ed.; CRC Press: Florida, 1996; p 32. c) Shirakawa, H.; Masuda, T.; Takeda, K. In *The Chemistry of Triple-Bonded Functional Groups (supplement C2)*; Patai, S., Ed.; Wiley: Chichester, 1994; p 945. d) Costa, G. In *Comprehensive Polymer Science*; Eastmond, G. C., Ledwith, A., Russo, S., Sigwalt, P., Eds.; Pergamon Press: Oxford, 1989; p 155.

5) a) Masuda, T.; Deng, Y. X.; Higashimura, T. *Bull. Chem. Soc. Jpn.* **1983**, *56*, 2798. b) Masuda, T.; Okano, Y.; Tamura, K.; Higashimura, T., *Polymer* **1985**, *26*, 793.

6) For example, decomposition of *cis-transoidal* poly(phenylacetylene) produced with a Rh catalyst is so rapid that the M_n values estimated by GPC with $CHCl_3$ eluent are not reproducible. A similar degradation also takes place in other solvents such as THF although the rate is low.

7) For reviews for gas-permeable polymer membranes, see: a) Masuda, T.; Teraguchi, M.; Nomura, R. In *Polymer Membranes for Gas and Vapor Separation*: *Chemistry and Materials Science*; Freeman, B. D., Pinnau, I., Eds.; ACS Symp. Ser. 733; Am. Chem. Soc.: Washigton, DC, 1999; Chapter 2. b) Kesting, R. E.; Fritzsche, A. K. *Polymeric Gas Separation Membranes*; Wiley: New York, 1993. c) Stern, S. A. *J. Membr. Sci.* **1994**, *94*, 1. d) Cabasso, I. In *Encyclopedia of Polymer Science and Engineering 1*, 2nd ed.; Kroschwitz, J. I., Ed.; Wiley: New York, 1987; p 509. e) Aoki, T.; Oikawa, E. In *The Polymeric Materials Encyclopedia*; Salamone, J. C., Ed.; CRC Press: Florida, 1996; p 6492.

8) Aoki, T.; Shinohara, K.; Kaneko, T.; Oikawa, E. *Macromolecules* **1996**, *29*, 4192.

9) a) Tsuchihara, K.; Masuda, T.; Higashimura, T. *J. Polym. Sci., Part A: Polym. Chem.* **1993**, *31*, 547. b) Tsuchihara, K.; Masuda, T.; Higashimura, T. *Macromolecules* **1992**, *25*, 5816. c) Ito, H.; Masuda, T.; Higashimura, T. *J. Polym. Sci., Part A: Polym. Chem.* **1996**, *34*, 2925.

10) Izumikawa, H.; Masuda, T.; Higashimura, T. *Polym. Bull.* **1991**, *27*, 193.

11) The shape of CD spectrum of poly(**1**) significantly differs from that of poly(**2**), and the magnitude of [θ] of poly(**2**) around 380 nm was approximately 1.7 times as large as that of poly(**1**). On the other hand, the CD intensity of poly(**1**) around 300 nm was much larger than that of poly(**2**).

12) The stereochemistry of the monomers was determined by the NOE enhancement in the ^{1}H NMR of **5** as shown below. Irradiation of the methyl protons (a) at 0.82 ppm caused an NOE enhancement of the signal attributable to the proton (b) at 2.19 ppm, whereas no NOE enhancement was detected for the methylene protons (c) at 0.52–0.69 ppm. (Scheme for ref. 12)

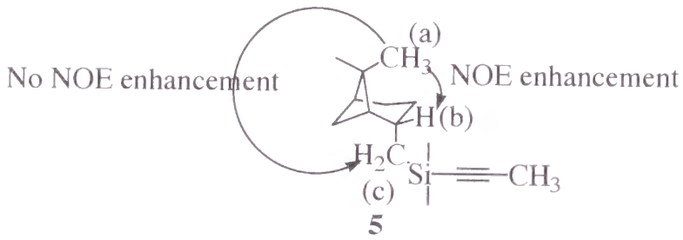

5

13) Chang, T. L.; Holzknecht, L. J.; Mark, J. H. B.; Ridgway, T. H.; Zimmer, H. *J. Polym. Sci., Polym. Chem.* **1989**, *27,* 989.

14) Takahashi, S.; Kuroyama, Y.; Sonogashira, K.; Hagihara, N. *Synthesis* **1980**, 627.

Part II

Synthesis and Properties of Novel Functional Substituted Polyacetylenes

Chapter 4

Copolymerization and Copolymer Properties of 1-[*p*-(Pentaphenyl)phenyl]-2-phenylacetylene

Abstract

Copolymerization of a diphenylacetylene having hexaphenylbenzene group, 1-[*p*-(pentaphenyl)phenyl]-2-phenylacetylene (**1**), with a few other diphenylacetylene derivatives (i.e., diphenylacetylene, 1-phenyl-2-[*p*-(trimethylsilyl)phenyl]acetylene, 1-phenyl-2-(*p*-*n*-octylphenyl)acetylene, (**2a–c**, respectively) and properties of the formed copolymers were investigated. No polymer was obtained in homopolymerization of **1** with $TaCl_5$–*n*-Bu_4Sn catalyst owing to steric hindrance. On the other hand, copolymerization with **2a–c** proceeded at various feed mole ratios to give copolymers in moderate yields. Copoly(**1/2a**) (feed ratio 25/75) was soluble in toluene and $CHCl_3$ and its weight-average molecular weight (M_w) was ca. $31x10^4$ and relatively high. Copoly(**1/2b**) and copoly(**1/2c**) (both feed ratios 5/95) were soluble in common organic solvents, and had a large M_w up to ca. $1x10^6$. These copolymers were yellow to orange solids. Oxidative cyclodehydrogenation of hexaphenylbenzene groups in copoly(**1/2a**) was attempted to convert them to more conjugated groups.

Introduction

Hexaphenylbenzene can be synthesized in quantitative yield by Diels-Alder reaction of 2,3,4,5-tetraphenylcyclopentadienone with diphenylacetylene, followed by aromatization accompanying elimination of carbon monoxide. This reaction has been utilized to polycycloaddition of bis(cyclopentadienone) derivatives with diacetylenes to synthesize various phenyl-substituted poly(phenylene).[1]

Recently Müllen and coworkers have reported that hexaphenylbenzene derivative undergoes cyclodehydrogenation under a mild condition to become hexa-*peri*-hexabenzocoronene.[2] This compound is a fused aromatic ring with a highly conjugated system. Incorporation of the hexa-*peri*-hexabenzocoronene into polymers and properties and functions of the formed polymers are very interesting. However, synthesis of polymers containing hexa-*peri*-hexabenzocoronene moieties has hardly been attempted.[3]

Substituted polyacetylenes are known as conjugated polymers and have alternating carbon-carbon double bonds in the main chain.[4] Among them, poly(diphenylacetylene) is infusible and insoluble in any solvent. This polymer, however, possesses interesting characteristics. For instance, all the carbons involved are sp^2 carbons, and the polymer is fairly thermally stable (the onset temperature of weight loss in air (T_0) is ca. 500 °C).[5] Meanwhile, diphenylacetylenes with bulky ring substituents give polymers in high yields, which are completely soluble in common organic solvents. Interestingly, the formed polymers have extremely high

Scheme 1

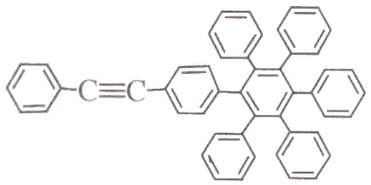

1

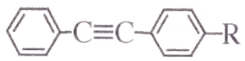

2a: R = H
2b: R = Me_3Si
2c: R = *n*-Oct

molecular weight (M_w > 1x10^6) and can afford tough free-standing films.[6] Such properties, i.e., solubility, thermal stability and film-forming ability, are important to find practical applications. Recently it has been found that some poly(diphenylacetylene) derivatives show intense electroluminescence and photoluminescence.[7]

In this chapter, copolymerizations of diphenylacetylene having hexaphenylbenzene (**1**) with some diphenylacetylenes and properties of the formed copolymers were investigated. The comonomers used were diphenylacetylene (**2a**), 1-phenyl-2-[*p*-(trimethylsilyl)phenyl]acetylene (**2b**), and 1-phenyl-2-(*p*-*n*-octylphenyl)acetylene (**2c**) (Scheme 1). Conversion of the hexaphenylbenzene moiety in copolymer into a more conjugated group was attempted by applying the oxidative cyclodehydrogenation reaction.

Results and Discussion

Copolymerization of Diphenylacetylene Having Hexaphenylbenzene Group. Table 1 summarizes the results of the copolymerization of **1** with diphenylacetylenes **2a–c**. No polymer was obtained in the homopolymerization of **1** by $TaCl_5$–*n*-Bu_4Sn (run 1). This result is attributable to the steric hindrance of **1**. On the other hand, copolymerization of **1** with **2a** proceeded at various feed mole ratios to give copolymers in relatively good yields. The copolymer obtained in run 3 (**1**/**2a** in the feed = 25/75) was soluble in $CHCl_3$ and its M_w reached a relatively large value of 31x10^4. A free-standing film could be fabricated by solution casting. On the other hand, when **1** was 20 mol% in the feed, the copolymer was insoluble (run 4), which is compatible with the finding that poly(**2a**) is insoluble in any solvent. Since poly(**2b**) and poly(**2c**) are completely soluble in common organic solvents unlike poly(**2a**), it is expected that use of **2a** and **2c** as comonomers is effective in enhancing copolymer solubility. When copolymerizations were carried out at a feed mole ratio of **1**/**2b**, **2c** = 5/95 (runs 6, 7), copoly(**1**/**2b**) and copoly(**1**/**2c**) were obtained in good yields, and were completely soluble in toluene and $CHCl_3$. Their M_w values were as high as ca. 1 x10^6 and free-standing films could be fabricated.

Table 1. Copolymerization of **1** (M_1) with **2a–c** (M_2) by $TaCl_5$–*n*-Bu_4Sn at Various Feed Ratios[a]

run	M_1 in feed	$[M]_{0,total}$	convn. of M_2	polymer[b]		
	mol%	M	%	yield, wt%	$M_w/10^3$[c]	$M_n/10^3$[c]
			comonomer: **2a**			
1	100	0.050	–	0	–	–
2	50	0.10	79	16	73	36
3	25	0.10	62	17	310	190
4	20	0.20	71	45	insoluble	
5	0	1.0	100	71	insoluble	
			comonomer: **2b**			
6[d]	5	0.20	100	61	1100	200
			comonomer: **2c**			
7[d]	5	0.20	100	62	1000	200

[a] Polymerized in toluene at 80 °C for 24 h; $[TaCl_5]$ = 10 mM, [*n*-Bu_4Sn] = 20 mM. [b] Methanol-insoluble product. [c] By GPC. [d] $[TaCl_5]$ = 20 mM, [*n*-Bu_4Sn] = 40 mM.

Structure and Properties of Copolymers. In the IR spectrum of the present copolymers, no absorption was observed around 2200 cm^{-1} ($\nu_{C\equiv C}$) which is seen in the monomers. Otherwise, the spectra of the copolymers were close to superpositions of the spectra of **1** and the comonomers. ^1H NMR spectra showed only very broad signals due to the high viscosity of copolymer solutions because of their high molecular weight, and no useful information was available.

Figure 1 depicts the UV-visible spectra of **1** and copoly(**1/2c**). Copoly(**1/2c**) has two absorption maxima in the region of 370–450 nm, and the cutoff wavelength is ca. 460 nm. All the copolymers show similar spectra, and they are basically the same as those of other poly(DPAs) reported before.[6] These spectra correspond to the yellow to orange color of the copolymers.

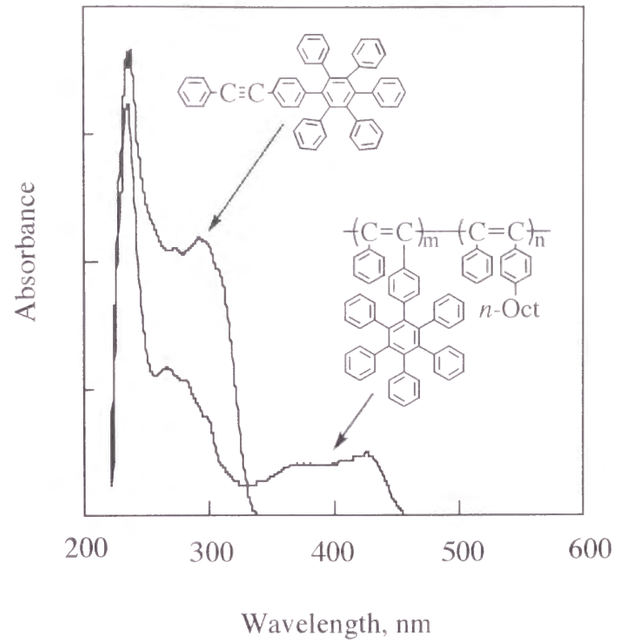

Figure 1. UV-visible spectra of **1** and copoly(**2a/c**) (in THF).

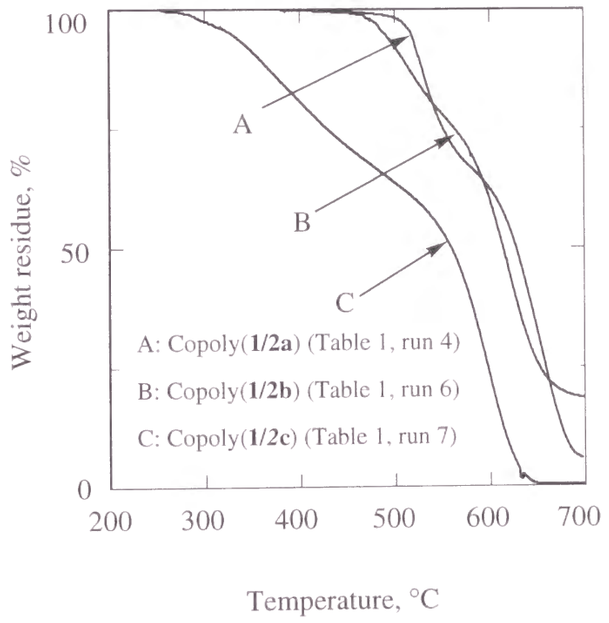

Figure 2. TGA curves of the copoly(**1/2c**) (heating rate 10 °C/min, in air).

Scheme 2. Oxidative cyclodehydrogenation of copoly(**1/2a**) (Table 1, run 3).

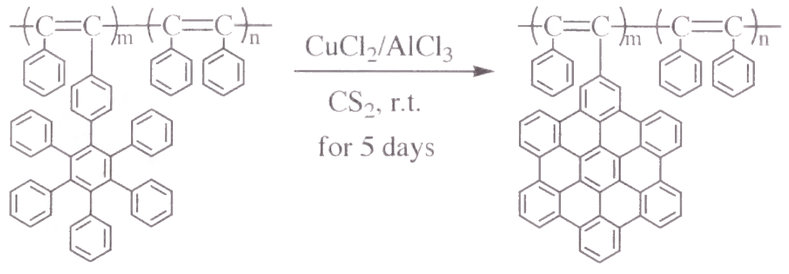

(feed mole ratio 25:75)
soluble
orange-colored solid

quantitative yield
insoluble
brown-colored solid

Thermogravimetric analyses (TGA) of the present copolymers were conducted in air (Figure 2). Copoly(**1/2a**) (run 4) and copoly(**1/2b**) (run 6) were fairly thermally stable, and no weight loss was observed up to ca. 420 °C. On the other hand, copoly(**1/2c**) (run 7) began to lose weight at 260 °C, and hence the *n*-octyl group proves to considerably reduce the thermal stability.

Copoly(**1/2a**) was subjected to the oxidative cyclodehydrogenation reaction under the conditions shown in Scheme 2. The reaction proceeded to give an insoluble dark-brown product. Thus, the solubility and color of the polymer were considerably changed with this reaction. Similar changes were observed with the same reaction of a vinyl copolymer containing hexaphenylbenzene moieties.[3a] These features indicate that the cyclodehydrogenation reaction has proceeded with copoly(**1/2a**) as well.

Experimental

Materials. *n*-Bu_4Sn was commercially obtained and distilled twice over CaH_2 before use. $TaCl_5$ was used as received. **2a** was purchased and purified by sublimation, and **2b** was prepared by the method reported in the literature.[6b] **1** and **2c** were synthesized with reference to the literature according to Scheme 3.[3a,6a]

Scheme 3

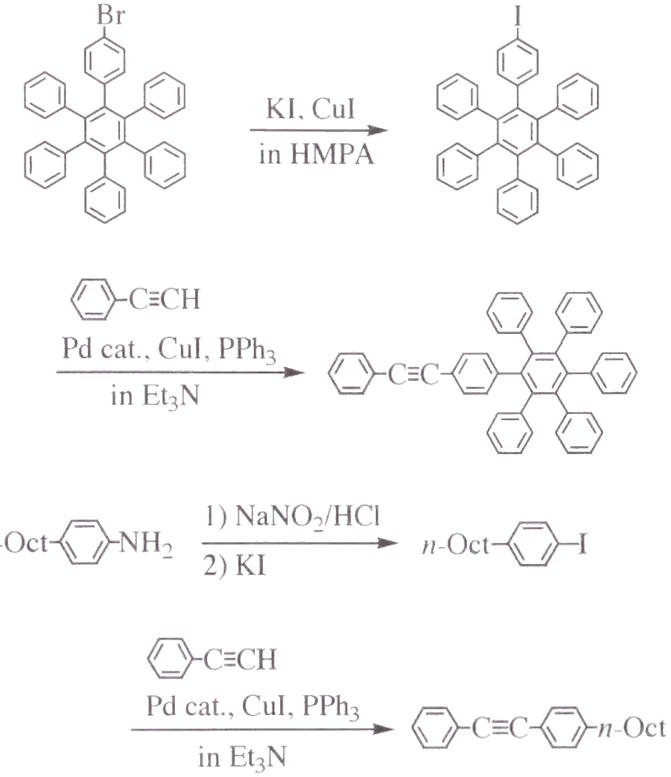

Synthesis of monomer 1: (4-Bromophenyl)pentaphenylbenzene, the starting material, was prepared according to reference.[3a] Since the corresponding iodide undergoes the following coupling reaction much faster than this bromide, the latter compound was converted to the former, i.e., the iodide.[8] Then the coupling reaciton of the iodide with phenylacetylene was carried out. The detailed procedures are as follows: A mixture of the bromide (2.7 g, 4.4 mmol), KI (7.8 g, 47 mmol), CuI (4.2 g, 22 mmol), and hexamethylphosphoric triamide (HMPA) (40 mL) was stirred for 6 h at 200 °C under nitrogen. The reaction was monitored by ^{1}H NMR (the peaks at 6.98 and 6.68 ppm of the bromide diminished and new peaks of the iodide appeared at 7.18 and 6.59 ppm). The reaction mixture was cooled to room temperature and the reaction was quenched by the addition of 2N HCl aq. (100 mL). Subsequently the mixture was poured into benzene (200 mL). The organic layer was washed with

water (3x70 mL) and dried over anhydrous Na_2SO_4. Benzene was evaporated to afford pale yellow solid (the crude product was used in the following reaction without further purification). A mixture of the crude iodide (2.5 g), phenylacetylene (0.45 g, 4.4 mmol), $(Ph_3P)_2PdCl_2$ (31 mg, 0.044 mmol), Ph_3P (47 mg, 0.18 mmol), CuI (50 mg, 0.26 mmol), and Et_3N (0.8 mL, 6.6 mmol) in toluene (50 mL) was stirred under dry nitrogen at 80 °C for 7 h. After the reaction had been finished (the completion was confirmed by ^1H NMR), the insoluble salt was filtered off and the salt was washed with toluene. The filtrate was washed with 2N HCl aq. and water, and dried over anhydrous Na_2SO_4. Toluene was evaporated and the crude product was purified by both flash column chromatography (silica gel; eluent: a gradient from hexane/toluene 4/1 to hexane/toluene 1/1) and recrystallization to give white solid. Overall yield 43% (based on bromide). IR (KBr) 3083, 3058, 3027, 1945, 1875, 1802, 1750, 1601, 1578, 1509, 1497, 1443, 1399, 1075, 1028, 911, 847, 810, 756, 735, 698, 583, 563, 544 cm^{-1}; ^1H NMR ($CDCl_3$) δ 7.46–7.40 (m, 2H), 7.33–7.27 (m, 3H), 7.07–7.02 (d, 2H), 6.94–6.80 (m, 27H); ^{13}C NMR ($CDCl_3$) δ 141.08, 140.59, 140.46, 140.40, 140.30, 140.17, 139.56, 131.41, 131.33, 130.00, 128.26, 128.04, 126.76, 126.58, 125.39, 125.23, 123.29, 119.72, 89.78, 88.91.

***Synthesis of monomer 2c*:** **2c** was prepared from 4-*n*-octylaniline as starting material by the same method as for the *n*-Bu analog reported in reference[6a]; colorless oil, overall yield 67%. IR (neat) 3031, 2926, 2855, 2218, 1597, 1512, 1487, 1466, 1443, 1377, 1071, 912, 831, 754, 691 cm^{-1}; ^1H NMR ($CDCl_3$) δ 7.55 (d, 2H, aromatic), 7.46 (d, 2H, aromatic), 7.35 (m, 3H, aromatic), 7.18 (d, 2H, aromatic), 2.61 (t, 2H), 1.69–1.55 (m, 2H), 1.40–1.21 (m, 10H), 0.91 (t, 3H); ^{13}C NMR ($CDCl_3$) δ 143.42, 131.52, 131.48, 128.44, 128.28, 128.02, 123.47, 120.32, 89.58, 88.69, 35.91, 31.87, 31.26, 29.45, 29.25, 22.67, 14.11.

Procedures. Polymerizations were carried out in a Schlenk tube equipped with a three-way stopcock under dry nitrogen with use of $TaCl_5$–*n*-Bu_4Sn catalyst which is the most effective catalyst for the polymerization of diphenylacetylenes.[6] Copolymers were isolated by precipitation into a large amount of methanol, and the copolymer yields were determined

by gravimetry. The conversions of comonomers **2a–c** were determined by gas chromatography (GC) using docosane as internal standard, while that of **1** could not be evaluated because its boiling point was too high. A detailed procedure of polymerization has been described elsewhere.[9] Oxidative cyclodehydrogenation and its work-up were performed according to reference 3.

Measurements. The molecular weights of copolymers were evaluated by GPC [eluent, $CHCl_3$; columns, Shodex K-803, K-804, K-805 for low molecular weight polymers, and Shodex K-805, K-806, K-807 for high molecular weight polymers (Showa Denko, Co., Japan)]. IR, UV, and NMR spectra were measured on a Shimadzu FTIR-8100 spectrophotometer, a Jasco V-530 spectrophotometer, a JEOL EX-400 spectrometer, respectively. Thermogravimetric analyses (TGA) were carried out with a Perkin Elmer TGA-7 analyzer (in air, heating rate 10 °C/min).

References

1) a) Harris, F. W.; Stille, J. K. *Macromolecules* **1968**, 1, 463. b) Mukamal, H.; Harris, F. W.; Stille, J. K. *J. Polym. Sci., Part A-1*: **1967**, *5*, 2721. c) Stille, J. K.; Harris, F. W.; Rakuits, R. O.; Mukamal, H. *J. Polym. Sci., Part B:* **1966**, 4, 791.

2) a) Iyer, V. S.; Wehmeier, M.; Brand, J. D.; Keegstra, M. A.; Müllen, K. *Angew. Chem., Int. Ed. Engl.* **1997**, *36*, 1604. b) Müller, M.; Iyer, V. S.; Kübel, C.; Enkelmann, V.; Müllen, K. *Angew. Chem., Int. Ed. Engl.* **1997**, 36, 1607. c) Müller, M.; Mauermann-Düll, H.; Wagner, M.; Enkelmann, V.; Müllen, K. *Angew. Chem., Int. Ed. Engl.* **1995**, *34*, 1583.

3) a) Kübel, C.; Chen, S.-L.; Müllen, K. *Macromolecules* **1998**, *31*, 3014. b) Wolfe, J. F.; Arnold, F. E. *Macromolecules* **1981**, *14*, 909. c) Wolfe, J. F.; Loo, B. H.; Arnold, F. E. *Macromolecules* **1981**, *14*, 915.

4) Shirakawa, H.; Masuda, T.; Takeda, K. In *The Chemistry of Triple-Bonded Functional Groups (supplement C2)*; Patai, S., Ed.; Wiley: Chichester, 1994; Chapter 17.

5) Niki, A.; Masuda, T.; Higashimura, T. *J. Polym. Sci., Part A: Polym. Chem.* **1987**, *25*, 1553.

6) a) Kouzai, H.; Masuda, T.; Higashimura, T. *J. Polym. Sci., Part A: Polym. Chem.* **1994**, *32*, 2523. b) Tsuchihara, K.; Masuda, T.; Higashimura, T. *Macromolecules* **1992**, *25*, 5816.

7) a) Zheng, Q.; Sun, R.; Zhang, X.; Masuda, T.; Kobayashi, T. *Jpn. J. Appl. Phys.* **1997**, *36*, 1675. b) Tada, K.; Hidayat, R.; Hirohata, M.; Teraguchi, M.; Masuda, T.; Yoshino, K. *Jpn. J. Appl. Phys.* **1996**, *35*, 1138. c) Hidayat, R.; Hirohata, M.; Tada, K.; Teraguchi, M.; Masuda, T.; Yoshino, K. *Jpn. J. Appl. Phys.* **1997**, *36*, 3740.

8) a) Suzuki, H.; Kondo, A.; Inoue, M.; Ogawa, T. *Synthesis* **1984**, 121. b) Suzuki, H.; Kondo, A.; Ogawa, T. *Chem. Lett.* **1985**, 411.

9) Ito, H.; Masuda, T.; Higashimura, T. *J. Polym. Sci., Part A: Polym. Chem.* **1996**, *34*, 2925.

Chapter 5

Polymerization and Polymer Properties of Disubstituted Acetylenes Having an Adamantyl Group

Abstract

Three disubstituted acetylenes having an adamantyl group, i.e., 1-(*p*-adamantylphenyl)-2-chloroacetylene, 1-(*p*-adamantylphenyl)-1-propyne, and 1-(*p*-adamantylphenyl)-2-phenylacetylene (Cl*p*AdPA, *p*AdPP, and *p*AdDPA, respectively) polymerized in good yields in the presence of $MoCl_5$- or $TaCl_5$-based catalysts. The highest weight-average molecular weights of poly(Cl*p*AdPA), poly(*p*AdPP), and poly(*p*AdDPA) reached 3.6×10^5, 1.1×10^6, and 6.0×10^6, respectively. The polymers were yellow to white solids and completely soluble in toluene, $CHCl_3$, etc. These polymers were thermally fairly stable and the onset temperatures of weight loss in air were over 360 °C. Poly(*p*AdPP) and poly(*p*AdDPA) provided free-standing films by solution casting and their oxygen permeability coefficients (P_{O2}) at 25 °C were 8.6 and 55 barrers, respectively, which are relatively small compared with those of other substituted polyacetylenes.

Introduction

Adamantane is a bulky cage-shaped hydrocarbon with high symmetry. It possesses a high melting point (268 °C) and high thermal stability owing to the rigid and spherical structure.[1] The adamantane moiety has been introduced into the main chain or side chain of various types of polymers.[2] These polymers show unique properties such as high thermal stability, high thermooxidative stability, high glass transition temperatures (T_g) and good solubility. The examples of such polymers include poly(1-adamantyl methacrylate) and poly(1-adamantyl acrylate),[3,4] whose T_g values are over 140 °C and fairly high as compared with their methyl ester analogues and provide rigid and brittle membranes. Recently, syntheses of poly(ether ether ketone)s and poly(ether sulfones) with pendant adamantyl groups have been reported.[5] The polymers showed high T_g (> 225 °C) and good thermal stability (the onset temperatures of weight loss in air (T_0) are above 400 °C).

There have been a few reports regarding adamantane-bearing polyacetylenes. For instance, metathesis polymerization of 1-ethynyladamantane by $MoCl_5$ and WCl_6 gives a polymer insoluble in any solvent.[6] Thermal and Pd-catalyzed polymerizations of 1,3-diethynyladamantane yield a polymer, which is thermally stable (T_0 = 475 °C) but insoluble owing to gelation.[7] Thus, there has been no example of soluble, high-molecular-weight, adamantane-bearing polyacetylenes.

The polymerization of various substituted acetylenes by using group 5 and 6 transition metal catalysts has been studied.[8] Among them, 1-(*p-tert*-butylphenyl)-2-phenylacetylene (*pt*BuDPA) was polymerized in high yield by $TaCl_5$-based catalysts.[9] The formed polymer was soluble in common organic solvents unlike poly(diphenylacetylene), and its M_w was higher than $1x10^6$. This polymer shows excellent thermal stability (T_0 = 380 °C) and high gas permeability (P_{O2} = 1000 barrer). The *tert*-butyl group is a bulky spherical substituent, which is considered to be useful to make glassy polymers more permeable to gases. The adamantyl group is a *tert*-alkyl group like *tert*-butyl and much bulkier.

It is interesting to synthesize high-molecular-weight, soluble polyacetylenes

having adamantyl groups and to study the properties and functions of the formed polymers. It have been previously reported that the polymerizations of 1-chloro-2-phenylacetylene (ClPA)[10], 1-phenyl-1-propyne (PP)[11], and diphenylacetylene (DPA)[12] by $MoCl_5$- and $TaCl_5$-based catalysts to afford high-molecular-weight polymers in good yields. In this chapter, the author investigated the polymerization of three homologues of these monomers in which an adamantyl group is introduced at para position; i.e., 1-(*p*-adamantylphenyl)-2-chloroacetylene (Cl*p*AdPA), 1-(*p*-adamantylphenyl)-1-propyne (*p*AdPP), and 1-(*p*-adamantylphenyl)-2-phenylacetylene (*p*AdDPA). Further, properties of the formed polymers were examined.

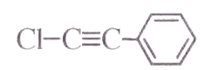

ClPA

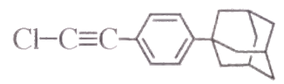

Cl*p*AdPA

PP

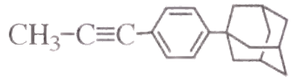

*p*AdPP

DPA

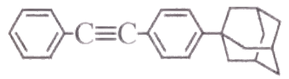

*p*AdDPA

Results and Discussion

Polymerization. It has been found in previous studies that Ta and/or Nb catalysts work well for the polymerization of sterically crowded disubstituted acetylenes such as 1-phenyl-1-propyne and diphenylacetylene.[8,12b,13] On the other hand, Mo catalysts are useful to the polymerization of chlorine-containing disubstituted acetylenes such as 1-chloro-2-phenylacetylene and 1-chloro-1-alkyne.[10,14] Hence, the polymerization of Cl*p*AdPA was carried out with Mo catal-

Table 1. Polymerization of Cl*p*AdPA by Various Catalysts[a]

catalyst	monomer	polymer[b]		
	convn., %	yield, %	$M_w/10^3$[c]	$M_n/10^3$[c]
$MoCl_5$	78	75	100	62
$MoCl_5$–*n*-Bu_4Sn	76	72	170	110
$MoCl_5$–Ph_4Sn	95	70	190	100
$MoCl_5$–Et_3SiH	100	74	160	90
$MoCl_5$–Ph_3SiH	89	82	140	76
$Mo(CO)_6$–CCl_4–$h\nu$[d]	77	51	360	210

[a] Polymerized in toluene at 30 °C for 24 h; $[M]_0$ = 0.50 M, [Cat] = 10 mM, [Cocat] = 20 mM. [b] Methanol-insoluble product. [c] Measured by GPC. [d] Polymerized in CCl_4.

ysts, whereas that of *p*AdPP and *p*AdDPA was examined with Nb and Ta catalysts.

Polymerization of Cl*p*AdPA. Table 1 shows the results for the polymerization of Cl*p*AdPA by using various $MoCl_5$-based catalysts. This monomer polymerized even with $MoCl_5$ alone in high yield, and the weight-average molecular weight (M_w) of the formed polymer was fairly high and $1x10^5$. When suitable organometallics such as *n*-Bu_4Sn, Ph_4Sn, Et_3SiH, and Ph_3SiH were used as cocatalysts, the M_w values of the polymers increased to $1.4x10^5$–$1.9x10^5$. The $Mo(CO)_6$–CCl_4–$h\nu$ catalyst was also effective to this monomer and the M_w of the polymer reached $3.6x10^5$, which is the largest value for this monomer. These molecular weights, however, were lower than those of poly(ClPA) formed under the same conditions and remained about 1/5 those of the corresponding poly(ClPA)s.[10] This is probably due to the bulkiness of the present monomer.

The time profile of polymerization for Cl*p*AdPA was examined by using the MoCl5–*n*-Bu_4Sn catalyst (Figure 1). Both monomer conversion and polymer yield increased with polymerization time; the monomer conversion reached ca. 85% after 24 h, and then the polymer yield was ca. 75%. The M_w of polymer became as large as

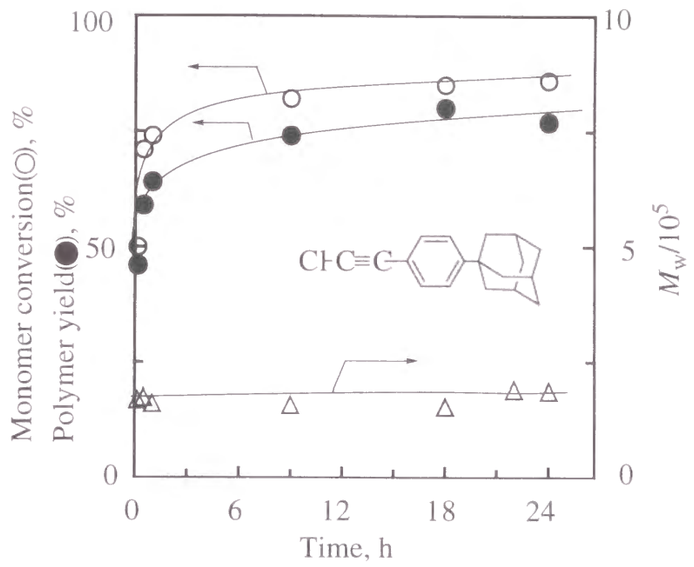

Figure 1. Time profile for the polymerization of Cl*p*AdPA by $MoCl_5$–*n*-Bu_4Sn (1:2) (in toluene, 30 °C, $[M]_0$ = 0.50 M, $[MoCl_5]$ = 10 mM).

Table 2. Polymerization of *p*AdPP by Various Catalysts[a]

catalyst	monomer	polymer[b]		
	convn., %	yield, %	$M_w/10^3$[c]	$M_n/10^3$[c]
$TaCl_5$	100	75	390	250
$TaCl_5$–*n*-Bu_4Sn	100	95	1000	710
$TaCl_5$–Ph_4Sn	100	99	1000	550
$TaCl_5$–Et_3SiH	100	83	940	500
$TaCl_5$–Ph_3SiH	100	95	660	360
$TaCl_5$–Ph_3Bi	100	83	1100	730
$NbCl_5$–*n*-Bu_4Sn	100	75	160	100

[a] Polymerized in toluene at 80 °C for 24 h; $[M]_0$ = 0.50 M, [Cat] = 10 mM, [Cocat] = 20 mM. [b] Acetone-insoluble product. [c] Measured by GPC.

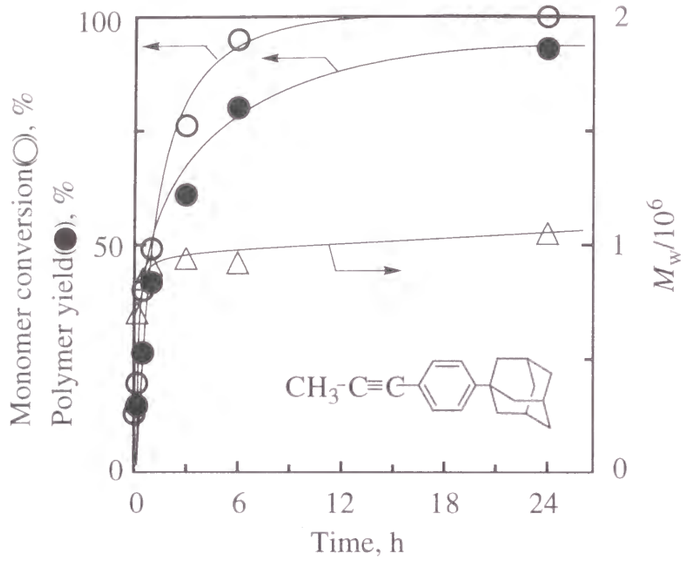

Figure 2. Time profile for the polymerization of *p*AdPP by $TaCl_5$–*n*-Bu_4Sn (1:2) (in toluene, 80 °C, $[M]_0$ = 0.50 M, $[TaCl_5]$ = 10 mM).

$2.0x10^5$ irrespective of polymerization time.

Polymerization of *p*AdPP. As seen in Table 2, *p*AdPP gave a polymer in high yield with $TaCl_5$ alone and the M_W of the formed polymer was $3.9x10^5$. Use of $TaCl_5$-cocatalyst systems achieved higher molecular weights up to M_W $6.6x10^5$–$1.1x10^6$. The $NbCl_5$–*n*-Bu_4Sn catalyst also gave a polymer in good yield but the M_W ($1.6x10^5$) of the polymer was rather low.

Figure 2 depicts the time profile of the polymerization of *p*AdPP by the $TaCl_5$–*n*-Bu_4Sn catalyst. The monomer was completely consumed after 24 h and the polymer yield also became virtually quantitative. The molecular weight of the polymer was around $1x10^6$ and hardly changed during the polymerization.

Polymerization of *p*AdDPA. When $TaCl_5$ alone was used as catalyst in the polymerization of the third monomer, *p*AdDPA, no methanol-insoluble polymer was obtained but the product was linear oligomers (Table 3). On the other hand,

Table 3. Polymerization of *p*AdDPA by Various Catalysts [a]

catalyst	polymer[b]		
	yield, %	$M_w/10^3$[c]	$M_n/10^3$[c]
$TaCl_5$	0	–	–
$TaCl_5$–*n*-Bu_4Sn	76	4300	2200
$TaCl_5$–Et_3SiH	76	3200	1200
$TaCl_5$–Ph_4Sn	17	6000	2900
$TaCl_5$–Ph_3SiH	0	–	–
$NbCl_5$–*n*-Bu_4Sn	4	2300	1100

[a] Polymerized in toluene at 80 °C for 3 h; $[M]_0$ = 0.10 M, [Cat] = 20 mM, [Cocat] = 40 mM. [b] Methanol-insoluble product. [c] Measured by GPC.

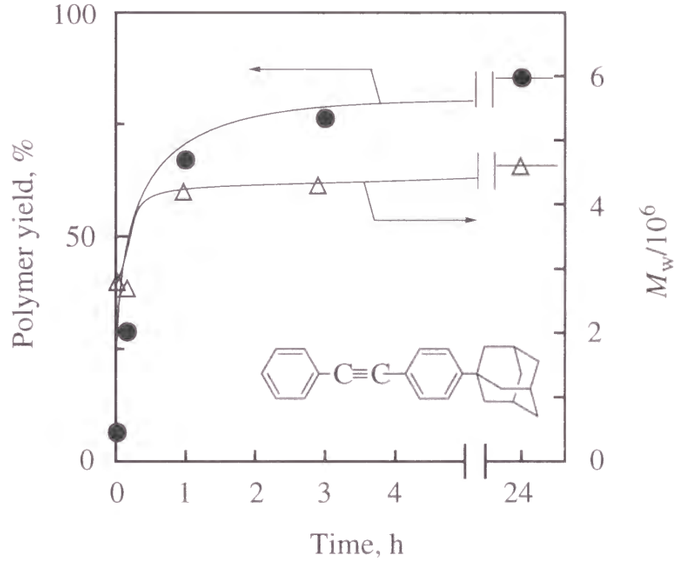

Figure 3. Time profile for the polymerization of *p*AdDPA by $TaCl_5$–*n*-Bu_4Sn (1:2) (in toluene, 80 °C, $[M]_0$ = 0.10 M, $[TaCl_5]$ = 20 mM).

this monomer polymerized in high yields with several $TaCl_5$-cocatalyst systems. Namely, polymers were obtained in over 70% yields when suitable organometallic cocatalysts such as Me_4Sn, *n*-Bu_4Sn, and Et_3SiH were employed in a twofold excess over $TaCl_5$. The M_w values of the polymers were higher than $1x10^6$. The polymer yields were much lower with Ph_4Sn and Ph_3SiH as cocatalysts. $NbCl_5$–*n*-Bu_4Sn was hardly effective. Poly(*p*AdDPA) was a yellow solid completely soluble in toluene and $CHCl_3$.

Polymerization of *p*AdDPA by $TaCl_5$–*n*-Bu_4Sn at 80 °C in toluene gave a polymer in ca. 75% yield in 3 h; the M_w was as high as $4.5x10^6$ (Figure 3). The molecular weight of polymer did not decrease even though the polymerization system was left over 24 h, indicating the absence of polymer degradation.

Polymer Structure. The IR spectra of all the polymers in this chapter exhibited no absorption around 2200 cm^{-1} ($\nu_{C\equiv C}$) which is seen in the monomers. Otherwise, similar bands were observed in the polymers and the corresponding monomers. The NMR spectra of the polymers also supported the absence of the carbon-carbon triple bond. Hence, the main chain of the polymers is considered to consist of alternating double bonds.

Figure 4 illustrates UV-visible spectra of the present polymers. Poly(Cl*p*AdPA) and poly(*p*AdPP) hardly show any absorption band in the visible region and the cutoff wavelengths of both spectra are 420 and 380 nm, respectively. These spectra are similar to those of poly(ClPA)[10] and poly(PP)[11]. Thus, the influence of the *p*-adamantyl group on the UV-visible spectra is negligible. Poly(*p*AdDPA) has two absorption maxima at 370 nm (ε_{max} 4750 M^{-1} cm^{-1}) and 430 nm (ε_{max} 5600 M^{-1} cm^{-1}), and the cutoff wavelength is ca. 500 nm, which is basically the same as those of other poly(DPAs) with ring substituents.[9,12b] These spectra correspond to the colors of the polymers (yellow to white). The spectrum of poly(*p*AdDPA) shows a red shift as compared with those of poly(Cl*p*AdPA) and (*p*AdPP), which is attributed to the presence of more phenyl groups.

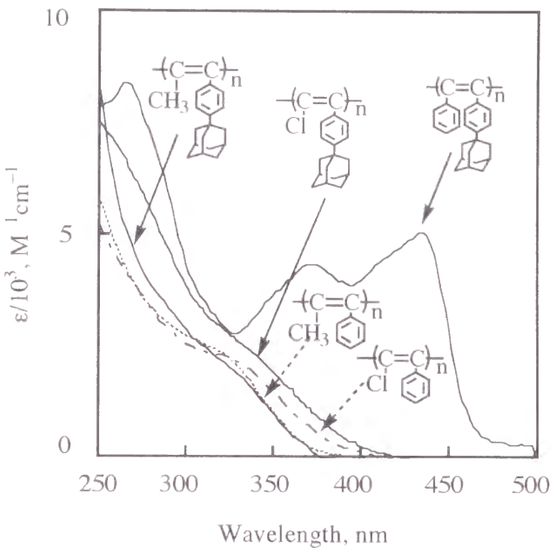

Figure 4. UV-visible spectra of adamantyl group-containing polyacetylenes (in THF).

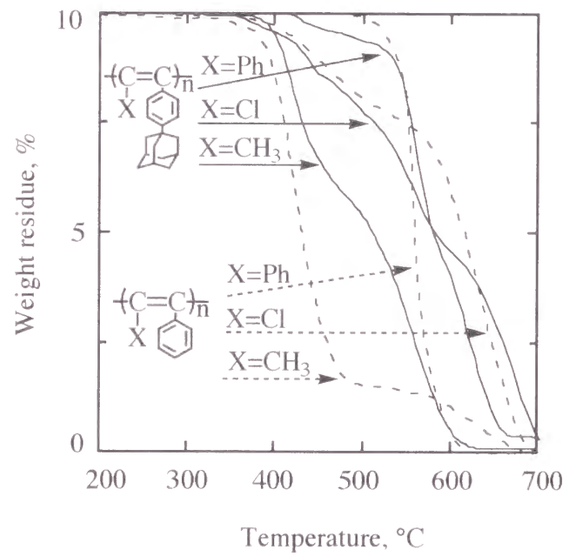

Figure 5. TGA curves of adamantyl group-containing polyacetylenes (in air, heating rate 10 °C/min).

Polymer Properties. Polymer properties were examined by using the samples of the poly(Cl*p*AdPA) obtained with $MoCl_5$–*n*-Bu_4Sn and poly(*p*AdPP) andpoly(*p*AdDPA) obtained with $TaCl_5$–*n*-Bu_4Sn in Tables 1, 2, and 3.

All the polymers completely dissolved in common solvents such as benzene, toluene, cyclohexane, THF, $CHCl_3$, and carbon tetrachloride, and did not dissolve in hexane, diethyl ether, 1,4-dioxane, acetone, ethyl acetate, DMF, DMSO, and methanol. Poly(*p*AdDPA) was partly insoluble in anisole and completely insoluble in dichloromethane and methyl benzoate, whereas poly(Cl*p*AdPA) and poly(*p*AdPP) were soluble in both solvents. All these polymers exhibited better solubility than the counterparts without *p*-adamantyl group; for instance, poly(DPA) is insoluble in any solvents, and poly(ClPA) and poly(PP) are insoluble in cyclohexane. Thus, introduction of adamantyl group has improved the polymer solubility. Free-standing films of poly(*p*AdDPA) and poly(*p*AdPP) could be obtained by casting them from a toluene solution. No tough film could be fabricated from poly(Cl*p*AdPA) because of its rather low molecular weight.

Thermogravimetric analyses (TGA) of the present and related polymers were conducted in air (Figure 5). The onset temperature of the weight loss in air (T_0) for poly(Cl*p*AdPA) and poly(*p*AdPP) were 360 and 380 °C, respectively, which are similar to those of poly(ClPA) and the poly(PP). The T_0 of poly(*p*AdDPA) was 420 °C, indicating high thermal stability of this polymer though somewhat inferior to poly(DPA). Thus, the introduction of an adamantyl group on the phenyl ring exhibits no significant adverse effect on the thermal stability. Among the present polymers, poly(*p*AdDPA) was superior in thermal stability. A reason for this is that aromatic substituents have no labile proton and protect the polymer main chain from the attack by oxygen owing to their steric effects. Measurements of differential scanning calorimetry (DSC) of the present polymers were conducted under nitrogen. No polymers indicated any peaks or inflections below their T_0 points. Thus, no glass transition was observed up to around 350 °C in these polymers.

Polyacetylenes having suitable substituents tend to show high gas permeability, and their gas permeation behavior has extensively been studied.[15-19] Among various acetylenic polymers, poly[1-(trimethylsilyl)-1-propyne] [poly-(TMSP)][20] and poly(*pt*BuDPA)[9] show very high gas permeability; their oxygen permeability coefficients (P_{O2}) reach 6000 and 1100 barrers [1 barrer = $1x10^{-10}$ cm^3 • (STP) • cm/(cm^2 • s • cmHg)], respectively. It is assumed that bulky round-shaped substituents such as *tert*-butyl and trimethylsilyl groups are effective for the high gas permeability of substituted polyacetylenes.

The P_{O2} value of poly(*p*AdDPA) at 25 °C was 55 barrers, which is close to that of natural rubber (23 barrers) (Figure 6). This P_{O2} value is much lower than that of poly(*pt*BuDPA).[9] The value of poly(*p*AdPP) was 8.6 barrer, which is similar to that of poly(PP)[11]. Thus, the gas permeability of substituted polyacetylenes greatly

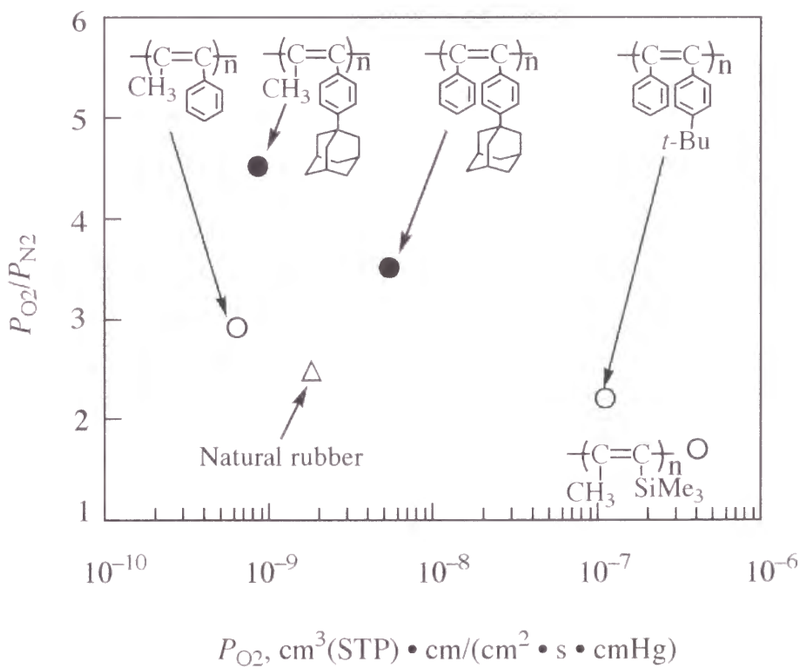

Figure 6. Oxygen permeability coefficients (P_{O2}) of adamantyl group-containing polyacetylenes (25 °C).

depends on the kind of substituents, and not only the bulkiness of substituents but also their shape, rigidity and mobility of substituents seem to be very important for gas permeability.[21] The separation factors between oxygen and nitrogen (P_{O_2}/P_{N_2}) of poly(*p*AdDPA) and poly(*p*AdPP) were 3.5 and 4.5, respectively, and higher than that of natural rubber (2.5). Permeability coefficients (unit: barrer) for other gases were as follows; poly(*p*AdPP): H_2 48, He 30, CH_4 2.7, CO_2 33; poly(*p*AdDPA): H_2 210, He 110, CH_4 160, CO_2 29.

Experimental

Materials. Transition-metal catalysts and organometallic cocatalysts were all commercially obtained and used without further purification. The three monomers (new compounds) were prepared by referring to the literature methods[22-24] (Scheme 1). The detailed methods for preparing the intermediates (i.e., *p*-adamantylphenylacetylene and *p*-adamantyliodobenzene) of the monomers have been described elsewhere.[25]

Scheme 1

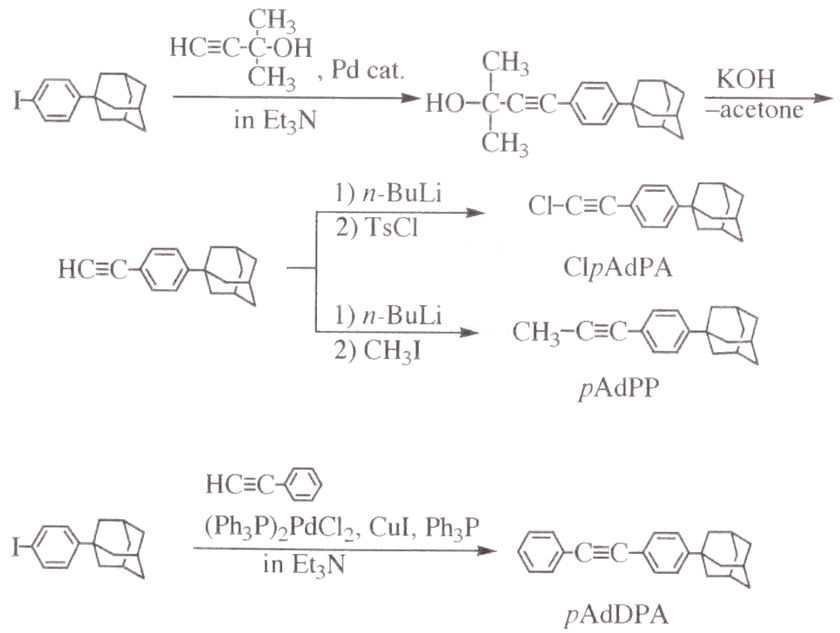

1-(p-Adamantylphenyl)-2-chloroacetylene: A 100-mL three-necked flask was equipped with a three-way stopcock, a dropping funnel, a rubber septum and a magnetic stirring bar. After the flask was flushed with nitrogen, a solution of *n*-butyllithium (8.0 mL, 1.6 M in hexane, 12.8 mmol) was placed in the flask at –78 °C. Then, a solution of (*p*-adamantylphenyl)acetylene[25] (3.0 g, 12.7 mmol) in THF (15 mL) was added dropwise, and the reaction mixture was left for 30 min at the same temperature. To the resulting alkynyllithium solution was added a solution of *p*-toluenesulfonyl chloride (2.9 g, 15.2 mmol) in THF (15 mL) dropwise, and stirring was continued for an additional 1 h at room temperature. After the completion of the reaction (disappearance of the starting acetylene) had been confirmed by thin layer chromatography (TLC), ice water (20 mL) was added. The product was extracted with diethyl ether, and the organic phase was washed with 2 N hydrochloric acid and water, and dried over anhydrous sodium sulfate. The volatile materials were evaporated, and the crude product was purified by flash column chromatography (eluent: hexane) to give a white solid (2.0 g, 59%), mp 151.5–152.8 °C, purity > 99% (by ^{1}H NMR); IR (KBr) 3036 (w), 2912 (s), 2849 (s), 2218 (m, $\nu_{C\equiv C}$), 1512 (m), 1447 (m), 837 (s), 808 (s), 552 (s) cm^{-1}; ^{1}H NMR ($CDCl_3$) δ 7.38 (d, J = 8.64 Hz, 2H), 7.28 (d, J = 8.64 Hz, 2H), 2.15–2.05 (m, 3H), 1.87 (d, J = 2.92 Hz, 6H), 1.83–1.68 (m, 6H); ^{13}C NMR ($CDCl_3$) δ 152.0 (Ar), 131.7 (Ar), 124.9 (Ar), 119.0 (Ar), 69.5 (ArC≡), 67.0 (≡CCl), 42.9 (Ad), 36.6 (Ad), 36.3 (Ad), 28.8 (Ad). Anal. Calcd for $C_{18}H_{19}Cl$: C, 79.82; H, 7.09; Cl, 13.09. Found: C, 79.80; H, 7.15; Cl, 13.17.

1-(p-Adamantylphenyl)-1-propyne: A 100-mL three-necked flask was equipped with a three-way stopcock, a dropping funnel, a rubber septum and a magnetic stirring bar. After the flask was flushed with nitrogen, a hexane solution of *n*-butyllithium (8.3 mL, 1.6 M, 13.3 mmol) was placed in the flask at –78 °C. A solution of (*p*-adamantylphenyl)acetylene[24] (2.6 g, 11.0 mmol) in THF (10 mL) was added dropwise at –78 °C under nitrogen, and the reaction mixture was left for 1 h. Then a solution of methyl iodide (0.82 mL, 13.2 mmol) in THF (5 mL) was added dropwise, and the reaction mixture was warmed up gradually to room temperature and

was stirred for 24 h. After the reaction had been completed (confirmed by TLC through the absence of the starting acetylene), a small amount of water was carefully added under ice-cooling and stirring. The solution was extracted with diethyl ether, and the organic phase was washed with 2 N HCl aq. solution and water, and dried over anhydrous sodium sulfate. After removal of the volatile compounds, the crude product was purified by flash column chromatography (eluent: hexane) to give a white solid (2.7 g, 98%), mp 146.0–148.0 °C, purity > 99% (by ^{1}H NMR); IR (KBr) 3034 (w), 2910 (s), 2849 (s), 2047 (m, $\nu_{C\equiv C}$), 1514 (m), 1502 (m), 1449 (m), 1016 (m), 839 (s), 808 (s), 556 (s) cm^{-1}; ^{1}H NMR ($CDCl_3$) δ 7.33 (d, J = 8.29 Hz, 2H), 7.26 (d, J = 8.78 Hz, 2H), 2.15–2.05 (m, 3H), 2.03 (s, 3H), 1.88 (d, J = 2.46 Hz, 6H), 1.82–1.69 (m, 6H); ^{13}C NMR ($CDCl_3$) δ 150.8 (Ar), 131.3 (Ar), 124.8 (Ar), 120.9 (Ar), 84.9 (ArC≡), 80.0 (≡CMe), 42.9 (Ad), 36.7 (Ad), 36.3 (Ad), 28.9 (Ad), 22.5 (Me). Anal. Calcd for $C_{19}H_{22}$: C, 91.13; H, 8.87. Found: C, 91.38; H, 8.89.

1-(p-Adamantylphenyl)-2-phenylacetylene: A 500-mL three-necked flask was equipped with a reflux condenser, a three-way stopcock, and a magnetic stirring bar, and flushed with dry nitrogen. *p*-Adamantyliodobenzene[25] (12.6 g, 37 mmol), $(Ph_3P)_2PdCl_2$ (77 mg, 0.11 mmol), CuI (129 mg, 0.168 mmol), Ph_3P (118 mg, 0.45 mmol), and triethylamine (80 mL) were placed in the flask, and the mixture was stirred for 1 h at 60 °C. Then, phenylacetylene (4.5 mL, 41 mmol) in triethylamine (70 mL) was added gradually, and stirring was continued for an additional 2 h (until TLC indicated no starting iodide). After triethylamine was evaporated, diethyl ether (ca. 400 mL) was added, and the insoluble salt was filtered off. The solution was washed with 2 N hydrochloric acid and then water. After drying over anhydrous sodium sulfate, the solution was concentrated at reduced pressure. Purification of the crude product by flash column chromatography (eluent: hexane) gave the desired product (yield 8.0 g, 70%) as a white solid, mp 173.5–175.0 °C, purity > 99% (by ^{1}H NMR); IR (KBr) 3032 (w) 2843 (s) 2220 (w, $\nu_{C\equiv C}$), 1597 (m), 837 (s), 806 (s), 762 (s), 694 (s) 556 (s) cm^{-1}; ^{1}H NMR ($CDCl_3$) δ 7.55–7.29 (9H, Ar), 2.15–2.05 (m, 3H), 1.90 (d, J = 2.92 Hz, 6H), 1.84–1.70 (m, 6H); ^{13}C NMR ($CDCl_3$) δ 151.7 (Ar), 131.5 (Ar), 131.4 (Ar),

128.3 (Ar), 128.0 (Ar), 124.9 (Ar), 123.5 (Ar), 120.2 (Ar), 89.6 (ArC≡), 88.7 (≡CPh), 42.9 (Ad), 36.7 (Ad), 36.3 (Ad), 28.9 (Ad). Anal. Calcd for $C_{24}H_{24}$: C, 92.25; H, 7.74. Found: C, 92.33; H, 7.84.

Polymerization. Polymerizations were carried out as described in Chapter 1. The conversions of *p*AdPP and Cl*p*AdPA were determined by gas chromatography (GC), while those of *p*AdDPA could not be evaluated because the boiling point of the monomer was too high. A detailed procedure of polymerization has been described elsewhere.[26]

Characterization. The molecular weights of polymers were evaluated by GPC with use of a polystyrene calibration. GPC curves were observed with a Shimadzu LC-9A liquid chromatograph [eluent, $CHCl_3$; columns, Shodex K-803, K-804, K-805 for low molecular weight polymers, and Shodex K-805, K-806, K-807 for high molecular weight polymers (Showa Denko, Co., Japan)].

IR, UV, and NMR spectra and gas permeability were measured in the same manner as described in Chapter 1. Measurements of TGA and DSC were conducted with a Perkin Elmer TGA-7 (in air, heating rate 10 °C/min) and a Perkin Elmer Pyris 1 (in nitrogen, heating rate 10 °C/min), respectively.

References

1) Fort, R. C., Jr.; Schleyer, P. v. R. *Chem. Rev.* **1964**, *64*, 277.
2) Khardin, A. P.; Radchenko, S. S. *Russ. Chem. Rev.* **1982**, *51*, 272.
3) Duling, I. N.; Schneidert, A.; Moore, R. E. French P. 1565698, 1969.
4) Duling, I. N.; Schneidert, A.; Moore, R. E. US P. 3639362, 1972.
5) Mathias, L. J.; Lewis, C. M.; Wiegel, K. N. *Macromolecules* **1997**, *30*, 5970.
6) Okano, Y.; Masuda, T.; Higashimura, T. *J. Polym. Sci., Polym. Chem. Ed.* **1985**, *23*, 2527.
7) a) Archibald, T. G.; Malik, A. A.; Baum, K.; Unroe, M. R. *Macromolecules* **1991**, *24*, 5261. b) Malik, A. A.; Archibald, T. G.; Baum, K.; Unroe, M. R. *J. Polym. Sci., Part A: Polym. Chem.* **1992**, *30*, 1747.

8) Masuda, T. In *The Polymeric Materials Encyclopedia*; Salamone, J. C., Ed., CRC Press: Boca Raton, FL, 1996; p 32.

9) Kouzai, H.; Masuda, T.; Higashimura, T. *J. Polym. Sci., Part A: Polym. Chem.* **1994**, *32*, 2523.

10) a) Masuda, T.; Yamagata, M.; Higashimura, T. *Macromolecules* **1984**, *17*, 126. b) Masuda, T.; Kuwane, Y.; Higashimura, T. *J. Polym. Sci., Polym. Chem.* Ed. **1982**, *20*, 1043.

11) a) Masuda, T.; Takahashi, T.; Higashimura, T. *Macromolecules* **1985**, *18*, 311. b) Masuda, T.; Niki, A.; Isobe, E.; Higashimura, T. *Macromolecules* **1985**, *18*, 2109.

12) a) Niki, A.; Masuda, T.; Higashimura, T. *J. Polym. Sci., Part A: Polym. Chem.* **1994**, **25**, 1553 (1987). b) Masuda, T.; Tachimori, H. *J. Macromol. Sci., Pure Appl. Chem.,* **1994**, *A31*, 1675.

13) Shirakawa, H.; Masuda, T.; Takeda, K. In *The Chemistry of Triple-Bonded Functional Groups (supplement C2)*; Patai, S., Ed.; Wiley: Chichester, 1994; Chapter 17.

14) Masuda, T.; Yoshimura, T.; Tamura, K.; Higashimura, T. *Macromolecules* **1987**, *20,* 1734.

15) Kesting, E.; Fritzsche, A. K. In *Polymeric Gas Separation Membranes*; Wiley: New York, 1993; pp 109–114.

16) Ichiraku, Y.; Stern, S. A.; Nakagawa, T. *J. Membr. Sci.* **1987**, *34*, 5.

17) Lin, X.; Qiu, X.; Zheng, G.; Xu, J. *J. Appl. Polym. Sci.* **1995**, *58*, 2137.

18) Pinnau, I.; Casillas, C. G.; Morisato, A.; Freeman, B. D. *J. Polym. Sci., Part B: Polym. Phys.* **1996**, *34*, 2613.

19) Toy, L. G.; Freeman, B. D.; Spontak, R. J.; Morisato, A.; Pinnau, I. *Macromolecules* **1997**, *30*, 4766.

20) Masuda, T.; Isobe, E.; Higashimura, T.; Takada, K. *J. Am. Chem. Soc.* **1983**, *105*, 7473.

21) Kanaya, T.; Teraguchi, M.; Masuda, T.; Kaji, K. *Polymer* **1999**, *40*, 7157.

22) Brandsma, L. In *Preparative Acetylenic Chemistry,* 2nd ed.; Elsevier: Amsterdam, 1988; pp 147–148.

23) Armitage, J. B.; Jones, E. R. H.; Whiting, M. C. *J. Chem. Soc.* **1952**, 1993.

24) Sonogashira, K.; Tohda, Y.; Hagihara, N. *Tetrahedron Lett.* **1975**, *50*, 4467.

25) Fujita, Y.; Misumi, Y.; Tabata, M.; Masuda, T. *J. Polym. Sci., Part A: Polym. Chem.* **1998**, *36*, 3157.

26) Tsuchihara, K.; Masuda, T.; Higashimura, T. *Macromolecules* **1992**, *25*, 5816.

Chapter 6

Polymerization and Polymer Properties of Acetylenes Having Azobenzene Moiety

Abstract

Polymerization of monosubstituted acetylenes with an azobenzene group at meta or para position (3EAB and 4EAB, respectively) was examined by using various catalysts (e.g., $MoCl_5$–*n*-Bu_4Sn, WCl_6–Ph_4Sn, and $[(nbd)RhCl]_2$–Et_3N). The $MoCl_5$–*n*-Bu_4Sn and WCl_6–Ph_4Sn catalysts yielded no polymer. In contrast, both monomers polymerized with $[(nbd)RhCl]_2$–Et_3N to give polymers in high yields. Whereas poly(4EAB) was insoluble in any organic solvents, poly(3EAB) was soluble in toluene, $CHCl_3$, etc. Poly(3EAB) was a yellow solid, whose M_W reached $4.9x10^5$. It provided a film by solution casting. The onset temperature of weight loss of poly(3EAB) in TGA in air was 230 °C. Trans-cis photoisomerization of azobenzene moieties in the poly(3EAB) took place upon UV irradiation.

Introduction

Azobenzene is a well-known photosensitive chromophore, which undergoes photoinduced and thermal geometric isomerizations.[1] A variety of polymers having azobenzene moieties in the main chain or side chain have been synthesized, and their properties have been investigated because of their photoactivities which may lead to various photonic applications.[2] The following polymers which contain azobenzenes in the main chain have been reported: a poly(phenyleneethynylene) having azobenzene moieties[3a] synthesized via Pd-catalyzed coupling reaction and a polyurea[3b] prepared by polycondensation of diisocyanate and 4,4'-diaminoazobenzene. On the other hand, there have been many examples of polymers carrying azobenzene moieties in the side chain. Thus, poly(4-vinylazobenezene),[4a] poly(methacrylates),[4b] poly(acrylates),[4c] polythiophenes,[4d,e] and poly(isocyanates)[4f–h] have been intensively investigated. Interestingly, UV irradiation of poly(isocyanates) having optically active azobenzene moieties causes trans-to-cis isomerization of azobenzene moieties, which induces inversion of the helical structure of the main chain.[4f–h] Some of these polymer films generate holographic surface relief gratings by photoirradiation.[5] Recently, the synthesis and photoisomerization behavior of azobenzene-containing dendrimers have been reported.[6]

Polyacetylenes possesses alternating double bonds along the main chain, which brings about unique electrical and optical properties.[7] There have, however, been a few reports regarding azobenzene-containing polyacetylenes. For instance, a 1,6-heptadiyne, to which an azobenzene group is tethered through an alkylene spacer at the 4-position, polymerizes with WCl_6- and $MoCl_5$-based catalysts in a ring-forming metathesis manner to afford a soluble polymer in moderate yields.[8] Polymerization of acetylenes that are connected with an azobenzene through alkylene spacing groups also proceeds with Rh and Fe catalysts, and the formed polymers show a smectic liquid-crystalline phase according to DSC analyses.[9] An acetylene with a ferrocenylazo group has been polymerized with a Schrock catalyst in a living fashion.[10]

Thus, there has been no example of the polymerization of acetylenes that have a directly bonded azobenzene moiety. The resulting polymers are expected to have a conjugation between the main chain and the azobenzene, which may endow novel optical and electronic properties. It is hence very interesting to synthesize polyacetylenes that possess directly connected azobenzene moieties and further study their properties. This chapter deals with the polymerization of 3-ethynylazobenzene and 4-ethynylazobenzene (3EAB and 4EAB, respectively). Polymers have been successfully obtained with use of suitable transition-metal catalysts, and properties of the formed polymers have been clarified.

Results and Discussion

Polymerization. Table 1 shows the results for the polymerization of 3EAB and 4EAB by various catalysts.[14] The $[(nbd)RhCl]_2$–Et_3N catalyst exhibited high activity in the polymerization of 3EAB; the monomer was completely consumed to afford polymer in 80% or higher yield. The polymer was an orange-colored solid soluble in low-polarity solvents such as toluene and $CHCl_3$. Though the $Fe(acac)_3$–Et_3Al catalyst also induced polymerization, its activity was lower. The polymer obtained with the Fe catalyst was a vermilion solid insoluble in any solvents; the insolubility seems to be attributable to the cis-cisoidal geometric structure like the case of poly(phenylacetylene). No polymer was obtained with classical metathesis catalysts such as WCl_6–Ph_4Sn and $MoCl_5$–n-Bu_4Sn, which is attributable to catalyst deactivation by the azo group. On the other hand, a Schrock carbene, which is relative tolerant to functional groups, afforded a soluble polymer in good yield, but the M_n was no more than 5000. The other monomer, 4EAB, also polymerized with $[(nbd)RhCl]_2$–Et_3N and $Fe(acac)_3$–Et_3Al, but the formed polymers were insoluble in any solvents. This is probably because the rigid planar *p*-azobenzene groups take a stacked structure. A Schrock carbene polymerized also 4EAB into a low molecular weight polymer.

Table 1. Polymerization of 3EAB and 4EAB by Various Catalysts[a]

run	catalyst	monomer convn., %	polymer[b] yield, %	$M_w/10^3$ [c]	$M_n/10^3$ [c]
		monomer: 3EAB			
1	$[(nbd)RhCl]_2$–Et_3N (1:2)[d]	100	99	350	80
2	$[(nbd)RhCl]_2$–Et_3N (1:2)[e]	100	80	490	110
3	$Fe(acac)_3$– Et_3Al (1:3)[f]	47	36	insoluble	
4	Schrock carbene[g]	100	76	16	5.2
5	Schrock carbene[h]	0	0	–	–
6	$MoCl_5$–n-Bu_4Sn (1:1)[i]	0	0	–	–
7	WCl_6–Ph_4Sn (1:1)[i]	0	0	–	–
		monomer: 4EAB			
8	$[(nbd)RhCl]_2$–Et_3N (1:2)[e]	100	100	insoluble	
9	$Fe(acac)_3$– Et_3Al (1:3)[f]	81	69	insoluble	
10	Schrock carbene[g]	100	75	14	6.8
11	Schrock carbene[h]	0	0	–	–

[a] Polymerized in toluene at 30 °C for 24 h; $[M]_0$ = 0.20 M, [Cat] = 2.0 mM. [b] Hexane-insoluble product. [c] Measured by GPC. [d] For 3 h, $[M]_0$ = 0.10 M. [e] For 3 h, $[M]_0$ = 0.25 M. [f] $[Fe(acac)_3]$ = 10 mM. [g] $\{Mo[OC(Me)(CF_3)_2]_2=N(2,6\text{-}i\text{-}Pr_2C_6H_3)=CH\text{-}CMe_2Ph\}$. [h] $\{Mo(O\text{-}t\text{-}Bu)_2=N(2,6\text{-}i\text{-}Pr_2C_6H_3)=CHCMe_2Ph\}$. [i] [Cat] = 20 mM.

Structure and Properties of Polymers. The structure and properties of poly(3EAB) were examined with the Rh-based sample (Table 1, run 2). The IR spectrum of poly(3EAB) exhibited no absorption at 3285 cm^{-1} ($\nu_{H-C\equiv}$) that is seen in the monomer (Figure 1(a)). Otherwise, similar bands were observed in the polymer and the monomer. The ^1H NMR spectrum of poly(3EAB) (Figure 1(b)) exhibits a relatively sharp signal due to main-chain cis-vinyl protons (5.87 ppm), indicating a high content of stereoregular cis-transoidal structure.[15,16] Since the vinyl-proton

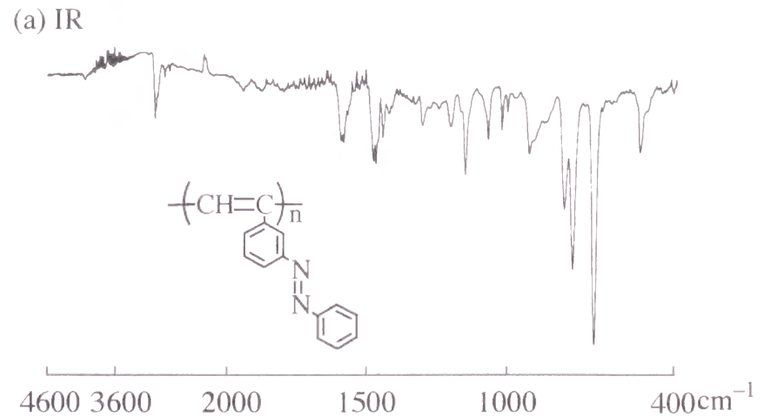

Figure 1. IR and ^1H NMR spectra of poly(3EAB) (Rh cat; IR, KBr pellet; NMR, $CDCl_3$ solution).

signal of the trans structure is overlapping with the aromatic region, the percent cis content of poly(3EAB) is determined to be 88% from the relative intensity of the signals at 5.87 ppm and that of the aromatic region.

Poly(3EAB) was soluble in toluene, benzene, THF, anisole, and $CHCl_3$ and insoluble in hexane, ethyl acetate, DMF, DMSO, and methanol. Poly(3EAB) provided a tough film by casting it from toluene solution. This polymer was stable enough in the solid state in air over a long period of time, while the molecular weight of the polymer decreased rapidly in $CHCl_3$. The M_w quickly decreased even during

GPC measurement when $CHCl_3$ was used as eluent. On the other hand, poly(3EAB) was relatively stable in THF, and the polymer degradation was rather slow; e.g., the M_w decreased to ca. 4/5 the initial value when THF solution of the polymer was left for 1 h.

The thermal stability of poly(3EAB) was examined by TGA in air (Figure 2). The weight loss began at 230 °C, which is higher than the temperature (ca. 200 °C) for poly(phenylacetylene). Thus, the introduction of azobenzene moieties in polyacetylene side groups exhibits no significant adverse effect on thermal stability.

The isomerization behavior of azobenzene moieties of the polymer in solution was investigated by UV-visible spectroscopy (Figure 3). The absorption maximum of the trans form was observed at 340 nm (ε_{max} = 2.3x10^4 M^{-1} cm^{-1}). When a solution of poly(3EAB) in THF was irradiated with UV light of wavelength 300–400 nm, the azobenzene moieties isomerized, resulting in the decrease of the absorption at 340 nm and in the increase of the absorption at 450 nm.

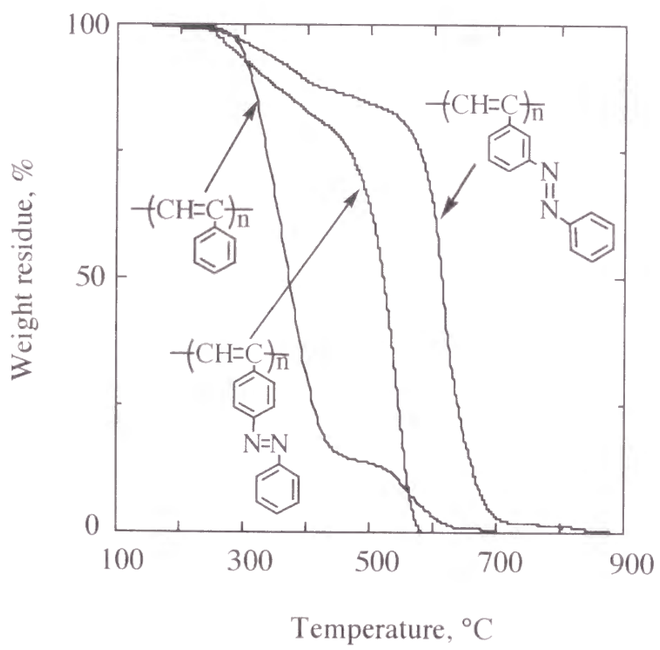

Figure 2. TGA curves of poly(3EAB) and poly(4EAB) (the samples prepared with Rh catalyst; heating rate 10 °C/min, in air).

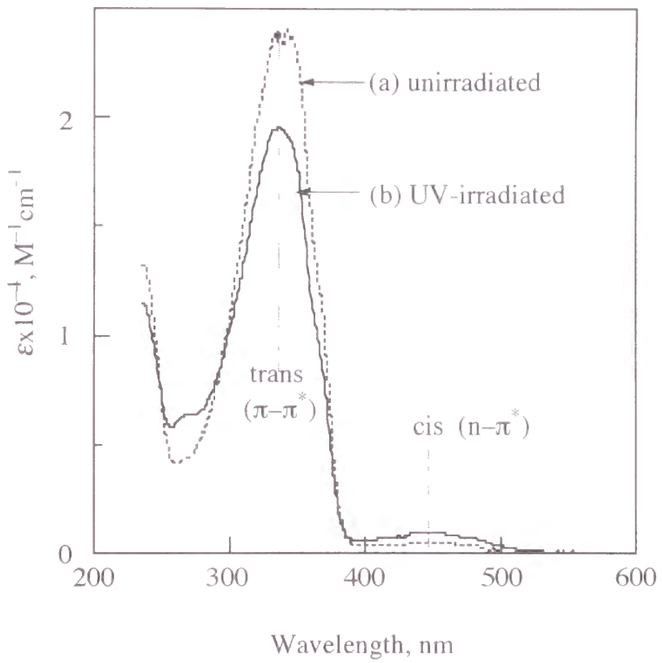

Figure 3. UV-visible spectra of poly(3EAB) in THF (a) before and (b) after UV irradiation at 300–400 nm for 2 h (with 200-W high pressure Hg-lamp).

Experimental

Materials. The two monomers were prepared with reference to the literature.[11,12] $[(nbd)RhCl]_2$ (Aldrich), other transition-metal catalysts (Strem), and organometallic cocatalysts (Aldrich or Kanto Chemicals) were used as purchased.

Synthesis of 3EAB: To a solution of nitrosobenzene (5.4 g, 50 mmol) in acetic acid (320 mL) was added 3-iodoaniline (10 g, 46 mmol), and the reaction mixture was stirred for 45 h at a reflux temperature. The solvent was evaporated, and the residue was diluted with diethyl ether. Then the ether solution was washed with water and dried over anhydrous Na_2SO_4. The ether was evaporated, and the crude product was purified by flash column chromatography to give 3-iodoazobenzene (12 g; yield, 87%) as an orange solid. The iodide (9.2 g, 30 mmol), $(Ph_3P)_2PdCl_2$ (98 mg, 0.14 mmol), CuI (154 mg, 0.81 mmol), Ph_3P (142 mg, 0.54 mmol), and triethylamine (100 mL) were placed in a three-necked flask. Then, trimethylsilyl-

acetylene (6.4 mL, 45 mmol) in triethylamine (30 mL) was gradually added, and stirring was continued for an additional 2 h (until TLC indicated no starting iodide). After triethylamine was evaporated, diethyl ether (ca. 200 mL) was added, and the insoluble salt was filtered off. The solution was washed with 2 N hydrochloric acid and then water, and dried over anhydrous Na_2SO_4. After evaporation of the ether, the crude product was purified by flash column chromatography (eluent: hexane) to give the coupling product (yield 8.2 g, 98%) as a red oil. To a solution of the coupling product (8.2 g, 29 mmol) in ethanol (80 mL) was added KOH powder (8 g, 0.14 mol), and the mixture was stirred for 2 h at room temperature. Then the reaction mixture was diluted with diethyl ether, and the ether solution was washed with water. The ether was evaporated and the crude product was purified by flash column chromatography to give 3EAB (5.5 g; yield, 88%) as an orange solid. Overall yield 76%, mp 64.0–65.0 °C, purity > 99% (by ^{1}H NMR). IR (KBr) 3285, 3061, 1593, 1568, 1479, 1469, 1261, 1074, 897, 806, 770, 687, 661 cm^{-1}; ^{1}H NMR ($CDCl_3$) δ 8.05–7.41 (9H, aromatic), 3.14 (1H); ^{13}C NMR ($CDCl_3$) δ 152.4, 152.3, 134.2, 131.3, 129.0, 126.2, 123.4, 123.0, 122.9, 122.8, 82.8, 77.9. Anal. Calcd for $C_{14}H_{10}N_2$: C, 81.53; H, 4.89; N, 13.58. Found: C, 81.80; H, 5.00; N, 13.47.

Synthesis of 4EAB: 4EAB was prepared by another method before.[13] Here, at first, 4-iodoazobenzene was prepared from 4-aminoazobenzene by the Sandmeyer reaction. Then, the coupling and desilylation reactions were carried out in the same way as for 3EAB. Overall yield 61.0%; mp 81.0–82.0 °C; purity > 99% (by ^{1}H NMR). IR (KBr) 3260, 3040, 1587, 1572, 1483, 1466, 1441, 1153, 1102, 1069, 843, 760, 679 cm^{-1}; ^{1}H NMR ($CDCl_3$) δ 7.95–7.48 (9H, aromatic) and 3.23 (1H); ^{13}C NMR ($CDCl_3$) δ 152.5, 152.1, 132.9, 131.3, 129.0, 124.6, 122.9, 122.8, 83.2, 79.4. Anal. Calcd for $C_{14}H_{10}N_2$: C, 81.53; H, 4.89; N, 13.58. Found: C, 81.67; H, 4.99; N, 13.76.

Procedures. A typical example of the polymerization procedure is as follows: A toluene solution of 3EAB and eicosane was placed in a Schlenk tube equipped with a three-way stopcock under a nitrogen atmosphere. To the monomer solution was added a solution of $[(nbd)RhCl]_2$ and Et_3N (mole ratio 1:2) in toluene at 30 °C. After 3 h, the polymerization was quenched by the addition of a mixture of toluene and acetic acid (4:1, volume ratio). The monomer conversion was determined by gas chromatography (GC). The formed polymer was isolated by precipitation in a large amount of hexane, and its yield was determined by gravimetry.

Characterization. The molecular weights of polymers were evaluated by GPC with use of a polystyrene calibration [eluent, THF; columns, Shodex KF-806Lx2, (Showa Denko, Co., Japan)].

IR, UV, and NMR spectra and TGA were measured in the same manner as described in Chapter 1.

References

1) a) Griffiths, J. *Chem. Soc. Rev.* **1972**, *1*, 481. b) *The Chemistry of Double-Bonded Functional Groups (supplement A3);* Patai, S., Ed.; Wiley: Sydney, 1997.

2) For reviews, see: a) *Macromolecular Symposia (Azobenzene-Containing Materials);* Natansohn, A., Ed., Wiley-VCH: Weinheim, **1999**; Vol. 139. b) Xie, S.; Natansohn, A.; Rochon, P. *Chem. Mater.* **1993**, *5*, 403. c) Kumar, G. S.; Neckers, D. C. *Chem. Rev.* **1989**, *89*, 1915.

3) a) Wright, M. E.; Porsch, M. J. *Polym. Prepr.* **1998**, *39* (2), 278. b) Lee, T. S.; Kim, D.-Y.; Jiang, X. L.; Li, L.; Kumar, J.; Tripathy, S. *Macromol. Chem. Phys.* **1997**, *198*, 2279.

4) a) Altomare, A.; Ciardelli, F.; Tirelli, N.; Solaro, R. *Macromolecules* **1997**, *30*, 1298. b) Wu, Y.; Demachi, Y.; Tsutsumi, O.; Kanazawa, A.; Shiono, T.; Ikeda, T. *Macromolecules* **1998**, *31*, 349. c) Ikeda, T.; Tsutsumi, O. *Science* **1995**, *268*, 1873. d) Zagórska, M.; Kulszewicz-Bajer, I.; Proñ, A.; Sukiennik, J.; Raimond, P.; Kajzar, F.; Attias, A.-J.; Lapkowski, M. *Macromolecules* **1998**, *31*, 9146. e) Lévesque, I.; Leclerc, M. *Macromolecules* **1997**, *30*, 4347. f) Müller, M.; Zentel, R. *Macromolecules* **1996**, *29*, 1609. g) Mayer, S.; Zentel, R.

Macromol. Chem. Phys. **1998**, *199*, 1675. h) Mayer, S.; Maxein, G.; Zentel, R. *Macromolecules* **1998**, *31*, 8522.

5) a) Andruzzi, L.; Altomare, A.; Ciardelli, F.; Solaro, R.; Hvilsted, S.; Ramanujam, P. S. *Macromolecules* **1999**, *32*, 448. b) Ballet, C.; Natansohn, A.; Rochon, P. *J. Phys. Chem.* **1996**, *100*, 8836. c) Kim, D. Y.; Li, L.; Jiang, X. L.; Shivshankar, V.; Kumar, J.; Tripathy, S. K. *Macromolecules* **1995**, *28*, 8835. d) Kim, D. Y.; Tripathy, S. K.; Li, L.; Kumar, J. *Appl. Phys. Lett.* **1995**, *66*, 1166.

6) a) Junge, D. M.; McGrath, D. V. *Chem. Commun.* **1997**, 857. b) Jiang, D.-L.; Aida, T. *Nature* **1997**, *388*, 454.

7) For reviews, see: a) Shirakawa, H.; Masuda, T.; Takeda, K. In *The Chemistry of Triple-Bonded Functional Groups* (*supplement C2*); Patai, S., Ed.; Wiley: Chichester, 1994; p 945. b) Masuda, T. In *The Polymeric Materials Encyclopedia*; Salamone, J. C., Ed.; CRC Press: Boca Raton, FL, 1996; p 32.

8) Jin, S. H.; Kang, S. W.; Park, J. G.; Lee, J. C.; Choi, K. S. *J. Macromol. Sci., Pure Appl. Chem.* **1995**, *A32*, 455.

9) a) Oh, S. Y.; Hong, S.-M.; Oh, S.-I. *Mol. Cryst. Liq. Cryst.* **1997**, *295*, 105. b) Goto, H.; Akagi, K.; Shirakawa, H. *Synth. Met.* **1997**, *84*, 373.

10) Buchmeiser, M. R.; Schuler, N.; Kaltenhauser, G.; Ongania, K.-H.; Lagoja, I.; Wurst, K.; Schottenberger, H. *Macromolecules* **1998**, *31*, 3175.

11) Tani, H.; Tanaka, S.; Toda, F. *Bull. Chem. Soc. Jpn.* **1963**, *36*, 1267.

12) Furlani, A.; Napoletano, C.; Russo, M. V.; Feast, W. J. *Polym. Bull.* **1986**, *16*, 311.

13) Tabata, M.; Yang, W.; Yokota, K. *Polym. J.* **1991**, *23*, 1135.

Part III

Properties and Functions of Poly(diphenylacetylenes) and Related Polymers

Chapter 7

Gas Permeability and Hydrocarbon Solubility of Poly[1-phenyl-2-[*p*-(triisopropylsilyl)phenyl]acetylene]

Abstract

The effect of film thickness, physical aging, and methanol conditioning on solubility and transport properties of glassy poly[1-phenyl-2-[*p*-(triisopropylsilyl)phenyl]acetylene] [poly(*pi*Pr$_3$SiDPA)] is reported at 35 °C. In general, gas permeability coefficients are very high and this polymer is more permeable to larger hydrocarbons (e.g. C_3H_8, C_4H_{10}) than to light gases such as H_2. Gas permeability and solubility coefficients are higher in as-cast, unaged films than in as-cast films aged at ambient conditions and increase to a maximum in both unaged and aged as-cast films after methanol conditioning. After methanol treatment, the oxygen permeabilities of unaged and aged films increase to 430 and 460 barrers, respectively. Thicker as-cast films have higher gas permeabilities than thinner as-cast films. The sensitivity of permeability to processing history may be due in large measure to the influence of processing history on nonequilibrium excess free volume and free volume distribution. Propane and *n*-butane diffusion coefficients are also sensitive to film processing history, presumably due to the dependence of diffusivity on free volume and free volume distribution.

Introduction

Relative to conventional glassy polymers, substituted, acetylene-based glassy polymers have desirable combinations of high gas and vapor permeability and high vapor selectivity for gas/vapor separations.[1] These properties are ascribed, in part, to extremely large fractional free volume in this family of polymers.[1-5] For example, poly[1-(trimethylsilyl)-1-propyne] [poly(TMSP)] and poly(4-methyl-2-pentyne) [poly(MP)] have overall fractional free volumes of 0.29 and 0.28, respectively, which are among the highest values ever reported for dense polymer films.[3-5] Furthermore, the fractional amount of nonequilibrium, unrelaxed free volume is 0.20–0.28 for poly(TMSP) and 0.15 for poly(MP), higher than that in any other glassy, hydrocarbon-based polymer.[4-8]

Glassy polymers are nonequilibrium materials whose properties change gradually with time (physical aging) due to local scale polymer chain motions which drive densification (i.e. reduction in free volume) of the material.[9] The free volume available to participate in physical aging is the nonequilibrium excess free volume. In substituted polyacetylenes such as poly(TMSP) and poly(MP), the majority of the overall free volume is present as excess free volume. Hence, the gas permeation and sorption properties of such polymers are particularly sensitive to film preparation protocol and aging.[10-12] For example, the oxygen permeability coefficient of poly(TMSP) can range from 2,600 barrers [1 barrer = 10^{-10} cm^3(STP)·cm/(cm^2·s·cmHg)] to 21,000 barrers at 25 °C depending on film history.[13] Previous studies have also shown that the permeability of poly(TMSP) decreases upon aging but can be restored to its initial value by soaking the aged film in methanol, a nonsolvent for the polymer.[10] Similarly, the nonequilibrium excess free volume in poly(TMSP) is reduced by aging but can be restored by soaking in methanol.

Poly[1-phenyl-2-[*p*-(triisopropylsilyl)phenyl]acetylene] (poly(*pi*Pr_3SiDPA) is a recently synthesized, poly(diphenyl acetylene) whose primary chemical structure is presented in Figure 1.[14] In this chapter, the influence of film thickness, methanol

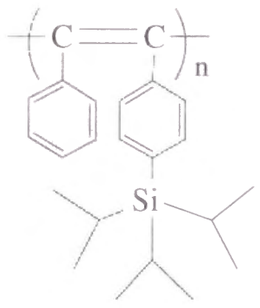

Figure 1. Chemical structure of poly(*pi*Pr_3SiDPA).

conditioning, and aging time on solubility, diffusivity, and permeability properties of poly(*pi*Pr_3SiDPA) is reported.

Results and Discussion

Characterization. The poly(*pi*Pr_3SiDPA) films used in this chapter were yellow and transparent. Based on DSC measurements, the polymer does not undergo any thermal transitions between 50 and 250 °C, indicating that the glass transition temperature of poly(*pi*Pr_3SiDPA) is greater than 250 °C. The equilibrium uptake of liquid methanol in the poly(*pi*Pr_3SiDPA) films is 28 ± 2 wt% at room temperature and is independent of film thickness. Within the precision of the measurements, the density of poly(*pi*Pr_3SiDPA) films is also independent of film thickness and is 1.00 ± 0.06 and 0.98 ± 0.04 g/cm^3 for the as-cast and methanol-conditioned film samples, respectively. These densities were determined from films prepared at the different times to confirm the reproductivity of the poly(*pi*Pr_3SiDPA) films. Similar large uncertainties in the geometric density were reported for poly(TMSP): 0.71± 0.07 g/cm^3 for the as-cast films and 0.91± 0.09 g/cm^3 for films aged for 4 years at ambient conditions.[15] Interestingly, the geometric density reported for as-cast poly(TMSP) films varies from 0.61 to 0.81 g/cm^3.[6,15-19] The difference in these density values is 0.20 g/cm^3. The wide range of reported density values of poly(TMSP) suggest that the glassy state of poly(TMSP) is very sensitive to film preparation history and may change substantially with time as nonequilibrium excess

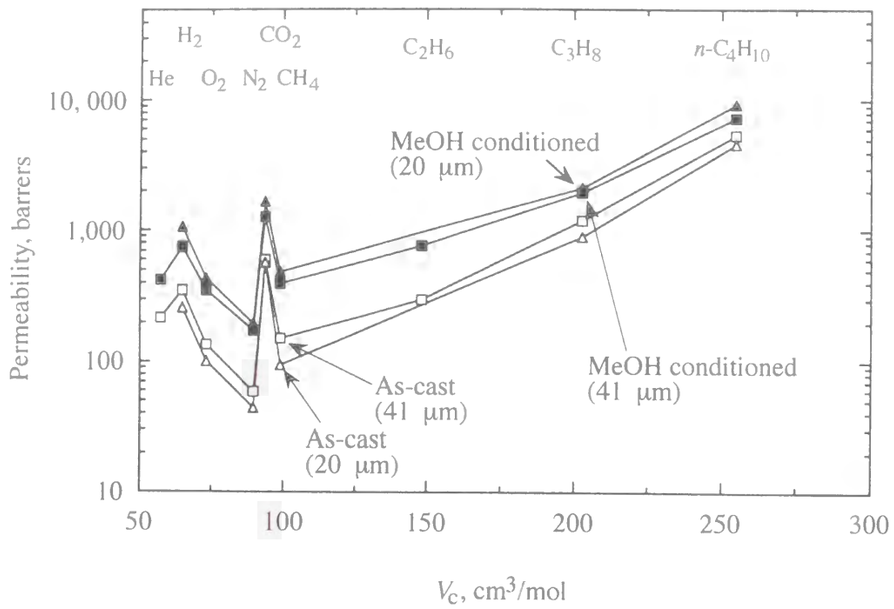

Figure 2. Effect of penetrant size (V_c=critical volume) and film thickness on gas permeability coefficients of as-cast and methanol-conditioned, unaged poly(*pi*Pr_3SiDPA) films at 35 °C. 20-μm-thick (△), 41-μm-thick (□). Methanol-conditioned films: 20-μm-thick (▲), 41-μm-thick (■).

volume relaxes. Like poly(TMSP), the free volume of poly(*pi*Pr_3SiDPA) is also sensitive to preparation history and will vary with time. These factors contribute to the large uncertainty in the density values.

Based on these density values, *FFV* is 0.15 ± 0.05 for as-cast poly(*pi*Pr_3SiDPA) and 0.17 ± 0.03 for methanol-conditioned poly(*pi*Pr_3SiDPA). Clearly, the *FFV* of poly(*pi*Pr_3SiDPA) is much lower than that of poly(TMSP) (0.29) and poly(MP) (0.28).[3,4] It is similar to that of conventional glassy polymers, such as polycarbonate (0.17) and polysulfone (0.16).[4]

Gas Permeability. Gas permeability of conventional glassy polymers, such as polysulfone, generally decreases with increasing penetrant size.[1] As shown in Figure 2, poly(*pi*Pr_3SiDPA) follows this trend only for noncondensable gases with critical volumes less than or equal to that of nitrogen. For gases with larger critical volumes, the permeability of poly(*pi*Pr_3SiDPA) films increases with increasing critical

volume. For example, C_1–C_4 hydrocarbon permeability coefficients in poly(*pi*Pr_3SiDPA) increase with increasing penetrant size. This permeability behavior is opposite to that of conventional glasses but is similar to that reported for high-free-volume, glassy polymers such as poly(TMSP) and poly(MP).[1-3] The permeability of carbon dioxide in poly(*pi*Pr_3SiDPA) is also extremely high compared to that of other gases with similar critical volumes (e.g., nitrogen, methane). These results suggest that the size-sieving behavior of poly(*pi*Pr_3SiDPA) is weak, since larger, but more soluble penetrants (e.g. *n*-butane) are much more permeable than smaller, less soluble penetrants (e.g. nitrogen).

The effects of film thickness and methanol conditioning on gas permeability of as-cast, unaged films are reported in Figure 2. The thicker as-cast film has higher gas permeabilities than the thinner as-cast film. For example, the oxygen permeability is 30% higher in the thick film (130 barrers) than in the thin film (100 barrers). After methanol conditioning, the permeabilities of both films are increased significantly, and

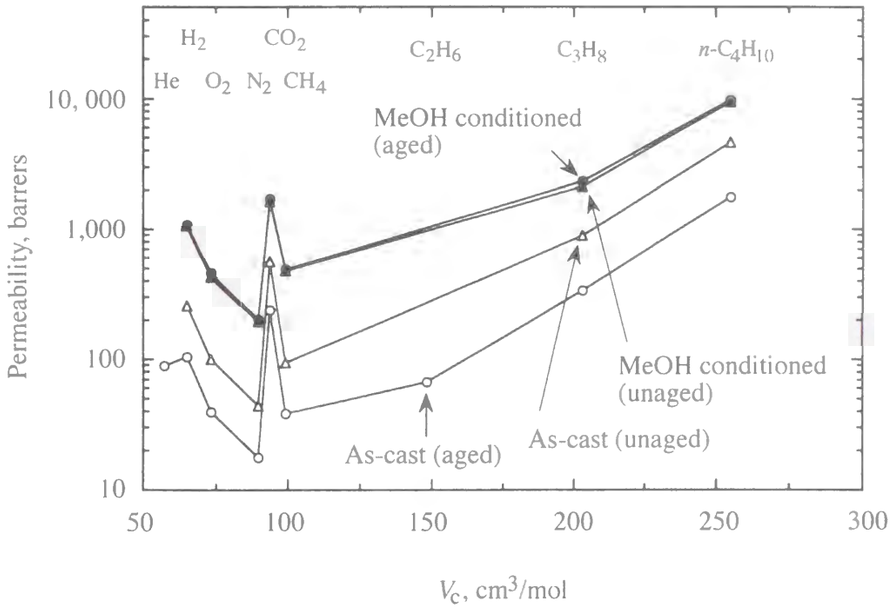

Figure 3. Effect of physical aging on gas permeability coefficients of as-cast and methanol-conditioned, 20-μm-thick poly(*pi*Pr_3SiDPA) films at 35 °C. As-cast films: unaged (△), aged (○). Methanol-conditioned films: unaged (▲), aged (●). The aging protocol is storage at ambient conditions for 7 days.

the thicker film has slightly lower permeabilities than the thinner film. For example, methanol conditioning increases the oxygen permeability of the thick and thin films to 350 and 430 barrers, respectively. These oxygen permeabilities differ by only 19%. Therefore, methanol conditioning significantly increases the permeability of both thick and thin films to all gases and reduces the difference between the permeabilities of these films.

Figure 3 presents the effect of physical aging for one week at ambient conditions on the gas permeability of 20-μm-thick poly(*pi*Pr_3SiDPA) films before and after methanol conditioning. The unaged, as-cast film has much higher gas permeabilities than the aged film. For example, the oxygen permeability is 150% higher in the unaged as-cast film (100 barrers) than in the aged film (40 barrers). After methanol conditioning, the permeabilities of both unaged and aged films increase substantially and become similar in value. For example, after methanol treatment, the oxygen permeability of the unaged and aged films increases to 430 and 460 barrers, respectively, values that are equivalent within the uncertainty in the experiment. Thus, methanol conditioning appears not only to increase permeability coefficients but also to increase the stability of permeation properties (i.e., decrease the rate of physical aging). The fundamental basis for the latter observation is not well understood but could be related to changes in the distribution of free volume elements resulting from the methanol-conditioning step.

Based on the results presented in Figures 2 and 3, the gas permeability of poly(*pi*Pr_3SiDPA) is significantly influenced by film thickness, physical aging, and methanol conditioning. In particular, methanol conditioning increases permeability. Previous studies have reported similar effects on the permeation properties of poly(TMSP) and poly(MP).[10-12] Poly(TMSP) and poly(MP) are swollen by methanol, the nonequilibrium excess free volume of the polymers increases, and gas permeability increases. For example, the oxygen permeability of poly(TMSP) decreased from 7,000 to 1,000 barrers when a film was aged under vacuum for 30 days at room temperature.[10] However, after immersion in methanol for 24 h at ambient conditions,

the aged film recovered its initial oxygen permeability value of 7,000 barrers. Similarly, as characterized by the Langmuir sorption capacity parameter C'_H, the nonequilibrium excess free volume in poly(TMSP) was reduced by aging but could be restored to its initial value by methanol-conditioning the film.

Hydrocarbon Solubility. *n*-Butane and propane sorption isotherms in poly(*pi*Pr_3SiDPA) are presented in Figures 4 and 5, respectively. Hydrocarbon uptake is higher in the unaged as-cast films than in the aged films and increases in these films after methanol conditioning. For example, at a *n*-butane relative pressure of 0.28 (70 cmHg), the methanol-conditioned, unaged film sorbs 43 cm^3(STP) *n*-C_4H_{10} /cm^3 poly(*pi*Pr_3SiDPA), which is similar to that sorbed by the methanol-conditioned, aged film [42 cm^3(STP)/cm^3]. Without methanol treatment, the *n*-butane sorption levels are only 39 and 29 cm^3(STP)/cm^3 in the unaged and aged films, respectively. Hence, methanol-conditioned films sorb 45–48% more *n*-butane than the aged sample. The above sorption order is consistent with the ranking of gas permeabilities described previously. The hydrocarbon uptake appears to decrease less with time in the methanol conditioned films than in the as-cast films, which is also consistent with the observed permeation behavior.

The *n*-butane and propane sorption isotherms in the various poly(*pi*Pr_3SiDPA) films are concave to the relative pressure axis. This concavity is characteristic of dual-mode sorption behavior, whose mathematical form is:[20-22]

$$C = k_D\, a + \frac{C'_H\, b\, a}{1 + b\, a} \qquad (1)$$

where k_D is the Henry's law coefficient [cm^3(STP) penetrant/cm^3 polymer], b is the Langmuir affinity parameter (dimensionless), and C'_H is the Langmuir capacity parameter (cm^3(STP) penetrant/cm^3 polymer). The Henry's law coefficient k_D represents the equilibrium partition coefficient of penetrant dissolved in the polymer

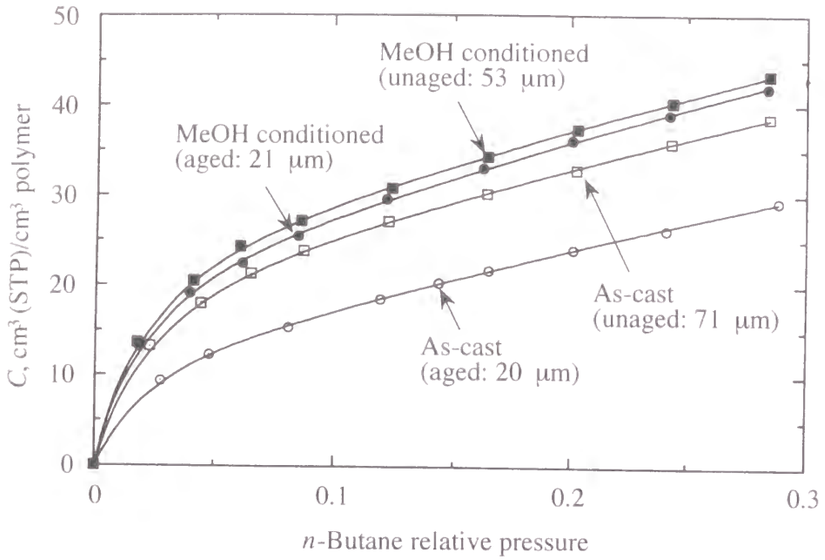

Figure 4. *n*-Butane sorption isotherms at 35 °C for as-cast unaged and aged poly(*pi*Pr$_3$SiDPA) films with and without methanol conditioning. Curves represent dual-mode fits to the data [eq. (1)]. p_{sat} (*n*-butane): 246.95 cmHg at 35 °C.[4] As-cast films: unaged, 71-μm-thick (□); aged, 20-μm-thick (○). Methanol-conditioned films: unaged, 53-μm-thick (■); aged, 21-μm-thick (●). The aging protocol is storage at ambient conditions for 7 days.

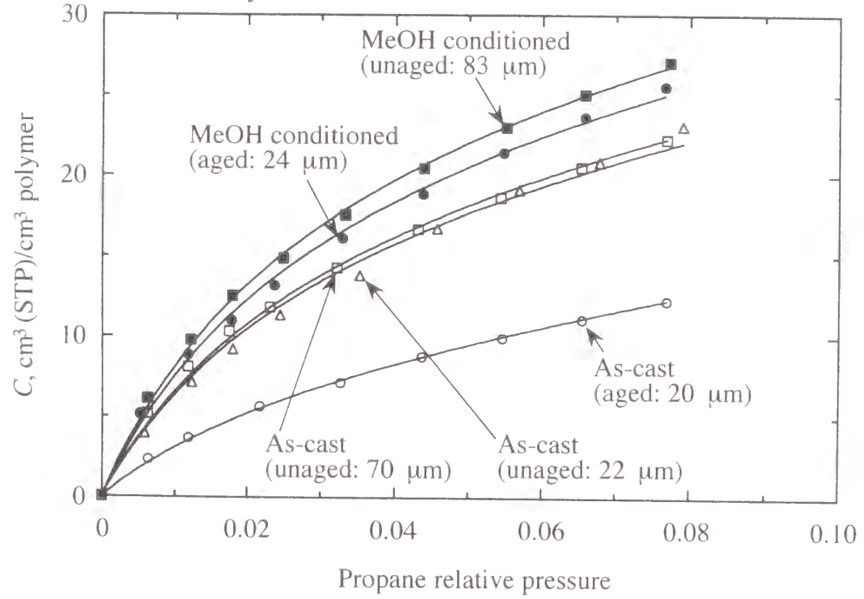

Figure 5. Propane sorption isotherms at 35 °C for as-cast unaged and aged poly(*pi*Pr$_3$SiDPA) films with and without methanol conditioning. Curves represent dual-mode fits to the data [eq. (1)]. p_{sat} (propane): 915.17 cmHg at 35 °C.[4] As-cast films: unaged, 22-μm-thick (△); unaged, 70-μm-thick (□); aged, 20-μm-thick (○). Methanol-conditioned films: unaged, 83-μm-thick film (■); aged, 24-μm-thick (●). The aging protocol is given in Table 2.

matrix. The Langmuir affinity parameter b characterizes the tendency of a penetrant to sorb into a Langmuir site. The Langmuir capacity parameter C_H' is a measure of the maximum sorption capacity of the Langmuir domains. The C_H' value is often related to the nonequilibrium excess free volume ($\hat{V}_g - \hat{V}_\ell$) in a glassy polymer by [4,8]

$$C_H' = \frac{(\hat{V}_g - \hat{V}_\ell)}{\hat{V}_g}\rho^* \qquad (2)$$

where $\hat{V}_g$ and $\hat{V}_\ell$ are the polymer specific volumes (cm^3/g) in the glassy and hypothetical equilibrium states, and ρ^* is the molar density (cm^3/cm^3) of penetrant in the Langmuir site. The nonequilibrium excess free volume fraction is (C_H'/ρ^*).

Dual-mode parameters obtained from a nonlinear least-squares regression analysis of the *n*-butane sorption data (Figure 4) are summarized in Table 1. For *n*-butane, the regression analysis was performed with all dual-mode parameters treated as adjustable constants. Within the uncertainties, the k_D and b values are the same for the four poly(*pi*Pr$_3$SiDPA) films studied, so all of the variability in the sorption isotherms in Figure 5 may be ascribed to differences in the nonequilibrium excess volume as a result of the differences in processing histories among the film.

According to the dual-mode sorption model, k_D and b are equilibrium parameters and k_D, which characterizes sorption, should not, therefore, change with physical aging or conditioning. The results in Table 1 are consistent with this point of view. For *n*-butane sorption, the C_H' value ranges from 14 cm^3(STP)/cm^3 for the unconditioned, aged film to 26 cm^3(STP)/cm^3 for the methanol-conditioned, as-cast film.

Table 1 also shows the excess free volume fraction calculated as (C_H'/ρ^*) for the various poly(*pi*Pr$_3$SiDPA) films. Based on the *n*-butane sorption data, the excess free volume fraction varies from 0.06 for the unconditioned, aged film to 0.12 for the methanol-conditioned films. The excess free volume fraction of the conditioned films is 100% higher than that of the unconditioned, aged sample. The methanol-treated

Table 1. Dual-Mode Parameters for *n*-Butane (n-C_4H_{10}) Sorption in Poly(piPr$_3$SiDPA) at 35 °C

poly(piPr$_3$SiDPA) film		film thickness [μm]	k_D $\left(\frac{cm^3(STP)\,n\text{-}C_4H_{10}}{cm^3\ poly(pi Pr_3 SiDPA)}\right)$	C'_H $\left(\frac{cm^3(STP)\,n\text{-}C_4H_{10}}{cm^3\ poly(pi Pr_3 SiDPA)}\right)$	b	C'_H/ρ^{*a}
as-cast	aged[b]	20	57 ± 7	14 ± 2	46 ± 16	0.06 ± 0.01
	unaged	71	60 ± 8	23 ± 2	44 ± 12	0.11 ± 0.01
methanol-conditioned[c]	aged[b]	21	68 ± 5	24 ± 1	50 ± 8	0.11 ± 0.01
	unaged	53	65 ± 5	26 ± 1	50 ± 7	0.12 ± 0.01

[a] $\rho^* = 220$ cm^3/cm^3 at 35 °C for n-C_4H_{10}.[4] [b] Aged at ambient conditions for 1 week. [c] Stored in methanol for at least 120 h at room temperature after film preparation and after any subsequent aging step.

films have an excess volume fraction similar to that of poly(MP) (0.12) but smaller than that of poly(TMSP)(0.21–0.28).[4-8] The unconditioned, aged film, however, has a (C'_H/ρ^*) value more comparable to that of conventional glassy polymers (0.02–0.06).[7]

For the propane sorption data shown in Figure 5, a regression analysis with all dual-mode parameters treated as adjustable constants yielded scattered k_D, C'_H, and b values with no clear trend. This result is consistent with earlier results for propane sorption in poly(TMSP)[8] and is most likely due to the narrow range of relative pressure explored. Therefore, the propane sorption data were reanalyzed by assuming, similar to the n-butane results, that k_D and b were unaffected by sample thickness, age, or methanol conditioning. Therefore, the data in Figure 5 were fit to the dual mode model with a single value of k_D and b for all isotherms, thereby confining all of the differences between the isotherms to C'_H. The resulting parameter values are recorded in Table 2. The (C'_H/ρ^*) values for propane sorption are, within the uncertainty associated with the parameters, the same as the equivalent values for n-butane sorption as was previously observed for poly(TMSP)[7]. Thus, based on the results, hydrocarbon solubility and gas permeability differences in as-cast, aged, and methanol-conditioned poly(piPr$_3$SiDPA) films are due in large measure to differences in the amount of nonequilibrium excess free volume.

Films of different thickness should have different solvent removal rates following casting. In a glassy polymer such as poly(piPr$_3$SiDPA), such differences could lead to different amounts of nonequilibrium excess volume that would, in turn, influence permeability, diffusivity, and solubility coefficients. However, for poly(piPr$_3$SiDPA) prepared under the conditions of this chapter, film thickness has, at most, a weak effect on sorption isotherms. The thicker, unaged as-cast film has slightly higher propane uptake than its thinner analog, consistent with the order of permeability for these samples (*cf.* Figure 1). However, this effect is very near the resolution of the experiment and it is not possible to make a clear distinction in the

Table 2. Dual-Mode Parameters for Propane (C_3H_8) Sorption in Poly(piPr$_3$SiDPA) at 35 °C

film	film	film thickness [μm]	k_D $\left(\frac{cm^3(STP)\ C_3H_8}{cm^3 poly(piPr_3SiDPA)}\right)$	C'_H $\left(\frac{cm^3(STP)\ C_3H_8}{cm^3\ poly(piPr_3SiDPA)}\right)$	b	C'_H/ρ^{*a}
as-cast	unaged	22	71[b]	22.7 ± 1.3	33[c]	0.094 ± 0.006
	aged[d]	20	71[b]	9.5 ± 0.1	33[c]	0.039 ± 0.001
	unaged	70	71[b]	23.4 ± 0.6	33[c]	0.097 ± 0.003
methanol-conditioned[e]	aged[f]	24	71[b]	27.3 ± 0.8	33[c]	0.11 ± 0.01
	unaged	83	71 ± 4	30[g]	33 ± 8	0.12[g]

[a] $\rho^* = 240$ cm^3/cm^3 at 35 °C for C_3H_8.[4] [b] Based on an analysis with k_D fixed at 71 cm^3(STP)/cm^3. [c] Based on an analysis with b fixed at 33. [d] Aged at ambient conditions for 21 days. [e] Stored in methanol for at least 120 h at room temperature after film preparation and after any subsequent aging step. [f] Aged at ambient conditions for 7 days. [g] Based on an analysis with C'_H fixed so that (C'_H/ρ^*) is 0.12, as determined from n-butane sorption data.

sorption properties of the thin and thick as-cast sample. The uncertainties in propane C'_H values in Table 2 reflect this point as well.

Hydrocarbon Diffusivity. The diffusivity of n-butane and propane was determined from kinetic sorption data. Representative kinetic curves obtained at low and high penetrant relative pressure are shown in Figures 6a and 6b, respectively, for propane sorption in a methanol-conditioned, 83-μm-thick poly(piPr$_3$SiDPA) film. M_t and M_∞ are the mass of penetrant (mg) sorbed at time t (s) and at equilibrium, respectively. In Figure 6a, the initial portion of the curve ($0.2 < M_t/M_\infty \leq 0.6$) is a linear function of $t^{1/2}$, consistent with Fickian diffusion controlling mass uptake. When these data are extrapolated to zero uptake ($M_t/M_\infty = 0$), however, they do not pass through the origin at $t = 0$, resulting in a small induction period. For propane sorption kinetics in poly(piPr$_3$SiDPA) at low penetrant relative pressures, this induction period is less than 5 s, as determined from the intersection of the extrapolated linear portion of the M_t/M_∞ curve with the abscissa. At higher penetrant relative pressure, propane sorption into the poly(piPr$_3$SiDPA) film occurs very quickly up to a fractional uptake of $M_t/M_\infty = 0.9$ and then approaches the final equilibrium state ($M_t/M_\infty = 1$) more gradually, as shown in Figure 6b. The induction period observed in Figure 6a and the protracted approach to equilibrium indicated in Figure 6b are often observed for organic-vapor diffusion into glassy polymers and are usually explained in terms of the time required to establish a constant surface concentration boundary condition and relaxation effects, respectively.[23,24]

For short times ($0 \leq M_t/M_\infty \leq 0.6$), the following equation is valid for one-dimensional Fickian diffusion in a plane sheet:[23]

$$\frac{d(M_t/M_\infty)}{dt^{1/2}} = \left(\frac{16D}{\ell^2\pi}\right)^{1/2} \tag{3}$$

Propane and n-butane diffusion coefficients in the poly(piPr$_3$SiDPA) films were calculated using equation 3 and the short-time kinetic data (0.2

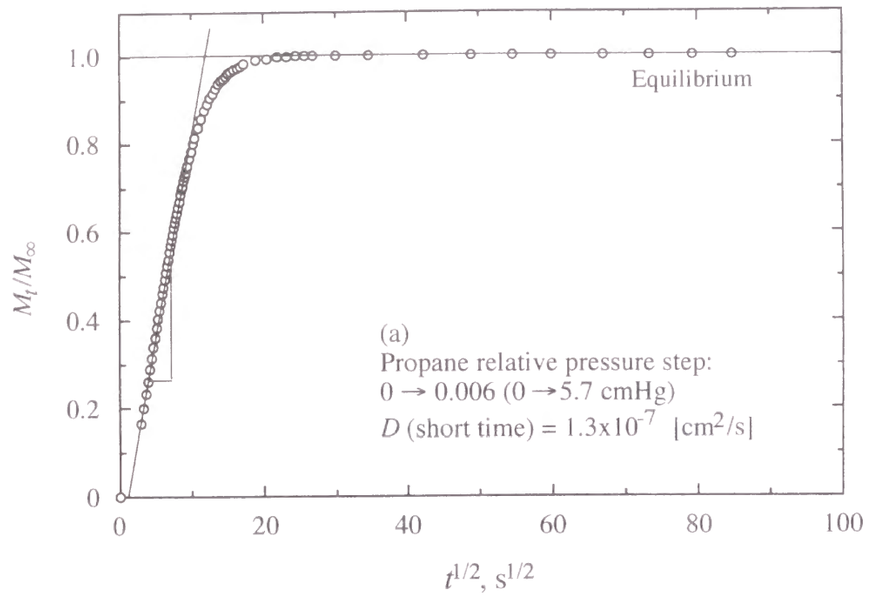

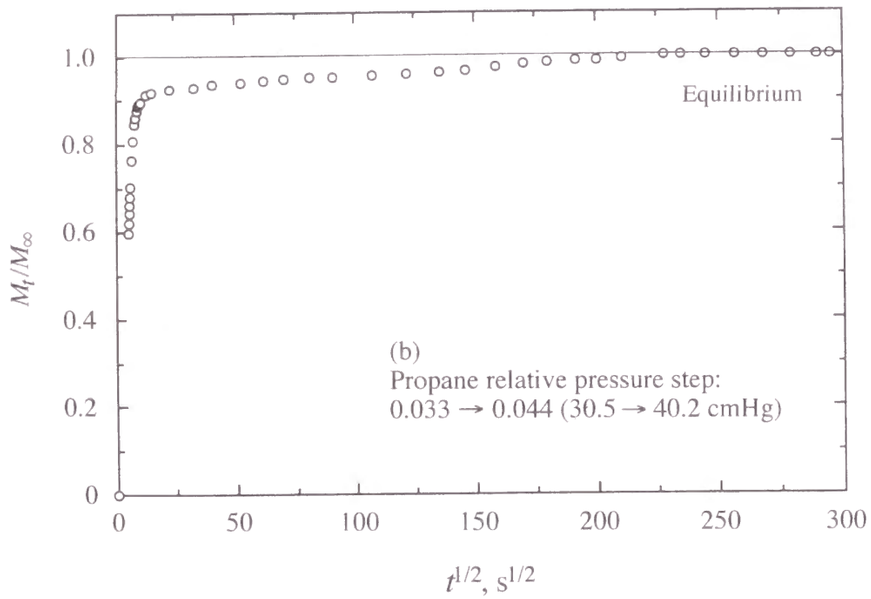

Figure 6. Kinetics of propane sorption in a methanol-conditioned, unaged, 83-μm-thick poly(piPr$_3$SiDPA) film at 35 °C. Propane relative pressure step (initial → final): (a) 0 → 0.006 (0 → 5.7 cmHg) and (b) 0.033 → 0.044 (30.5 → 40.2 cmHg). p_{sat} (propane): 915.17 cmHg at 35 °C[4].

< $M_t / M_\infty \leq 0.6$) measured at low penetrant pressures (e.g., Figure 6a). The *n*-butane sorption kinetics displayed similar characteristics and were analyzed in the same fashion.

The diffusion coefficients of *n*-butane and propane are presented in Figures 7 and 8, respectively, as a function of the average penetrant concentration, C_{av}:

$$C_{av} = \frac{C_i + C_f}{2} \tag{4}$$

where C_i and C_f are the penetrant concentrations (cm^3(STP) penetrant/cm^3 polymer) in the polymer at the beginning and end of the sorption experiment, respectively. The hydrocarbon diffusivities in poly(piPr$_3$SiDPA) films increase with increasing penetrant concentration, as shown in Figures 7 and 8. A similar concentration dependence was reported for the diffusion of propane in another substituted polyacetylene, poly(*tert*-butylacetylene).[25] Interestingly, at low penetrant pressures, *n*-pentane and ethanol diffusivities in poly(TMSP) decrease with increasing penetrant concentration.[26,27]

For *n*-butane, the thin, as-cast, aged film has the lowest diffusion coefficients, the lowest sorption levels (*cf.* Figure 4), and the lowest permeability coefficients (*cf.* Figure 3). The methanol conditioned films exhibit higher diffusion coefficients at low *n*-butane concentrations than the as-cast samples. (Unfortunately, the author do not have a full range of diffusion coefficient values for the thin methanol conditioned film to know if its diffusivity would be systematically higher than that of the other samples at all concentrations.) The methanol-conditioned films have higher sorption levels (*cf.* Figure 4) and higher permeability coefficients than the as-cast samples (*cf.* Figure 3). The thicker as-cast, unaged film has higher *n*-butane diffusion coefficients and higher *n*-butane solubility coefficients (*cf.* Figure 4) than the thinner, as-cast, aged film. All of these results are consistent with the samples having higher nonequilibrium excess free volume having higher *n*-butane solubility, diffusivity, and permeability coefficients.

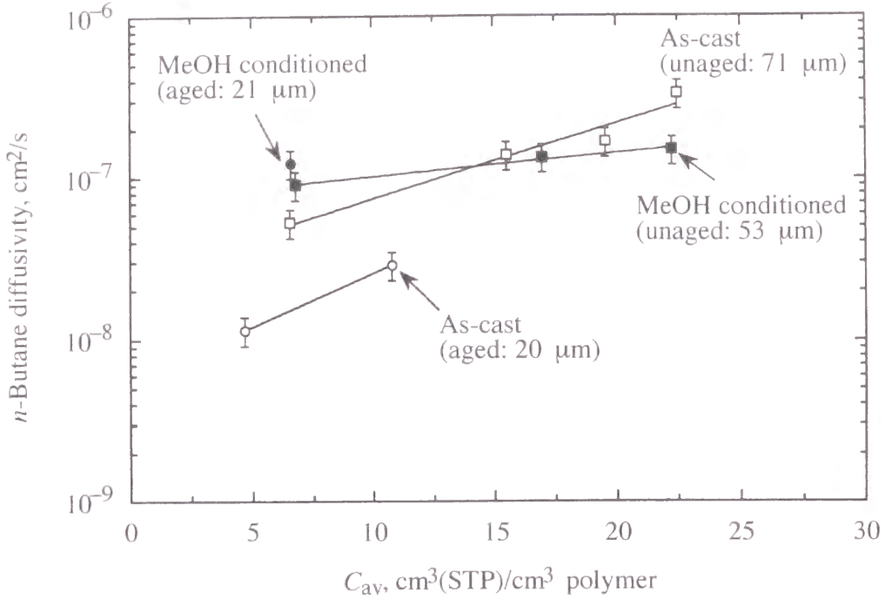

Figure 7. Effect of average penetrant concentration on *n*-butane diffusion coefficient in as-cast and methanol conditioned unaged and aged films at 35 °C. As-cast films: unaged, 71-μm-thick (□); aged, 20-μm-thick (○). Methanol-conditioned films: unaged, 53-μm-thick (■); aged, 21-μm-thick (●).

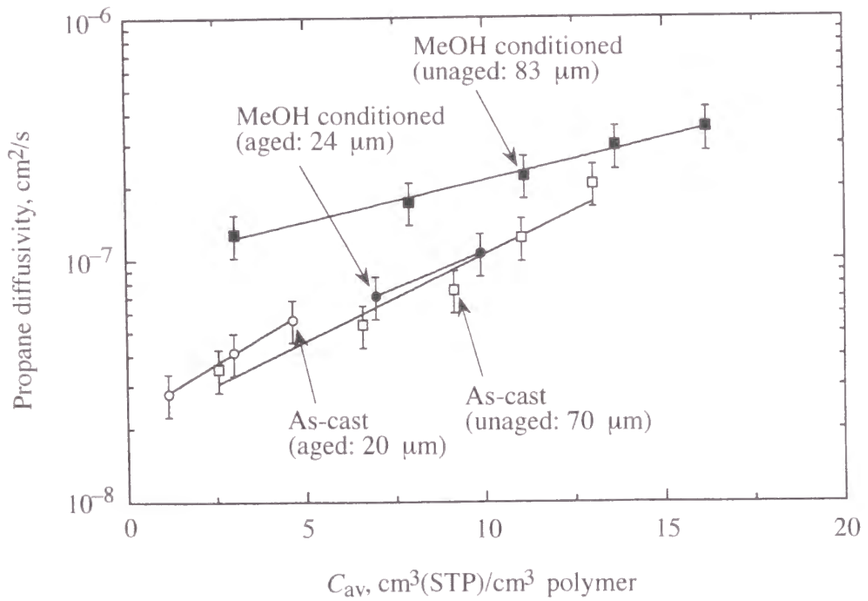

Figure 8. Effect of average penetrant concentration on propane diffusion coefficient in as-cast and methanol conditioned unaged and aged films at 35 °C. As-cast films: unaged, 70-μm-thick (□); aged, 20-μm-thick (○). Methanol-conditioned films: unaged, 83-μm-thick (■); aged, 24-μm-thick (●).

Curiously, the concentration dependence of the *n*-butane diffusion coefficient is weaker in the unaged, methanol conditioned film than in the as-cast unaged film so that at higher *n*-butane concentrations, the diffusivity of the as-cast sample is higher than that of the methanol conditioned, unaged sample. However, the *n*-butane uptake is higher at all relative pressures in the methanol conditioned, unaged film than in the as-cast, unaged film (*cf.* Figure 4). These results suggest that effects more subtle than simply overall nonequilibrium excess volume (as measured by C_H'/ρ^*), perhaps the distribution of non-equilibrium excess free volume elements and the distribution of penetrants within these free volume elements, probably also contribute in a significant way to the diffusion behavior of *n*-butane in these samples.

As shown in Figure 8, as-cast samples generally have lower propane diffusion coefficients than methanol conditioned films though the aged, methanol conditioned film had propane diffusion coefficients only slightly higher than those of the as-cast, unaged film. The order of the propane diffusion coefficients is not the same as the order of the propane sorption isotherms (*cf.* Figure 5), suggesting, like for *n*-butane, that propane diffusion coefficients are also sensitive to factors beyond simply average nonequilibrium excess volume.

Intrinsic Gas Transport Properties. Regardless of film preparation history and age, methanol conditioning increases the nonequilibrium excess free volume in poly(*pi*Pr$_3$SiDPA). C_H' values are highest and nearly identical for methanol-conditioned unaged and methanol-conditioned aged films, which have similar hydrocarbon uptake. These results are consistent with the permeability data. The average gas permeabilities and gas/nitrogen selectivities of a methanol-conditioned, unaged thick poly(*pi*Pr$_3$SiDPA) film shown in Figure 2 are presented in Table 3. The oxygen permeability of the conditioned films is comparable to that of silicone rubber and roughly one order of magnitude lower than that of poly(TMSP) and poly(MP).[2,3,10] Like poly(TMSP) and poly(MP), though, poly(*pi*Pr$_3$SiDPA) is more permeable to propane and *n*-butane than to hydrogen and nitrogen. Although the *FFV* of poly(*pi*Pr$_3$SiDPA) films is similar to that of conventional glassy polymers, their

Table 3. Gas Permeability Coefficients and Pure-Gas Selectivities over Nitrogen in Methanol-Conditioned, Unaged 41-μm-thick Poly(*pi*Pr_3SiDPA) Film at 35 °C

gas	permeability[a], barrers	gas/N_2 selectivity
H_2	740	4.4
He	420	2.5
N_2	170	1.0
O_2	350	2.1
CO_2	1,300	7.6
CH_4	390	2.3
C_2H_6	760	4.5
C_3H_8	1,900	11
n-C_4H_{10}	7,300	43

[a] Permeability values of the film shown in Figure 2.

Table 4. Infinite-Dilution Solubility, Diffusivity, and Permeability of Propane and *n*-Butane in Methanol-Conditioned Poly(*pi*Pr_3SiDPA) Films at 35 °C[a]

	propane	*n*-butane
S_0[b]	1.2	5.5
D_0[c]	9.8×10^{-8}	7.3×10^{-8}
P_0[d]	1.2×10^{-7}	4.0×10^{-7}

[a] Determined from sorption experiments on a 83-μm-thick as-cast film for propane and a 53-μm-thick as-cast film for *n*-butane. [b] S_0 [=] cm^3(STP)/cm^3·cmHg. [c] D_0 [=] cm^2/s. [d] $P_0 = S_0 \times D_0$ [=] cm^3(STP)·cm/(cm^2·s·cmHg).

gas permeabilities are much higher than those of common glasses due, presumably, to a much larger excess free volume fraction. These results underscore the importance of free volume distribution on gas transport properties.

Unlike conventional glassy polymers, hydrocarbon permeability in poly(*pi*Pr_3SiDPA) increases with increasing critical volume. The infinite-dilution solubility, diffusivity, and permeability of propane and *n*-butane in methanol-conditioned poly(*pi*Pr_3SiDPA) films are recorded in Table 4. Consistent with expectations based on penetrant condensability, infinite-dilution *n*-butane solubility is higher than propane solubility, while, in accord with penetrant-size expectations, *n*-butane diffusivity is lower than that of propane. However, the increase in solubility on going from propane to *n*-butane is stronger than the decrease in diffusivity and, as a result, poly(*pi*Pr_3SiDPA) is more permeable to *n*-butane than to propane. The same trend was reported for poly(TMSP).[5]

Experimental

Material. Synthesis of poly(*pi*Pr_3SiDPA) was performed as described in Chapter 1: in toluene at 80 °C for 24 h; $[M]_0 = 0.10$ M, $[TaCl_5] = 20$ mM, $[n\text{-}Bu_4Sn] = 40$ mM. The polymer yield was 80%. The weight-average molecular weight was 4×10^6. Detailed polymer properties are given in Chapter 1.[14]

Film Preparation. Isotropic, dense films of poly(*pi*Pr_3SiDPA) were prepared by casting a 1 wt% toluene solution of the polymer onto a glass plate. The plate was covered with a glass dish to slow the rate of solvent evaporation. Films were dried at ambient conditions for 2 weeks for thin samples (10–25 μm in thickness) and 3 weeks for thicker samples (40–85 μm in thickness). They were then stored under vacuum at room temperature for 24 h to remove residual solvent. Some as-cast poly(*pi*Pr_3SiDPA) films were used directly for gas permeation and sorption experiments. Other thin as-cast films (10–25 μm in thickness) were stored (i.e., aged) for an additional 1 or 3 weeks at ambient conditions before testing. Some unaged and aged films were also immersed in methanol until sorption equilibrium was attained

(~ 120 h). These conditioned films were removed from methanol and dried gradually at ambient conditions for 20–24 h (i.e., until the weight of the films became constant) before being used in sorption or permeation experiments.

Characterization. Density was determined from film weight and volume at ambient conditions. The fractional free volume (*FFV*) was estimated from

$$FFV = \frac{V - 1.3V_W}{V} \tag{5}$$

where V is the polymer specific volume (reciprocal of density) and V_W is the specific van der Waals volume estimated from van Krevelen's group contribution method.[28] Thermal properties were determined using a Perkin-Elmer Pyris 1 differential scanning calorimeter (DSC) operated at a heating rate of 10 °C/min from 50 to 250 °C with a nitrogen purge.

Gas Permeation. Pure-gas permeabilities of the various poly(*pi*Pr_3SiDPA) films were determined using a constant-pressure/variable-volume method at 35 °C.[2-5] The gases used were He, H_2, N_2, O_2, CH_4, C_2H_6, C_3H_8, *n*-C_4H_{10}, and CO_2. The feed pressure was 50 psig (4.4 atm) for all gases, except *n*-butane (10 psig, 1.7 atm); the permeate pressure was maintained at 0 psig (1 atm). Before beginning the gas permeation measurements, the permeation cell containing the polymer film to be tested was allowed to equilibrate at 35 °C for 20–24 h.

Gas Sorption. The sorption of pure propane and *n*-butane in the poly(*pi*Pr_3SiDPA) films was determined gravimetrically as a function of pressure at 35 °C using a Cahn 2000 electrobalance sorption system.[4,8] After loading the polymer film into the sample chamber, the sorption system was evacuated for 20–24 h at 35 °C to degas the polymer film. Hydrocarbon penetrant was then introduced into the sorption chamber, and penetrant uptake was recorded as a function of time.

References

1) Freeman, B. D.; Pinnau, I. *Trends. Polym. Sci.* **1997**, *5*, 167.

2) Pinnau, I.; Toy, L. G. *J. Membr. Sci.* **1996**, *116*, 199.
3) Morisato, A.; Pinnau, I. *J. Membr. Sci.* **1996**, *121*, 243.
4) Toy, L. G.; Nagai, K.; Freeman, B. D.; Pinnau, I.; He, Z.; Masuda, T.; Teraguchi, M. submitted to *Macromolecules.*
5) Merkel, T. C.; Bondar, V.; Nagai, K.; Freeman, B. D. submitted to *Macromolecules.*
6) Volkov, V. V. *Polym. J.* **1991**, *23*, 457.
7) Srinivasan, R.; Auvil, S. R.; Burban, P. M. *J. Membr. Sci.* **1994**, *86*, 67.
8) Morisato, A.; Freeman, B. D.; Pinnau, I.; Casillas, C. G. *J. Polym. Sci., Part B: Polym. Phys.* **1996**, *34*, 1925.
9) Struik, L. C. E. *Physical Aging in Amorphous Polymers and Other Materials*; Elsevier: Amsterdam, 1978.
10) Nagai, K.; Higuchi, A.; Nakagawa, T. *J. Polym. Sci., Part B: Polym. Phys.* **1995**, *33*, 289.
11) Nagai, K.; Nakagawa, T. *J. Membr. Sci.* **1995**, *105*, 261.
12) Morisato, A.; He, Z.; Pinnau, I. In *Polymer Membranes for Gas and Vapor Separation: Chemistry and Materials Science*; Freeman, B. D., Pinnau, I., Eds.; ACS Symp. Ser. 733; Am. Chem. Soc., 1999; Chapter 4, p 56.
13) Nagai, K. *Maku (Membrane)* **1997**, *22*, 206.
14) Chapter 1 of this thesis; *J. Polym. Sci., Part A: Polym. Phys.* **1998**, *36*, 2721.
15) Yampol'skii, Y. P.; Shishatskii, S. M.; Shantorovich, V. P.; Antipov, E. M.; Kuzmin, N. N.; Rykov, S. V.; Khodjaeva, V. L.; Plate, N. A. *J. Appl. Polym. Sci.* **1993**, *48*, 1935.
16) Witchey-Lakshmanan, L. C.; Hopfenberg, H. B.; Chern, R. T. *J. Membr. Sci.* **1990**, *48*, 321.
17) Jia, J.; Baker, G. L. *J. Polym. Sci., Part B: Polym. Phys.* **1998**, *36*, 959.
18) Ichiraku, Y.; Stern, S. A.; Nakagawa, T. *J. Membr. Sci.* **1987**, *34*, 5.
19) Nakanishi, K.; Odani, H.; Kurata, M.; Masuda, T.; Higashimura, T. *Polym. J.* **1987**, *19*, 293.

20) Barrer, R. M.; Barrie, J. A.; Slater, J. *J. Polym. Sci.* **1958**, *27*, 177.

21) Michaels, A. S.; Vieth, W. R.; Barrie, J. A. *J. Appl. Phy.* **1963**, *34*, 1.

22) Vieth, W. R.; Tam, P. M.; Michaels, A. S. *J. Colloid and Interface Sci.* **1966**, *22*, 360.

23) Crank, J. In *The Mathematics of Diffusion,* 2nd ed.; Oxford University Press: Oxford, 1975.

24) Berens, A. R.; Hopfenberg, H. B. *J. Polym. Sci., Part B: Polym. Phys.* **1979**, *17*, 1757.

25) Morisato, A.; Miranda, N. R.; Freeman, B. D.; Hopfenberg, H. B.; Costa, G.; Grosso, A.; Russo, S. *J. Appl. Polym. Sci.* **1993**, *49*, 2065.

26) Doghieri, F.; Biavati, D.; Sarti, G. C. *Ind. Eng. Chem. Res.* **1996**, *35*, 2420.

27) Doghieri, F.; Sarti, G. C. *J. Polym. Sci., Part B: Polym. Phys.* **1997**, *35*, 2245.

28) van Krevelen, D. W. In *Properties of Polymers,* 3rd ed.; Elsevier: Amsterdam, 1990.

Chapter 8

Relationship between the Gas Permeability and Local Mobility of Disubstituted Acetylene Polymers: Investigation by Quasielastic Neutron Scattering

Abstract

The local mobility of three substituted polyacetylenes (i.e., poly[1-(trimethylsilyl)-1-propyne] [poly(TMSP)], poly[1-phenyl-2-[*p*-(trimethylsilyl)phenyl]acetylene] [poly(pMe$_3$SiDPA)], and poly[1-phenyl-2-[*p*-(triisopropylsilyl)phenyl]acetylene] [poly(piPr$_3$SiDPA)]) was investigated by means of quasielastic neutron scattering technique, aiming at elucidation of the relationship between the local mobility of substituents in the polymer and the gas permeability. Although all of the polymers have bulky trialkylsilyl groups, their P_{O2} values were quite different, i.e., in the order of poly(TMSP) > poly(pMe$_3$SiDPA) > poly(piPr$_3$SiDPA). It was found that the local flux, which is defined as the product of the relaxation rate (Γ) and mobile fraction (f_m) increased with the gas permeability coefficient. This result indicates that local flux is one of the important factors to control gas permeability.

Introduction

In general, substituted polyacetylenes exhibit relatively high gas permeability among all the examined polymers.[1,2] Among them, poly[1-(trimethylsilyl)-1-propyne] [poly (TMSP)] is a colorless solid polymer soluble in common solvents such as toluene and chloroform, and provides a free-standing membrane by solution casting. It shows extremely high permeability to various gases; e.g., the oxygen permeability coefficient (P_{O2}) ~ 4000 barrers [1 barrer = $1x10^{-10}$ cm^3 (STP) · cm/(cm^2 · s · cmHg) (25 °C).[3-7] This polymer shows unique features in the gas permeation behavior. For instance, it is glassy at room temperature unlike poly(dimethylsiloxane) [poly(DMS)], and its gas permeation is explained in terms of the dual-mode sorption and diffusion mechanism, which involves both the Langmuir-type sorption and the Henry-type solution.

It was found several years ago that poly[1-phenyl-2-[*p*-(trimethylsilyl)phenyl]-acetylene] [poly(*p*Me_3SiDPA)] also permeates gases fairly well.[8,9] Thus its P_{O2} value is 1100 barrers (25 °C), corresponding to about 1/4 that of poly(TMSP) and about twice that of poly(DMS). Poly(*p*Me_3SiDPA) is thermally much more stable than poly(TMSP), which will be an important factor when their practical application as separation membranes is considered. The high gas permeability of poly(TMSP) and poly(*p*Me_3SiDPA) suggests that both stiff main chain and round-shaped side groups play an important role in the gas permeation through substituted polyacetylene membranes.

In Chapter 1, however, it has turned out that the P_{O2} values (25 °C) of poly[1-phenyl-2-[*p*-(triisopropylsilyl)phenyl]acetylene] [poly(*pi*Pr_3SiDPA)] and poly[1-phenyl-2-[*p*-(triphenylsilyl)phenyl]acetylene] [poly(*p*Ph_3SiDPA)] are 20 and 3.8 barrers, respectively,[10] which are much smaller than that of poly(*p*Me_3SiDPA). A possible explanation for the relatively low permeability of poly(*pi*Pr_3SiDPA) and poly(*p*Ph_3SiDPA) is that, if the round-shaped substituent is too large, its mobility is low, which leads to low permeability.

Inelastic and quasielastic neutron scatterings (INS and QENS) are powerful

tools for investigation of molecular motion. In the measurements, the scattering intensity is recorded as functions of energy and momentum transfer of neutrons, providing information about both time and spatial scales of motion simultaneously. Generally speaking, quasielastic neutron scattering scans the ranges of 10^{-13} to 10^{-8} s in time and of 1 to 600 Å in space, which are suitable for studying the motions of polymer molecules. Thus, many studies have so far been carried out on the dynamics of macromolecules;[11,12] e.g., reptation motions in polymer melts,[13] hydrodynamic interactions in polymer solutions,[14] dynamics in glassy states[15,16] and near glass transition temperature,[17,18] and rotational motions of methyl groups.[19,20]

In this chapter, the author investigated the local mobility of poly(TMSP), poly(*p*Me_3SiDPA) and poly(*pi*Pr_3SiDPA) by means of a quasielastic neutron scattering technique to obtain information about whether the relatively low permeability of poly(*pi*Pr_3SiDPA) is caused by its low mobility.

Results and Discussion

Gas Permeability of Several Substituted Polyacetylenes. Figure 1 represents the permeabilities of poly(TMSP), poly(*p*Me_3SiDPA), and poly(*pi*Pr_3SiDPA) membranes to various gases as polygonal lines; these data are based on references 6, 9, and 10. It is very clear that the gas permeability varies to a large extent, depending on the polymer structure, i.e., in the order of poly(TMSP) > poly(*p*Me_3SiDPA) > poly(*pi*Pr_3SiDPA). It is a very interesting subject to elucidate the reason of such large variations. On the other hand, the patterns of these polygonal lines are very similar to one another, which suggests that the mechanisms of gas permeation through these polyacetylenes are essentially the same.

Elastic Scattering. In order to obtain information on the atomic motion from the temperature factor, which gives the mean square displacement of H atoms, the elastic scattering was first measured. In Figure 2, logarithm of the elastic scattering intensity $I_{el}(Q)$ is plotted against Q^2 for poly(TMSP), poly(*p*Me_3SiDPA) and poly(*pi*Pr_3SiDPA), where the elastic intensity is normalized to unity at $Q = 0$. In

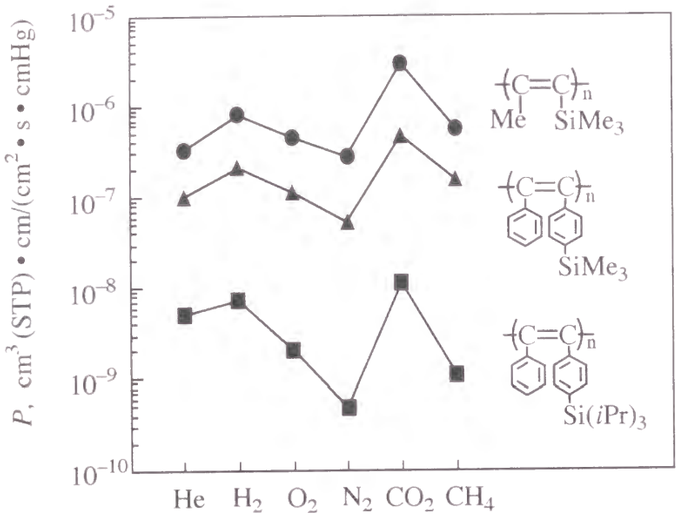

Figure 1. Gas permeability coefficients (P) of polyacetylenes having silyl groups (25 °C).

the Gaussian approximation,[25] the Q dependence of incoherent elastic scattering intensity $I_{el}(Q)$ is given by

$$I_{el}(Q) = \exp\left[-< u^2 > Q^2 / 3\right] \qquad (1)$$

for isotropic three-dimensional motions. Here, $<u^2>$ is a mean square displacement of an atom. As seen in Figure 2, the relation of eq. (1) perfectly holds for the three samples, and hence the mean square displacement $<u^2>$ from the slopes of the straight lines was evaluated. As mentioned above, the scattering intensities of the present samples are dominated by incoherent scattering from hydrogen atoms, so that $<u^2>$ reflects the amplitudes of motion of hydrogen atoms. The evaluated mean square displacements $<u^2>$ are listed in Table 1. Poly(TMSP) has the largest $<u^2>$ among them, which corresponds to the largest gas permeability coefficient as shown in Figure 1. Probably the large amplitude of motions in poly(TMSP) accelerates the mobility of gases, leading to the large gas permeability.

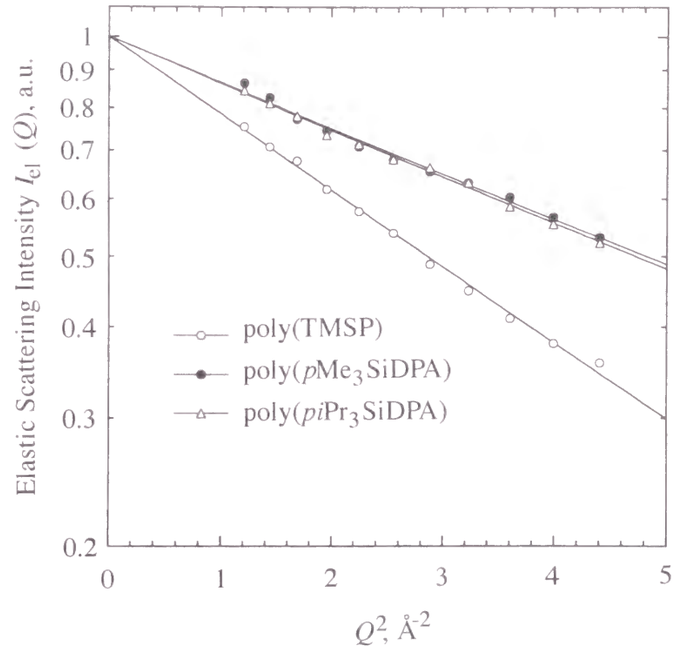

Figure 2. Q dependence of elastic scattering intensity I_{el} (Q) for poly(TMSP), poly(pMe$_3$SiDPA) and poly(piPr$_3$SiDPA).

Table 1. Results of Quasielastic Neutron Scattering for Poly(TMSP), Poly(pMe$_3$SiDPA), and Poly(piPr$_3$SiDPA)

polymer	$<u^2>$, Å^2	Γ, meV	f_m
poly(TMSP)	0.72	0.45	0.045
poly(pMe$_3$SiDPA)	0.44	0.34	0.012
poly(piPr$_3$SiDPA)	0.43	0.21	0.0053

Quasielastic Scattering. For the purpose to obtain information about the relaxational motions, the author observed quasielastic neutron scattering spectra or dynamic scattering laws $S(Q,\omega)$ of poly(TMSP), poly(pMe$_3$SiDPA) and poly(piPr$_3$SiDPA) at 296 K, which are shown in Figure 3. These spectra were normalized to the total scattering intensity in the present energy region of 0 to 3 meV. The dotted curve in the figure is the resolution function of the spectrometer. All the spectra contain the elastic scattering contribution within the resolution function,

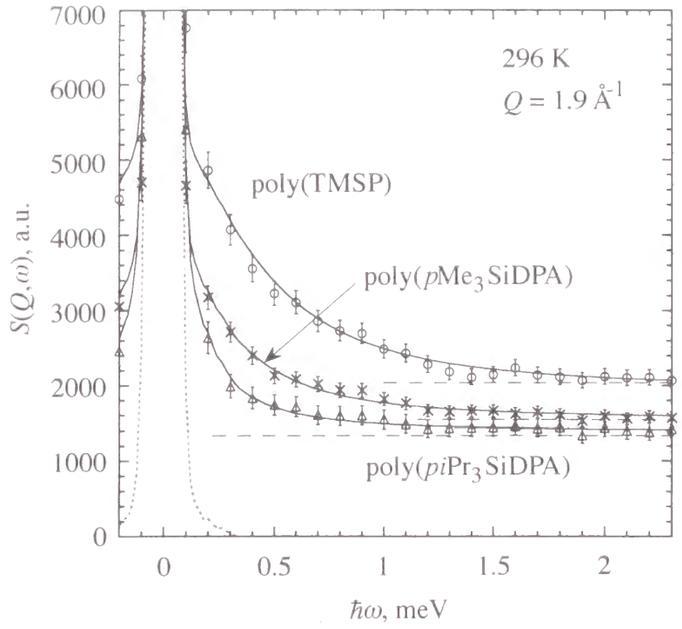

Figure 3. Quasielastic neutron scattering spectra $S(Q,\omega)$ for poly(TMSP), poly(pMe$_3$SiDPA) and poly(piPr$_3$SiDPA) measured at Q = 1.9 Å^{-1}. The dotted curve is the resolution function of the spectrometer. The solid curves are the results of fits with eq. (2) (see text). The dashed lines represent the inelastic contribution.

showing that there exist immobile molecules (or segments) and/or that such motion is localized in a limited space.[12] In addition to the elastic scattering, the quasielastic spectral broadening is observed in an energy region below about 1.5 meV over the inelastic flat background indicated by dashed lines. The quasielastic and inelastic components originate from relaxational and vibrational motions in the polymers, respectively.

In order to analyze the spectra of Figure 3, it was assumed that the dynamic scattering law $S(Q,\omega)$ is phenomenologically described by

$$S(Q,\omega) = (1 - f_m)\delta(\omega) + f_m S_{rel}(Q,\omega) + B_{in}(Q) \qquad (2)$$

Here, $\delta(\omega)$ and f_{m} are a δ-function describing the scattering law from the immobile part and the fraction of the mobile part, respectively, and $S_{\mathrm{rel}}(Q,\omega)$ and $B_{\mathrm{in}}(Q)$

represent relaxational and vibrational spectra, respectively. It was further assumed that the relaxational spectrum $S_{\mathrm{rel}}(Q,\omega)$ is described by a Lorentzian:

$$S_{rel}(Q,\omega) = \frac{1}{\pi}\frac{\Gamma}{\Gamma^2 + \omega^2} \qquad (3)$$

where Γ is a relaxation rate, corresponding to the inverse of the relaxation time τ ($\Gamma = h/\tau$, h being Planck's constant). After convoluting the model function [eq. (2)] with the energy resolution function of the spectrometer, it was fitted to the observed spectra. The solid curves in Figure 3 show the results of the fits. The agreements are excellent, which confirms that the above simple phenomenological model can adequately describe the observed spectra.

We also analyzed the same spectra in terms of a three-site rotating jump motion[26] of methyl groups by taking into account their mobile fraction because the incoherent scattering cross-section of methyl groups is much larger than the other scattering cross-sections. It was found that the relaxation (jump) rate of methyl protons and the mobile fraction evaluated in the three-site rotating model are almost the same as those in the above phenomenological model, which suggests that the quasielastic scattering intensity is mainly governed by the rotational motion of methyl groups in these polymers. In the case of poly(piPr$_3$SiDPA), strictly speaking, one must take into account rotational motions of i-propyl group for detailed analysis.

The evaluated relaxation rate Γ and the mobile fraction f_{m} are summarized in Table 1. Both the relaxation rate and the mobile fraction decrease in the order of poly(TMSP) > poly(pMe$_3$SiDPA) > poly(piPr$_3$SiDPA), and obviously depend on the molecular structure. Since the mobile fraction does not necessarily increase with increasing mobility in polymers, the observed correlation between the mobility and the mobile fraction is characteristic to these three polymers.

Relationship between the Local Mobility and the Gas Permeability. In order to see the relations of the relaxation rate and the mobile fraction to the gas permeability, Γ and f_{m} are plotted as a function of the CO_2 permeability coefficient P

for the three polymers in Figure 4 (a) and (b), respectively. The larger the relaxation rate and the mobile fraction, the larger the permeability; this suggests that both the relaxation rate and the mobile fraction are important factors to determine the gas permeability. The local flux can be defined as the product of the relaxation rate and the mobile fraction, Γ x f_m, and employed as a measure of local mobility. It is expected that the gas permeability is governed by the local flux. The local flux Γ x f_m is plotted in Figure 4 (c) versus the CO_2 permeability coefficient. This plot strongly suggests the existence of a correlation between the local flux and the gas permeability. It is, however, noted that the local flux Γ x f_m of poly(*pi*Pr$_3$SiDPA) is about one order of magnitude smaller than that of poly(TMSP), while the gas permeability coefficient of poly(*pi*Pr$_3$SiDPA) is about two orders of magnitude lower than that of poly(TMSP) for several kinds of gases (see Figure 1). A reason may be that the gas permeability coefficient (*P*) has been employed in place of the diffusion coefficient (*D*), which does not involve the factor of solubility (*S*) (however, the contribution of *S* to *P* is rather small and *D* is correlated with *P* well[6]).

The gas permeation through glassy polymers is explained in terms of the dual-mode mechanism, which postulates the presence of two phases, i.e., one governed by the Langmuir sorption and the other controlled by the Henry law.[1,2] Introduction of long *n*-alkyl and phenyl groups in substituted polyacetylenes generally decreases gas permeability,[6] which is explicable by the decrease of molecular-scale voids and in turn by the decrease of the contribution of the Langmuir term. On the other hand, the following explanation is plausible in the case of the polymers in this chapter. We assume that the Langmuir and Henry terms work in series unlike the conventional idea that they work in parallel. It is rather unlikely that the presence of very bulky groups such as *i*-Pr$_3$Si and Ph$_3$Si decreases the molecular scale voids and hence the Langmuir term will not largely vary among the present polymers. Then, the order of magnitude of gas permeability in the present polymers will be affected by the Henry term, which is strongly governed by the local mobility. This chapter has demonstrated a possibility that, besides the presence of molecular-scale voids, the local mobility of polymer molecules plays an important role in the gas permeability of glassy polymers.

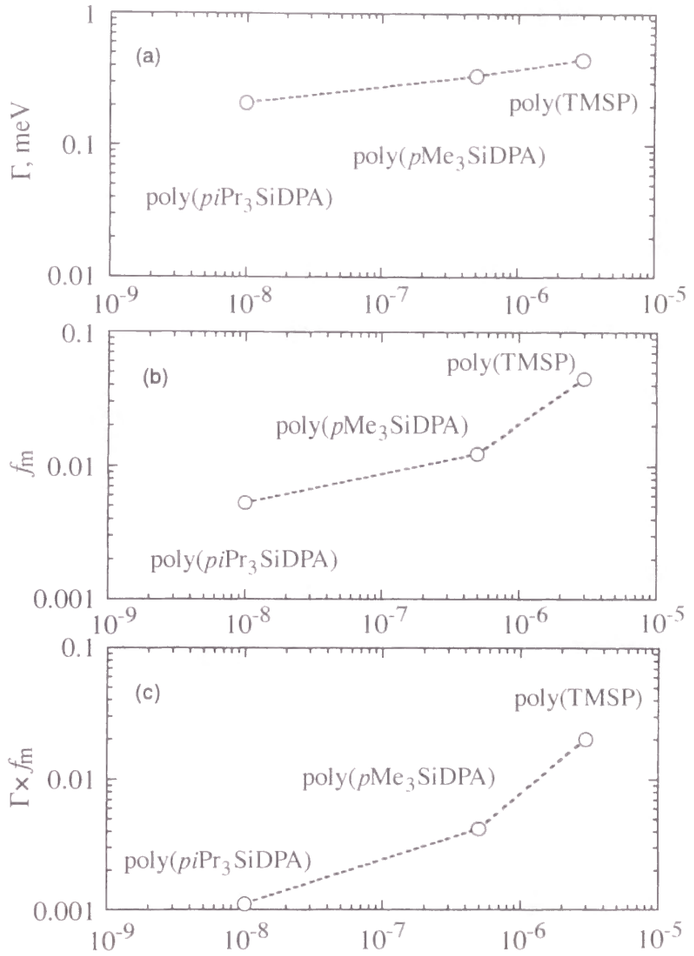

Figure 4. (a) Relaxation rate Γ, (b) mobile fraction f_m, and (c) apparent local flux Γ x f_m as a function of carbon dioxide permeability coefficient P_{CO2}.

In conclusion, the author has revealed in this chapter that there is a definite correlation between the gas permeability of poly(TMSP), poly(*p*Me$_3$SiDPA), and poly(*pi*Pr$_3$SiDPA) and their local flux Γ x f_m, and that this can explain the relatively low gas permeability of poly(*pi*Pr$_3$SiDPA).

Scheme 1

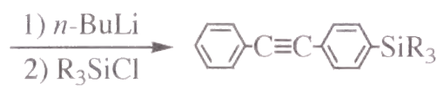

pMe_3SiDPA (R = Me_3Si, overall yield 77%)
piPr_3SiDPA (R = *i*Pr_3Si, overall yield 14%, mp 151.0–152.7°C)

Experimental

Materials. 1-Trimethylsilyl-1-propyne was purchased from Shin-etsu Chemical Industries Ltd., Japan and distilled twice from calcium hydride under nitrogen atmosphere. Diphenylacetylene derivatives were prepared by the method described in Chapter 1[9,10,21] according to Scheme 1. Both monomers were purified by flash column chromatography and recrystallization. Anal. Calcd for $C_{17}H_{18}Si$ (*p*Me_3SiDPA): C, 81.5; H, 7.3; Si, 11.2. Found: C, 81.7; H, 7.2; Si, 11.1. Anal. Calcd for $C_{23}H_{30}Si$ (*pi*Pr_3SiDPA): C, 82.6; H, 9.1; Si, 8.3. Found: C, 82.6; H, 9.1; Si, 8.3.

Both $TaCl_5$ and Ph_3Bi were commercially obtained and used without further purification. Commercial *n*-Bu_4Sn was distilled twice from calcium hydride under nitrogen atmosphere before use.

Polymerizations were carried out in toluene at 80 °C for 24 h under dry nitrogen. The detailed procedure was described in Chapter 1.

The molecular weights of polymers were determined by gel permeation chromatography (polystyrene calibration, eluent $CHCl_3$). The results of the polymerizations are summarized in Table 2.

Quasielastic Neutron Scattering Measurements. Quasielastic neutron scattering measurements were performed with a cold triple-axis spectrometer HER at the beam port C1-1 of the JRR-3M reactor in Tokai, Japan. They were done with a fixed scattered wavenumber of k_f = 1.25 $Å^{-1}$ and an energy resolution (FWHM) of

Table 2. Polymerization of TMSP, *p*Me_3SiDPA, and *pi*Pr_3SiDPA[a]

polymer	yield, %	M_w	M_n	M_w/M_n
poly(TMSP)[b]	90	$4.2x10^6$	$2.4x10^6$	1.7
poly(*p*Me_3SiDPA)[c]	80	$7.7x10^6$	$4.1x10^6$	1.9
poly(*pi*Pr_3SiDPA)[d]	82	$9.5x10^6$	$5.4x10^6$	1.7

[a] Polymerized in toluene at 80 °C for 24 h. [b] $[M]_0$ = 1.0 M, $[TaCl_5]$ = 10 mM, $[Ph_3Bi]$ = 10 mM. [c] $[M]_0$ = 0.50 M, $[TaCl_5]$ = 20 mM, $[n\text{-}Bu_4Sn]$ = 40 mM. [d] $[M]_0$ = 0.10 M, $[TaCl_5]$ = 20 mM, $[n\text{-}Bu_4Sn]$ = 40 mM.

about 0.2 meV using a horizontal focusing analyzer. Two types of scans were made at a room temperature (296 K); i.e., an energy scan in a region of –0.2 to 3 meV at constant Q (= 1.9 $Å^{-1}$) and an elastic Q-scan, Q being the magnitude of scattering vector. Motions observed under these experimental conditions are in a time range of 1.4 x 10^{-12} to 2 x 10^{-11} s and in a spatial scale at around 3.3 Å.

After correcting for background, the observed spectra were converted to differential scattering cross-sections $\partial^2\sigma/\partial\Omega\partial E$. In the samples used here, the observed differential scattering cross-section is dominated by incoherent scattering from hydrogen atoms because of its large incoherent atomic scattering cross-section.[24] Thus, the incoherent scattering laws $S(Q,\omega)$ were directly calculated from the data.

References

1) Kesting, R. E.; Fritzsche, A. K. *Polymeric Gas Separation Membranes*; Wiley: New York, 1993.
2) Stern, S. A. *J. Membr. Sci.* **1994**, *94*, 1.
3) Masuda, T.; Isobe, E.; Higashimura, T.; Takada, K. *J. Am. Chem. Soc.* **1983**, *105*, 7473.
4) Takada, K.; Matsuya, J.; Masuda, T.; Higashimura, T. *J. Appl. Polym. Sci.* **1985**, *30*, 1605.
5) Ichiraku, Y.; Stern, S. A.; Nakagawa, T. *J. Membr. Sci.* **1987**, *34*, 5.

6) Masuda, T.; Iguchi, Y.; Tang, B.-Z.; Higashimura, T. *Polymer* **1988**, *29*, 2041.

7) Witchey-Lakshmanan, L. C.; Hopfenberg, H. B.; Chern, R. T. *J. Membr. Sci.* **1990**, *48*, 321.

8) Tsuchihara, K.; Masuda, T.; Higashimura, T. *J. Am. Chem. Soc.* **1991**, *113*, 8548.

9) Tsuchihara, K.; Masuda, T.; Higashimura, T. *Macromolecules* **1992**, *25*, 5816.

10) Chapter 1 of this thesis; *J. Polym. Sci., Part A: Polym. Chem.* **1998**, *36*, 2721.

11) Higgins, J. S. *Developments in Polymer Characterization-4*; Dawkins, J. V., Ed., Applied Science Publishers: London, 1983; Chapter 4.

12) Bee, M. *Quasielastic Neutron Scattering*; Adam Hilger: Bristol, 1988.

13) a) Richter, D.; Ewen, B.; Farago, B.; Wagner, T. *Phys. Rev. Lett.* **1989**, *18*, 2140.
b) Richter, D.; Willner, L.; Zirkel, A.; Farago, B.; Fetters, L. J.; Huang, J. S. *Macromolecules* **1994**, *27*, 7437.

14) Higgins, J. S. *Brit. Polym. J.* **1987**, *19*, 103.

15) Kanaya, T.; Kaji, K.; Ikeda, S.; Inoue, K. *Chem. Phys. Lett.* **1988**, *150*, 334.

16) Inoue, K.; Kanaya, T.; Ikeda, S.; Kaji, K.; Shibata, K.; Misawa, M.; Kiyanagi, Y. *J. Chem. Phys.* **1991**, *95*, 5332.

17) Kanaya, T.; Kawaguchi, T.; Kaji, K. *J. Chem. Phys.* **1993**, *98*, 8262.

18) a) Kanaya, T.; Kawaguchi, T.; Kaji, K. *J. Chem. Phys.* **1996**, *104*, 3841. b) Kanaya, T.; Kawaguchi, T.; Kaji, K. *J. Chem. Phys.* **1996**, *105*, 4342.

19) Frick, B.; Fetters, L. J. *Macromolecules* **1994**, *27*, 974.

20) Arrighi, V.; Higgins, J. S.; Burgess, A. N.; Howells. W. S. *Macromolecules* **1995**, *28*, 2745 and 4622.

21) Tsuchihara, K.; Masuda, T.; Higashimura, T. *J. Polym. Sci., Part A: Polym. Chem.* **1993**, *31*, 547.

22) Masuda, T.; Isobe, E.; Higashimura, T. *Macromolecules* **1985**, *18*, 841.

23) Masuda, T. *Macromolecular Syntheses* **1992**, *11*, 45.

24) Bacon, G. E. *Neutron Diffraction;* Clarendon Press: Oxford, 1975.

25) Springer, T. *Quasielastic Neutron Scattering for the Investigation of Diffusive Motions in Solids and Liquids*; Springer-Verlag: Berlin, 1972.

26) Barns, J. D. *J. Chem. Phys.* **1973**, *58*, 519.

Chapter 9

Relationship between the Gas Permeability and Free Volume of Substituted Polyacetylenes and Related Polymers: Investigation by the Spin Probe Technique

Abstract

The spin probe technique was systematically applied to study a family of high permeability and high free volume glassy polymers. Rotation correlation times τ_c or frequencies $\nu = 1/\tau_c$ of 2,2,6,6-tetramethylpyperidine-1-oxyl (TEMPO) were measured in amorphous teflons–random copolymers of tetrafluoroethylene and 2,2-bistrifluoromethyle-4,5-difluro-1,3-dioxole, polyacetylenes and polynorbornenes. Polymers distinguished by unusually high, for the glassy state, permeability and free volume exhibit large rotational mobility of TEMPO. The correlation times correspond to fast rotation of the spin probe previously observed only in rubbery polymers. Correlations between the frequency ν and gas permeability and diffusion coefficients were observed. However, in some polymers, the spin probe's rotation rate is also sensitive to side-chain local mobility, which does not affect translational diffusion coefficients of gas molecules in polymers.

Introduction

The search for novel polymeric materials with optimized combinations of gas permeability and permselectivity is an important problem in membrane science. A rational basis for this search is the determination of relationship between chemical structure, physical properties and transport parameters such as permeability and diffusion coefficients. While many physical properties can influence gas permeability, free volume or free volume size distribution seems to be the most important property related to gas transport and even sorption parameters of polymers. As a result, several methods have been proposed to probe free volume in polymers. A common feature of such methods as positron annihilation[1], inverse gas chromatography[2], electrochromic[3], photochromic[4], and spin probe[5] methods is that different probe particles are introduced into a material under investigation and, after following their behavior in the polymer, certain conclusions can be made regarding free volume or average free volume element size in the material. Some of these methods, e.g. positron annihilation, have proven to be effective as standard approaches for reliable characterization of free volume in polymers. In contrast, the spin probe technique has only been only sporadically used in relation to free volume in and transport properties of polymers.

One of earliest results of the use of spin probes to study mass transfer properties of polymers was reported by Wasserman *et al.*[6] who demonstrated the correlation between rotational and translational diffusion coefficients of the stable free radical (spin probe) TEMPO. This result suggested that correlations might exist between gas diffusion coefficients and the rotation frequency of spin probes; and, in fact, such correlations were observed.[7] It was also shown that the rotation frequency of spin probes and gas diffusion coefficients exhibit a similar dependence on glass transition temperatures.[8] This effect could be explained by the analogous effects of free volume on these parameters. Whether or not a spin probe can be accommodated by a free volume element depends sensitively on the size of the spin probe and is reflected in the frequency of the probe's rotation as sensed by ESR method.[9] Based

on studies with spin probes of various sizes, a rough estimate of the size of free volume elements can be made. Interestingly, such estimates are in a reasonable agreement with the results of other methods, e.g. inverse gas chromatography.[10]

A disadvantage of these earlier studies is that the spin probe technique has been applied only to a limited set of conventional polymers with relatively low free volume. It is quite desirable to apply this method to glassy polymers such as poly[1-(trimethylsilyl)-1-propyne] [poly(TMSP)] and other amorphous polyacetylenes which exhibit extremely high free volume. Additionally, this method has rarely been used to characterize a systematic series of structurally related polymers. Meanwhile, this approach is common in studies of gas permeability and diffusivity of polymers, because it allows the rationalization of structure–properties relationships in polymers. The study in this chapter is meant to fill this gap.

The aim of this chapter is to investigate the mobility of the spin probe TEMPO in a large group of polymers belonging to different classes, including poly(TMSP) and other polyacetylenes, high permeability, high free volume amorphous glassy fluoropolymers (AF2400 and AF1600), a substantial group of norbornene polymers. For most of these materials, gas permeability and diffusion coefficients are known, which allows a comparison between parameters characterizing translation and rotational diffusion of low molecular mass compounds in polymers as well as the role of free volume and local group mobility on spin probe parameters. In other words, a question can be asked and probably answered if free volume effects are the main factor that influences a spin probe rotation frequency in glassy polymers, i.e. in the absence of segmental mobility, or there are other factors that affect the spin probe mobility.

Results and Discussion

Two perfluorinated copolymers of 2,2-bisfluoromethyl-4,5-difluoro-1,3-dioxole and tetrafluoroethylene had the following structure, composition, and physical properties (glass transition temperature, molecular mass and fractional free

volume). Their transport parameters have been reported elsewhere.[11]

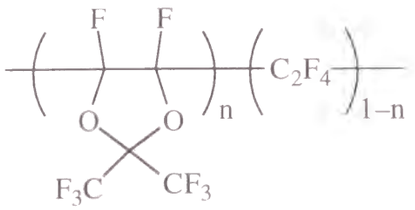

	n	T_g, °C	M_w	FFV, %
I	0.87	240	300,000	37.4
II	0.65	165	100,000	32.0

The repeat unit structures and catalysts used to prepare the polyacetylenes are shown in Table 1. All of the polymers have molecular mass in the range of $4x10^5$ to $2x10^6$ and were studied in powder form.

The structures, catalytic systems used, and glass transition temperatures of the norbornene polymers are given in Table 2.

During the last decades, interesting novel membrane materials, distinguished by unusually loose chain packing and, consequently, extremely high values of gas permeability and diffusion coefficients attracted much attention. These materials such as Teflon AF, poly(TMSP), and other substituted polyacetylenes exhibit extraordinary high free volume as determined by the Bondi method or by positron annihilation lifetimes spectroscopy (PALS). Accordingly, one of the aims of this chapter is to investigate the behavior of the TEMPO spin probe in such materials and to compare

Table 1. Polyacetylenes and Catalytic Systems Used

no.	R_1	R_2	catalytic system	ref.
III	H	$Si(CH_3)_3$	$VOCl_3$–*i*-Bu_3Al	12
IV	CH_3	$Si(CH_3)_3$	$TaCl_5$–*i*-Bu_3Al	13
V	Ph	*p*-$C_6H_4Si(CH_3)_3$	$TaCl_5$–*n*-Bu_4Sn	14
VI	Ph	*p*-$C_6H_4C(CH_3)_3$	$TaCl_5$–*n*-Bu_4Sn	15
VII	Cl	Ph	$Mo(CO)_6$-CCl_4-*hν*	16
VIII	Cl	*n*-C_6H_{13}	$MoCl_5$–*n*-Bu_4Sn	16

Table 2. Norbornene Polymers and Catalytic Systems Used

no.	repeat unit	catalytic system	T_g, °C	$v\times10^{-9}$, s^{-1}	P_{O2}, barrer[a]	ref.
IX		WCl_6[PhC≡CH]	31	0.1	2.8	17
X	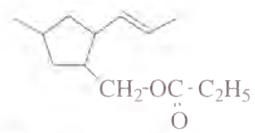	WCl_6[PhC≡CH]	–	0.1	–	18
XI	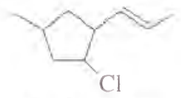	$WCl_6[Si(C_3H_5)_4]$	–	0.1	2.3	18
XII	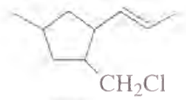	$RuCl_3$ $3H_2O$	–	0.3	0.46	18
XIII		Re_2O_7/Al_2O_3 Et_4Pb	–	0.5	1.0	18
XIV	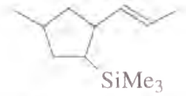	WCl_6[PhC≡CH]	113	0.5	30	17
XV	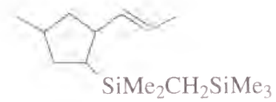	WCl_6[PhC≡CH]	24	0.8	16	17
XVI	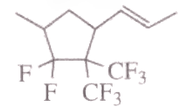	$WCl_6\left[Me_2Si\diamond SiMe_2\right]$	169	1.0	50	19
XVII		pentenyl nickel chloride ethylaluminum sesquichloride	>390	0.6	2.5	20
XVIII	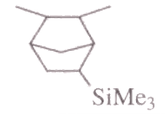	idem	>370	1.0	–	20

[a] 1 barrer = $1x10^{-10}$ cm^3(STP)•cm/(cm^2•s• cmHg).

the parameters of its rotational mobility with those of conventional, more densely packed glassy and rubbery polymers. Another objective is to record the variation of spin probe mobility in a series of structurally related polymers. Such systematic

studies of the effect of polymer structure on gas permeability (P) and diffusion (D) coefficients have provided many useful insights.[10] At last, it is interesting to test, using a wider set of polymers, the correlations of transport parameters, such as D and P, with the rotation frequency of TEMPO. Early studies were reported regarding systematic and interesting correlations between these variables.[7]

Table 3 presents the mobility of TEMPO (as characterized by the rotation frequency ν) at ambient temperature (25 °C) in high free volume polymers. The rotation frequencies for conventional polymers are also provided for comparison. From these results, both glassy AF2400, AF1600 and the majority of the amorphous polyacetylenes are characterized by ν values significantly higher than those of conventional polymers. The polymers with larger free volume permit higher TEMPO mobility. Thus AF2400 copolymer, which contains more perfluorodioxole than AF1600 has higher TEMPO mobility than AF1600. Poly(TMSP) (IV), the polymer with the highest free volume among all glassy polymers, as estimated e.g., by positron annihilation[10] or Bondi's[23] methods, also has rather high rotation frequency of 0.8×10^9 s^{-1}, much larger than the rotational frequency values for conventional glassy polymers. Most other polyacetylenes are characterized by somewhat lower frequencies of TEMPO rotation.

While the probe mobility is extraordinarily higher in the large free volume perfluorocopolymers and polyacetylenes, it is important to recall that the methodology of determining probe mobility in large free volume and conventional polymers is somewhat different. The ν values recorded in Table 3 for conventional glassy polymers were obtained using the "traditional" method of ESR spectroscopy, which corresponds to the region of so-called "slow" movement of a spin probe (4×10^{-9}–10^{-7} s^{-1}).[5,21] A comparison of rotational frequencies of spin probes measured by the "traditional" ESR method and the method of ESR spectroscopy with saturation transfer showed[24,25] that the correlation times (or rotation frequencies) determined by the "traditional" method characterize not the average value, but the upper limit of the spectrum of rotation frequencies of the spin probe in

Table 3. Mobility of TEMPO ν and Gas Permeability–Diffusivity of High Free Volume and Conventional Polymers at Ambient Temperatures

no.	polymer	$\nu \times 10^{-9}$, s^{-1}	P_{O2}, barrer	$D_{CO2} \times 10^7$, $cm^2 \cdot s^{-1}$
perfluorodioxole copolymers				
I	AF2400	1.2	1140	–
II	AF1600	0.8	170	7.0
polyacetylenes				
III	-CH=C($SiMe_3$)-	0.7	–	–
IV	-C(Me)=C($SiMe_3$)-	0.8	2600	250
V	-CPh=C(p-$C_6H_4SiMe_3$)-	0.7	1100	–
VI	-CPh=C(p-$C_6H_4CMe_3$)-	0.6	1100	–
VIII	-C(Cl)=C(n-C_6H_{13})-	1.5	32	14
VII	-C(Cl)=C(Ph)-	0.4	5.1	1.7
conventional polymers[a]				
glassy				
	PS	0.25	1 – 2	0.8
	PMMA	0.1	0.09	0.07
	PVC	0.08	0.045	0.025
	PVAc	0.01	0.45	–
rubbery				
	NR	2.3	23	12.5
	PIB	0.5	1.3	0.58
	PDMS	90	600	110

[a] PS – polystyrene; PMMA - poly(methyl methacrylate); PVC - poly(vinyl-chloride); PVAc - poly(vinyl acetate); NR-natural rubber; PIB-poly(isobutylene); PDMS - polydimethylsiloxane.

the polymer. This upper limit corresponds to the fastest rotational movements of the probe in the polymer. As a rule, the average value of the rotational frequency of TEMPO is smaller at least an order of magnitude than the value measured by the "traditional" ESR method. Thus, in polystyrene, this average value is about 0.01×10^9 s^{-1} at room temperature. On the other hand, frequency measured by the "traditional" method in the region of "fast" movements (i.e. in the range of 2×10^{10}–3×10^8 s^{-1}), which is characteristic of TEMPO probe rotation in rubbers and the high free volumes polymers studied in this chapter, as a rule, characterize namely the average value of the rotation frequency distribution of the spin probe.[24,25] Therefore, the difference between the average rotation frequencies in the two groups of polymers compared in Table 3 is even more dramatic than the values in the table may suggest.

Gas permeability and diffusion coefficients in Table 3 can be compared with spin probe mobility to identify correlations between spin probe mobility and small molecule transport properties in a polymer matrix. Based on this comparison there is an approximate correlation between rotation frequency and the D and P values. Indeed, the copolymer AF1600 is distinguished by lower ν values and permeability coefficients than AF2400. Polymer VII, which has the lowest mobility of the spin probe among the polyacetylenes, is the least permeable. However, the correlation of ν versus P and D is fairly poor and can hardly be used, for example, for a prediction of the gas transport parameters based on the ESR spectra of sorbed spin probe molecules. For example, in fluoropolymer AF1600 and poly(TMSP), TEMPO rotates with same frequency whereas P and D values differ significantly. TEMPO rotational frequency ν is higher in AF2400 than in poly(TMSP), though the relation between gas permeability of these polymer is opposite. It seems that there are other factors that influence ν and P values independenly in addition to the effects of free volume in glassy polymers.

An interesting case for comparison is polyacetylene VIII, which contains a long alkyl side group. This polymer has the highest rotation frequency 1.5×10^9 s^{-1} of

all the polyacetylenes. Meanwhile, its diffusivity is lower than that of poly(TMSP) (IV) by an order of magnitude and its permeability is lower than that of poly(TMSP) by two orders of magnitude. A common structural feature of polyacetylenes is a very rigid main-chain. Hence the introduction of a side-chain alkyl group which is very flexible relative to the main-chain can increase local mobility in the vicinity of the spin probe molecule. The same effect is observed if one compares gas permeability and diffusivity of poly(TMSP) and polydimethylsiloxane (PDMS), the most permeable rubber. Poly(TMSP) is, of course, much more permeable than PDMS. However, the mobility of TEMPO is much higher in PDMS than in poly(TMSP). This result is ascribed to the extremely high mobility of the main-chains in PDMS.

An analysis of the data in Table 2 for norbornene polymers leads to similar conclusions. This table presents a long series of norbornene polymers prepared via ring opening metathesis polymerization and two addition type norbornene polymers XVII and XVIII. Again only a rough correlation of spin probe mobility and gas permeability is observed. The most permeable polymer of this group, the fluorine containing polymer XVI, has the highest frequency, 1×10^9 s^{-1}. On the other hand, the mobility of the spin probe is small in polynorbornenes with low gas permeability (IX, XI). Analogous to the substituted polyacetylenes, an introduction of groups which provide more flexible side chains is accompanied by a noticeable growth of the TEMPO rotation frequency. For example, the introduction of a methylene spacer between the chlorine and cyclopentane ring in XII results in a marked decrease in permeability, in comparison with polymer XI, but an increase in ν.

It is also interesting to compare the silicon-containing polynorbornenes XIV and XV. It is well known that the $Si(CH_3)_3$ groups impart high gas permeability, large free volume, and elevated T_g in glassy polymers.[10] Indeed, poly(trimethylsilyl norbornene) (XIV) exhibits a rather high oxygen permeability coefficient and high spin probe mobility. However, the introduction of longer silicon-containing side-chains, like in polymer XV, results in a substantial decrease in the glass transition temperature that is caused by a self-plasticization effect. As Table 2 shows the T_g

value of polymer XV is even lower that that of non-substituted polynorbornene IX. A large local mobility that makes the chains of XV more flexible induces also relatively large rotational mobility of TEMPO spin probe. Meanwhile the permeability of polymer XV is lower than those in polynorbornenes containing bulky groups attached directly, that is without spacers, to the main-chain (XIV, XVI). These results can again be interpreted as an indication that spin probe rotational frequency is much more sensitive to local (small scale) mobility in glassy polymers than gas permeability.

Two addition type norbornene polymers form a group of another molecular design. Both polymers have relatively high TEMPO mobility. The silicon-containing norbornene polymer XVIII, in spite of its rather large molecular mass (ca. $2x10^5$), has poor film forming properties, so its gas permeability could not be determined. However, the high rotational mobility of TEMPO implies that it should exhibit rather high permeability coefficients.

The temperature dependence of the TEMPO rotation frequency was determined for several polymers in the range of 14 to 105 °C. The rotation frequency exhibited an Arrhenius temperature dependence in every case. Examples of these results for AF2400, AF1600, and poly(TMSP) are shown in Figures 1 and 2, respectively. The mobility of the spin probe in AF2400 is higher than in AF1600 at all temperatures. The mobility of poly(TMSP) (IV) is higher than in other polyacetylenes at all temperatures too.

The Arrhenius parameters for several high free volume polymers are shown in Table 4. They are compared with those characteristics for conventional glassy and rubbery polymers. The apparent activation energies for the spin probe mobility in most polyacetylenes as well as AF2400 and AF1600 do not differ substantially from the values observed for conventional glassy polymers. However, pre-exponential factors are larger by approximately an order of magnitude. Again a noticeable exception is polyacetylene VIII, which contains a flexible side-chain. Its activation energy is twice as large as that for the other high free volume glassy polymers, and its

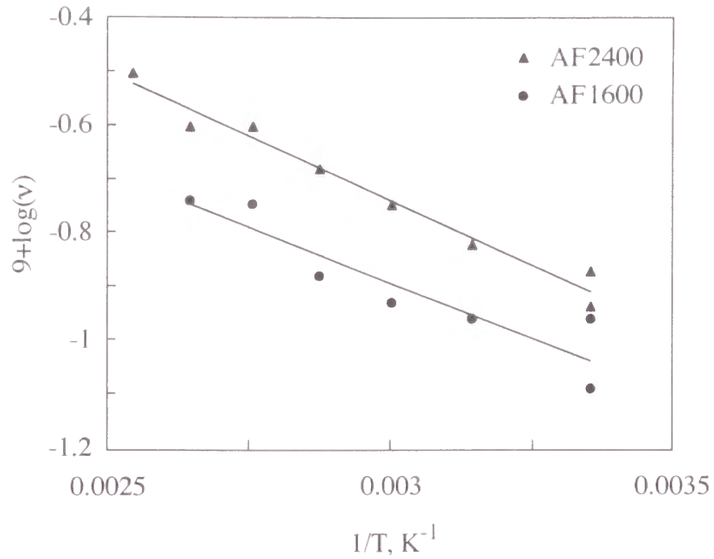

Figure 1. Temperature dependence of rotational frequency of TEMPO in: (1) AF2400; and (2) AF1600.

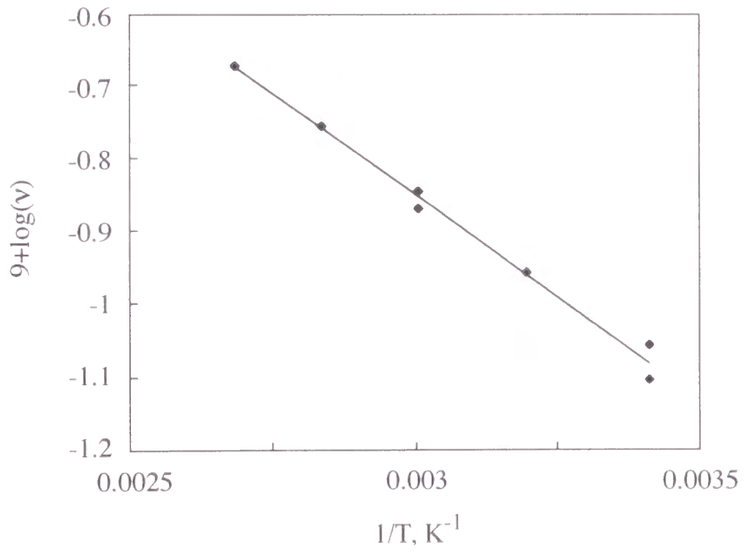

Figure 2. Temperature dependence of rotational frequency of TEMPO in poly(TMSP) (IV).

Table 4. Parameters of Arrhenius Dependence of TEMPO Mobility[a]

no.	polymer	$\nu_0 \times 10^{-10}$, s^{-1}	E, kcal/mol
I	AF2400	4.8	2.2±0.2
II	AF1600	2.15	1.9±0.3
IV	-C(Me)=C($SiMe_3$)-	6.3	2.5±0.1
V	-CPh=C(*p*-$C_6H_4SiMe_3$)-	6.6	2.5±0.3
VI	-CPh=C(*p*-$C_6H_4CMe_3$)-	4.5	2.8±0.3
VII	-C(Cl)=C(*n*-C_6H_{13})-	3.2	2.7±0.6
VIII	-C(Cl)=C(Ph)-	303	4.4±0.4
XVIII	PTMSNB(add)	7.1	2.6±0.2
	PS[b]	0.62	1.9
	PMMA[b]	0.05	1.0
	PVC[b]	0.24	2.1
	PVAc[b]	0.012	1.2
	NR	1.8×10^4	6.7
	PIB	4×10^6	10.8

[a] These parameters were obtained by fitting data of type shown in Figures 1 and 2 to the Arrhenius type equation: $\nu = \nu_0 \exp(-E/RT)$. The lines in Figures 1 and 2 represent the best fit of the data to this model. [b] The value obtained by the "traditional" method of ESR spectroscopy.

pre-exponential factor is larger by two orders of magnitude. Thus, the difference in TEMPO rotational frequencies between poly(TMSP) and polymer VIII increases with temperature, and at 100 °C it amounts to a factor of about 4. Bearing in mind the Arrhenius parameters of spin probe rotation, the rotational frequency of TEMPO in polyacetylene VIII is intermediate between the TEMPO rotational frequencies in glassy and rubbery polymers. This result will be considered in more detail below.

An important difference between rubber and glassy polymers is the much steeper temperature dependence of specific volume of the former as expressed by the inequality $\alpha_l > \alpha_g$., where α_l and α_g are the slopes of the temperature dependences of

the specific volume of a polymer $V_g(T)$ above and below the glass transition temperature, respectively. In other words, the variation of free volume with temperature is stronger above the glass transition temperature than below T_g. In the rubbery state, free volume is determined predominantly by segmental motion or larger scale chain mobility. This notion is consistent with the observation that larger apparent activation energies of rotation of spin probes are typical for rubbers than for glassy polymers.[5] Therefore, the higher activation energy and pre-exponential factor observed for polyacetylene VIII confirms the assumption that the high rotational frequency of TEMPO in this material is determined basically by the local mobility of its flexible side group.

The mobility of spin probes should be sensitive to the size of free volume but probably does not depend solely on this factor. If one approximates the Arrhenius temperature dependence of spin probe mobility by a linear function $\nu(T)$, then the slope $\beta = \Delta\nu/\nu_{av}\Delta T$, where $\Delta\nu$ is the difference between $\nu(T_{max})$ and $\nu(T_{min})$, can be compared with α_g in the polymers studied. Here T_{max} and T_{min} are the maximum and minimum temperatures in the temperature range studied. It is seen from Table 5 that the rotational frequency of TEMPO in different glassy polymers is much more strongly dependent on temperature than specific volume and, hence, free volume. Therefore, the rotational mobility of spin probes is not determined exclusively by the

Table 5. Parameters of Temperature Dependence of TEMPO Mobility and Thermal Expansion Coefficients α_g

polymer	$(\Delta\nu/\nu_{av}\Delta T) \times 10^4$, K^{-1}	$\alpha_g \times 10^4$, K^{-1}
AF2400	96	1.37
AF1600	96	1.22
PS	83	2
PMMA	44	2
PVC	91	3.5

size of a cavity in which they are located but also by activation of rotational diffusion. This phenomenon is equally true for rotation of spin probes in rubbers because there the difference in activation energies is much bigger than the difference between α_l and α_g.

Experimental

Polymers. Amorphous glassy perfluorinated copolymers purchased from E. I. DuPont Co. were used as-received in the form of powder.

All of the polyacetylenes shown in Table 1, with the possible exception of partially cross-linked poly[(trimethylsilyl)acetylene] (III), are soluble in common organic solvents and form good films. As a rule, the glass transition temperatures of these polymers are very high (often above the onset of decomposition) and usually are not detectable in DSC scans.

Polymer structures of poy(norbornenes) used in this chapter were shown in Table 2. Depending upon the type of catalyst used, norbornene derivatives can experience ring opening metathesis polymerization (ROMP) which gives a cyclolinear structure of the resulting polymers or they can undergo addition polymerization with opening of double bonds that leads to the polymers having an entirely different structure. As shown in Table 2, both types of norbornene polymers were investigated.

A stable nitroxyl radical, 2,2,6,6-tetramethylpyperidine-1-oxyl (TEMPO), was used as the spin probe. It was introduced into the polymers from the vapor phase at ambient temperature. Samples of the solid spin probe and polymers were kept together in a closed vessel long enough for uniform sorption of TEMPO into the polymer. Exposure times were selected to obtain a strong ESR spectrum of the sorbed free radical. In some cases the samples were heated to 50–80 °C in order to achieve a more uniform distribution of TEMPO in the sample. The criterion for uniform distribution of the probe molecules in the sample was the absence of spectral distortion caused by dipole-dipole and exchange interactions of the sorbed free

radicals. Some of the polyacetylenes show their own ESR signal, i.e. in absence of added TEMPO. Polyacetylene III (see Table 1) had the most intensive probe-free ESR signal with the following parameters: g-factor = 2.0023 and line width, ΔH = 3.95 G. The signals of the other polyacetylenes were much less intense. In every case, the intensity of the ESR signals ascribed to TEMPO was much larger than that of the ESR signals of the polymers themselves. Hence, the polymer signal offered no practical interference with TEMPO ESR signal and did not prevent meaningful analysis of the ESR spectrum of the spin probe. ESR spectra were recorded at temperatures ranging from 14 to 105 °C using an X-band ESR-spectrometer (Radiopan, Poland) under conditions which were far from saturation. Spin probe rotation correlation times τ_c (or frequencies of rotation of the spin probe $\nu = 1/\tau_c$) were calculated using traditional methods.[5,21] Figure 3 presents some examples of the ESR signals of the spin probe in polymers.

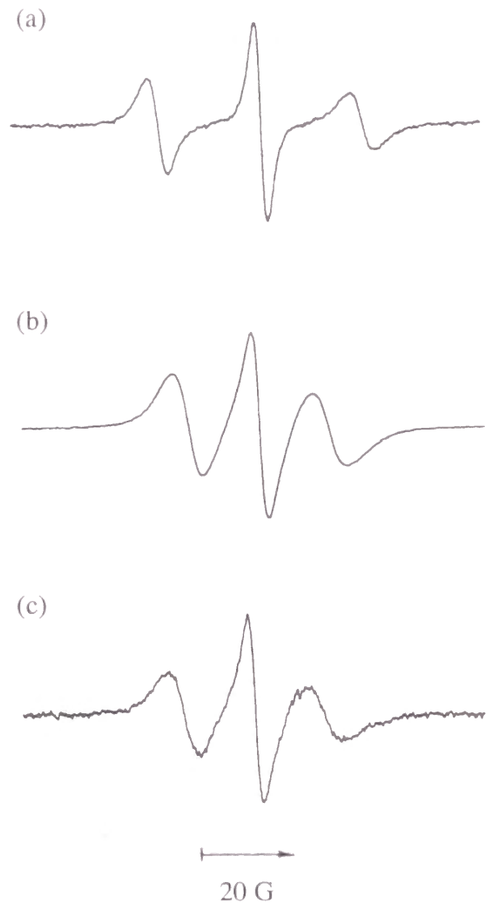

Figure 3. ESR spectra of the spin probe TEMPO in: (a) polyacetylene VII; (b) teflons AF2400 or I; and (c) AF1600 or II.

Gas permeability and diffusion coefficients were determined by a mass spectrometric technique described in detail elsewhere.[22]

References

1) Schrader, D. M.; Jean, Y. C. *Positron and Positron Chemistry*; Elsevier:

Amsterdam, 1988.

2) Yampolskii, Y. P.; Kaliuzhnyi, N. E.; Durgaryan, S. G. *Macromolecules* **1986**, *19*, 846.

3) Yampolskii, Y. P.; Shantarovcih, V. P.; Chernyakovskii, F. P.; Kornilov, A. I.; Plate, N. A. *J. Appl. Polym. Sci.* **1993**, *47*, 85.

4) Victor, J. G.; Torkelson, J. M. *Macromolecules* **1987**, *20*, 2241.

5) Wasserman, A. M.; Kovarskii, A. L. *Spin Probes and Labels in Physical Chemistry of Polymers*; Nauka: Moscow, 1986 (in Russian).

6) Wasserman, A. M.; Barashkova, I. I.; Yasina, L. L.; Pudov, V. S. *Vysokomol. Soed.* **1977**, *19*, 2083.

7) Yampolskii, Y. P.; Durgaryan, S. G.; Nametkin, N. S. *Dokl. Akad. Nauk USSR* **1981**, *261*, 708.

8) Yampolskii, Y. P.; Durgaryan, S. G.; Nametkin, N. S. *Vysokomol. Soed. A* **1982**, *24*, 536.

9) Yampolskii, Y. P.; Wasserman, A. M.; Kovarskii, A. L.; Durgaryan, S. G.; Nametkin, N. S. *Dokl. Akad. Nauk USSR* **1979**, *249*, 150.

10) Plate, N. A.; Yampolskii, Y. P. In *Polymeric Gas Separation Membranes*; Paul, D. R., Yampolskii, Y. P., Eds.; CRC Press: Boca Raton, 1994.

11) Alentiev, A. Y.; Yampolskii, Y. P.; Shantarovich, V. P.; Nemser, S. M.; Plate, N. A. *J. Membr. Sci.* **1997**, *126*, 123.

12) Mullagaliev, I. R.; Mudarisova, R. H.; Monakov, Y. B.; Onishenko, L. V.; Olhovskaya, L. I.; Rafikov, S. R. *Dokl. Akad. Nauk USSR* **1989**, *305*, 140.

13) Plate, N. A.; Antipov, E. M.; Teplyakov, V. V.; Khotimskii, V. S.; Yampolskii, Y. P. *Vysokomol. Soed. A* **1990**, *32*, 1123.

14) Tsuchihara, K.; Masuda, T.; Higashimura, T. *Macromolecules* **1992**, *25*, 5816.

15) Kouzai, H.; Masuda, T.; Higashimura, T. *J. Polym. Sci., Part A: Polym. Chem.* **1994**, *32*, 2523.

16) Masuda, T.; Iguchi, Y.; Tang, B.-Z.; Higashimura, T. *Polymer* **1988**, *29*, 2041.

17) Bondar, V. I.; Kukharskii, Y. M.; Yampolskii, Y. P.; Finkelshtein, E. S.;

Makovetskii, K. L. *J. Polym. Sci., Part B: Polym. Phys.* **1993**, *31*, 1273.

18) Finkelshtein, E. S.; Bespalova, N. B.; Portnykh, E. B.; Makovetskii, K. L.; Ostrovskaya, I. Y.; Shishatskii, S. M.; Yampolskii, Y. P.; Plate, N. A.; Kaliuzhnyi, N. E. *Polym. Sci.* **1993**, *35*, 589.

19) Yampolskii, Y. P.; Bespalova, N. B.; Finkelshtein, E. S.; Bondar, V. I.; Popov, A. V. *Macromolecules* **1994**, *27*, 2872.

20) Makovetskii, K. L.; Gorbacheva, L. I.; Golenko, T. G.; Ostrovskaya, I. Y. *Vysokomol. Soed. A* **1996**, *38*, 435.

21) Berliner, L. J. *Spin Labeling. Theory and Application*; Academic Press: New York, 1976.

22) Yampolskii, Y. P.; Novitskii, E. G.; Durgaryan, S. G. *Zavodsk. Lab.* **1980**, *46*, 256.

23) Morisato, A.; Shen, H. C.; Sankar, S. S.; Freeman, B. D.; Pinnau, I.; Casilas, C. G. *J. Polym. Sci., Part B: Polym. Phys.* **1996**, *34*, 2209.

24) Livshitz, V. A.; Kuznetsov, V. A.; Barashkova, I. I.; Wasserman, A. M. *Vysokomol. Soed. A* **1982**, *24*, 1085.

25) Wasserman, A. M.; Khazanovich, T. N. In *Polymer Yearbook*; Pethrick, R. A., Ed.; **1995**, *12*, 153.

Chapter 10

Optical Properties and Electroluminescence Characteristics of Poly(diphenylacetylenes) and Related Polymers

Abstract

Intense photoluminescence (PL) is observed in disubstituted acetylene polymers even though solitonic mid-gap absorption is observed upon doping, contrary to unsubstituted trans-polyacetylene and monosubstituted acetylene polymers in which strong PL is not observed. Intense green and blue electroluminescence (EL) is realized utilizing poly(diphenylacetylene) derivatives and poly(1-phenyl-1-alkyne) derivatives, respectively. Greenish-blue emission is also observed in poly(1-chloro-2-phenylacetylene) derivatives. The dependence of wavelength and intensity of PL and EL on the molecular structure of substituents is clarified in detail. The effects of molecular alignment and layer structure on the EL characteristics are also discussed. Upon intense light excitation, remarkable spectral narrowing due to stimulated emission is also observed in these disubstituted acetylene polymers.

Introduction

Among various conducting polymers, aromatic conducting polymers such as polythiophene, poly(*p*-phenylenevinylene), poly(*p*-phenylene) and their derivatives have been used as the emission layer in polymer electroluminescence (EL) devices.[1-9] However, polyacetylene and its derivatives have not been studied in detail regarding their use in EL devices.

This may be partly due to the early stage of experimental results showing that in trans-polyacetylene photoluminescence (PL) is not observed in the visible range but in cis-polyacetylene weak PL is observed.[10] That is, in conducting polymers having a degenerate ground-state structure, such as trans-polyacetylene, the photoexcited state was considered to relax to soliton states, resulting in the total suppression of PL. However, it was found that even in trans-polyacetylene, weak PL could be observed in the infrared region.[11] Therefore, the unique PL characteristics of polyacetylene can be interpreted not by a simple soliton model but also by the relative energy of the excited 1^1B_u and 2^1A_g States.[12] When the metastable 2^1A_g state is lower in energy than the 1^1B_u state, only weak PL can be observed. On the contrary, in polyacetylene derivatives in which the 1^1B_u state is lower in energy than the 2^1A_g state, strong PL is expected.

Recently, Yoshino *et al.* have reported the electrochemical and optical properties of poly[(*o*-trimethylsilylphenyl)acetylene] [poly(*o*Me_3SiPA)].[13] However, strong PL was not observed. More recently, they also reported that strong PL was observed in poly(diphenylacetylene) [poly(DPA)] derivatives and EL devices emitting green and blue light can be realized by utilizing disubstituted acetylene polymers.[6-9]

On the other hand, lasing of highly fluorescent conducting polymer has also attracted much attention, and several experimental results on spectral narrowing by stimulated emission in poly(*p*-phenylenevinylene) derivatives have been reported.[14] In this chapter, the author discusses the detailed dependence of PL and EL of polyacetylene derivatives as shown in Figure 1 on substituents and also device configurations. The spectral narrowing in polyacetylene derivatives upon intense

optical excitation is also discussed.

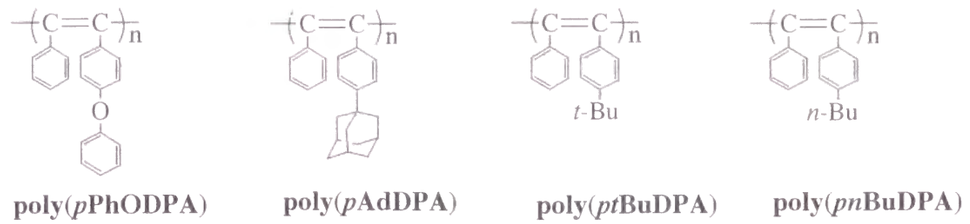

Figure 1. Molecular structures of polyacetylene derivatives used in this chapter.

Results and Discussion

As shown in Figure 2, the absorption edge of polyacetylene derivatives and the band gap evaluated from it depend on the substituents. Among various monosubstituted acetylene polymers, the band gaps of poly(*o*Me_3SiPA) (1.9 eV), poly(*o*CF_3PA) (2.2 eV) and poly(*o*Me_2PhSiPA) (2.0 eV) are much smaller than those of poly(IP) (3.0 eV) and poly(DPAP) (3.0 eV). However, it should be mentioned that in these monosubstituted acetylene polymers, strong PL was not observed, as already reported.[13] Though PL and EL of red color can be observed in these monosubstituted small-band-gap acetylene polymers such as poly(*o*Me_3SiPA), poly(*o*CF_3PA) and poly(*o*Me_2PhSiPA), they are extremely weak.

Among disubstituted acetylene polymers, poly(1-phenyl-1-alkyne) derivatives such as poly(PP), poly(PB), poly(PO) and also poly(α-NP) exhibit a large band gap (3.3–3.45 eV) compared with those of poly(diphenylacetylene) [poly(DPA)] derivatives such as poly(*pn*BuDPA) (2.55–2.75 eV) .

These disubstituted acetylene polymers are all highly PL emissive, in contrast to monosubstituted acetylene polymers. For example, the PL quantum efficiency of poly(*pn*BuDPA) was estimated to reach 60%. Figure 3 shows normalized PL spectra of typical disubstituted acetylene polymers. As is evident in this figure, poly(1-phenyl-1-alkyne) derivatives and poly(diphenylacetylene) derivatives exhibit blue and green emission, respectively. It should also be mentioned that even in the same group of derivatives, the PL peak energy also depends slightly on the molecular structure of the substituent.

PL intensity was also confirmed to be strongly dependent on the molecular structure of substituents even in the same group of polyacetylene derivatives. For example, as shown in Figure 4, among poly(*m*Me_3SiDPA), poly(*p*Me_3SiDPA) and poly(*pi*Pr_3SiDPA), poly(*pi*Pr_3SiDPA) exhibited the strongest PL and poly(*m*Me_3SiDPA) weakest PL.

These disubstituted acetylene polymers also exhibited strong EL. For example, the EL intensity of poly(*pn*BuDPA) was comparable to that of poly(2,5-dialk

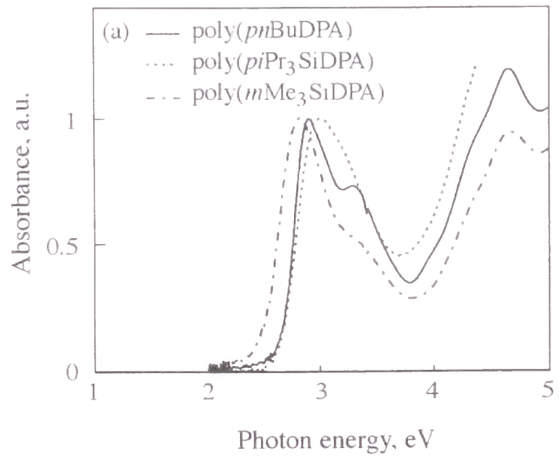

Figure 2. Optical absorption spectra of (a) poly(diphenylacetylene) derivatives, (b) poly(1-phenyl-1-alkynes) and (c) monosubstituted acetylene polymers.

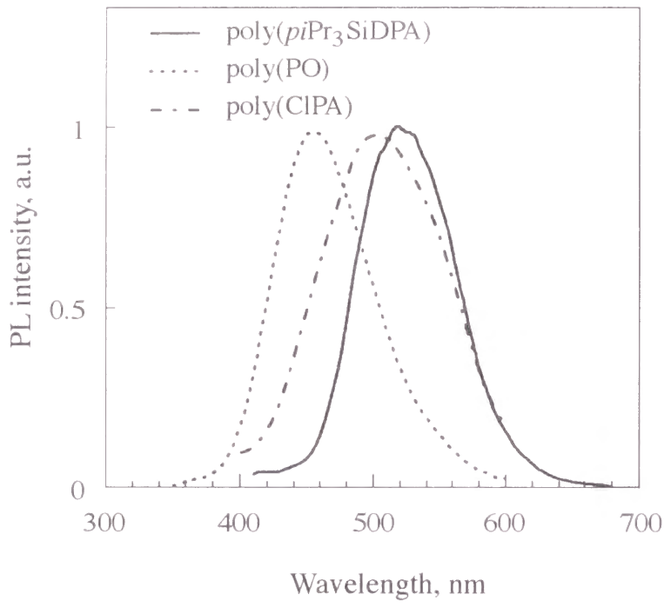

Figure 3. Photoluminescence spectra of poly(*pi*Pr_3SiDPA), poly(PO) and poly(ClPA).

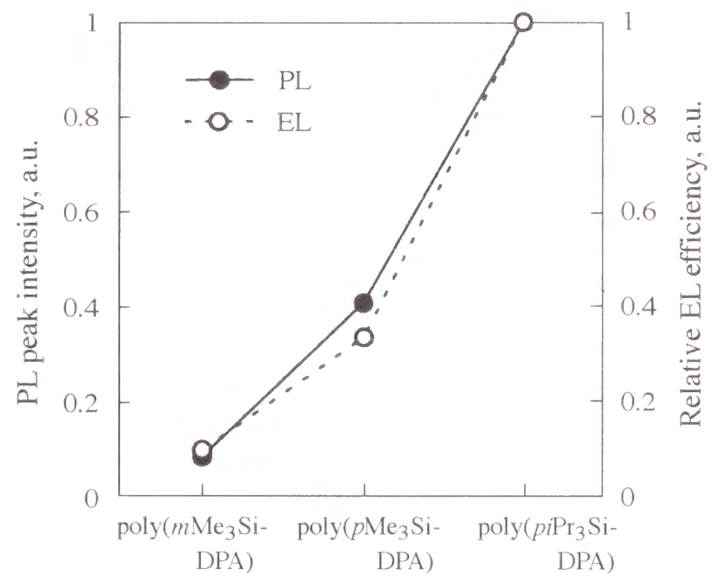

Figure 4. Dependencies of PL peak intensity and EL efficiency of poly(diphenylacetylene) derivatives on molecular structure of side group.

oxy-*p*-phenylenevinylene) derivatives at the same condition. As shown in Figure 5, poly(diphenylacetylene) derivatives also show green EL. The relative intensities among various polymers of this series were similar to those of PL, as shown in Figure 4 with a dashed line, for example.

It should also be noted from Figure 6 that poly(1-phenyl-1-alkynes) show intense blue EL. In this series of polyacetylene derivatives, polymers with longer alkyl chains exhibited stronger EL.

On the other hand, greenish-blue PL and EL were observed in poly(1-chloro-2-phenylacetylene) derivatives such as poly(ClPA) and poly(ClβNA), as shown in Figure 3.

It should be mentioned that in these disubstituted acetylene polymers, a drastic absorption spectrum change was commonly observed upon electrochemical doping due to the formation of mid-gap states (solitons), but still strong PL was observed.[9]

These experimental results suggest that the relative energy of the 2^1A_g and 1^1B_u excited states depends on the substituent. The magnitude of relaxation of the main chain configuration after photoexcitation may also depend on the substituent.

It has been already reported that in the three-layered structure of EL devices, color-variable EL depending on the polarity of the applied voltage can be realized utilizing the middle layer as an electron-blocking layer.[3-5]

On the other hand, multi-layered EL cells utilizing combinations of conducting polymers based on polyacetylene derivatives and cyano-substituted poly(*p*-phenylenevinylene) derivative have been fabricated. However, polarity-dependent EL was not realized at this stage of experimentation. In most cases so far studied, EL from a polymer with smaller band gap was obtained. That is, the emission from a conducting polymer with larger band gap may be suppressed by the transfer of either charge or energy to the polymer of smaller band gap.

In polymer films of mixtures of poly(1-phenyl-1-alkyne) derivative, poly(PO), and poly (diphenylacetylene) derivative, poly(*pn*BuDPA), the PL spectrum and intensity depend strongly on the concentration, as shown in Figure 7. As also shown

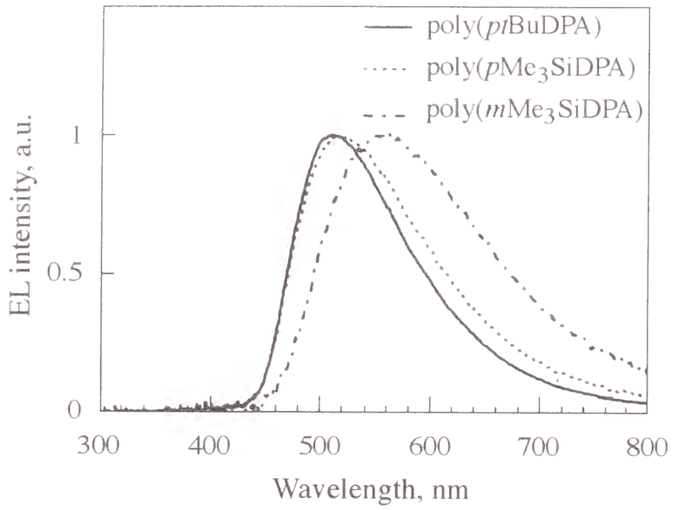

Figure 5. Electroluminescence spectra of poly(diphenylacetylene) derivatives.

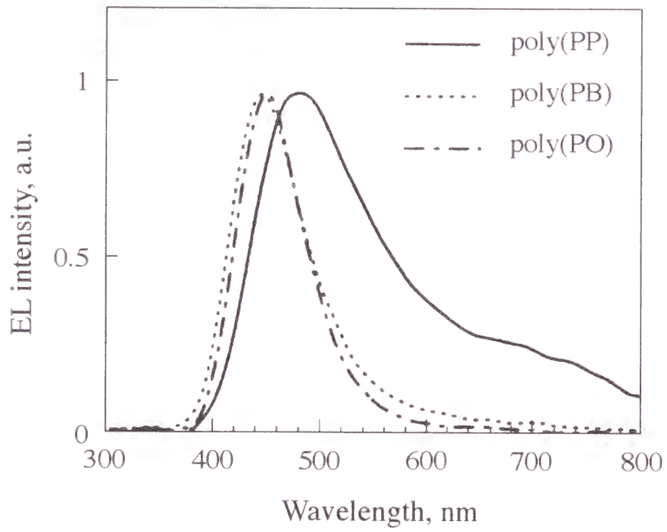

Figure 6. Electroluminescence spectra of poly(1-phenyl-1-alkynes).

in the inset of Figure 8, the spectrum of the mixture is composed of overlapped peaks originated from poly(*pn*BuDPA) and poly(PO). It should also be noted in Figure 8 that in the mixture the emission peaks originating from poly(*pn*BuDPA) and poly(PO) shift to higher energy compared with those of pure sample, which may be due to the change of main chain conformation in the mixture film.

The author has also been interested in the laser emission from conducting polymers upon intense excitation. It was already reported that remarkable spectral narrowing in poly(2,5-dialkoxy-*p*-phenylenevinylene) upon intense photoexcitation.[14] This spectral narrowing seems to be a common phenomenon in highly luminescent conducting polymers. Therefore, polyacetylene derivatives under intense light excitation have been also studied. Indeed, spectral narrowing upon intense photoexcitation was found as shown in Figure 9 in poly(*pn*BuDPA), for example.

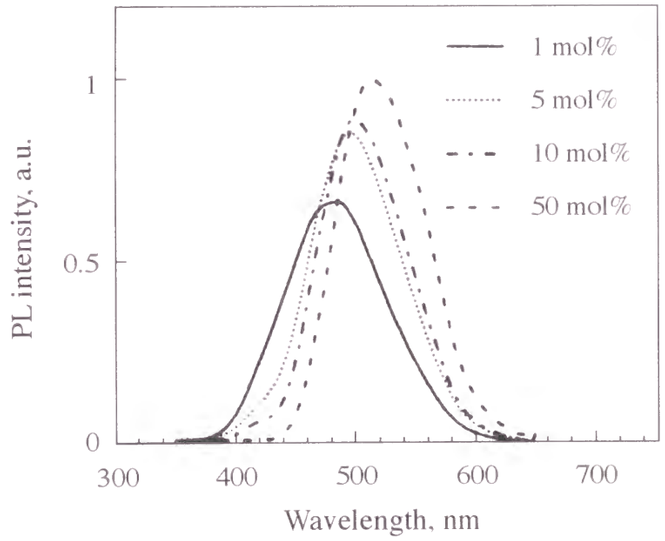

Figure 7. Photoluminescence spectra of poly(*pn*BuDPA)/poly(PO) composites at various poly(*pn*BuDPA) concentrations.

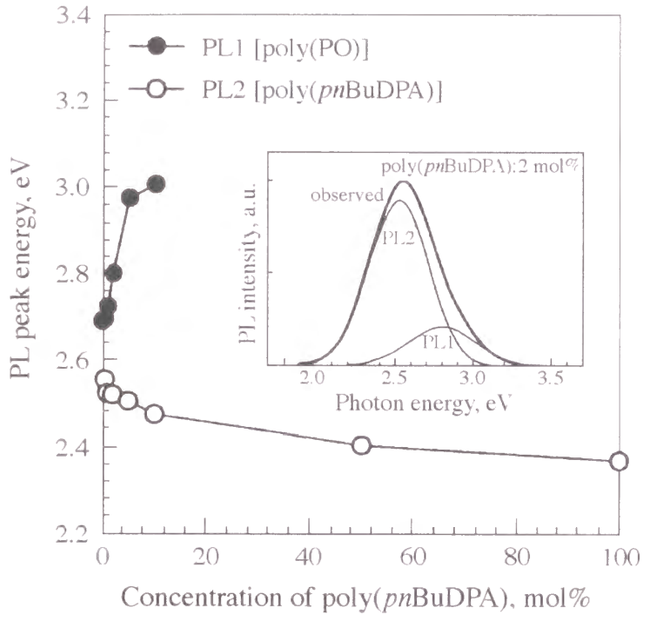

Figure 8. Dependence of peak energies of photoluminescence originating from poly(PO) and poly(*pn*BuDPA) in the photoluminescence spectra of poly(*pn*BuDPA)/poly(PO) composites on the poly(*pn*BuDPA) concentration. The photoluminescence spectrum of poly(*pn*BuDPA)/poly(PO) composites is composed of overlapping peaks originating from poly(*pn*BuDPA) and poly(PO), as shown in the inset.

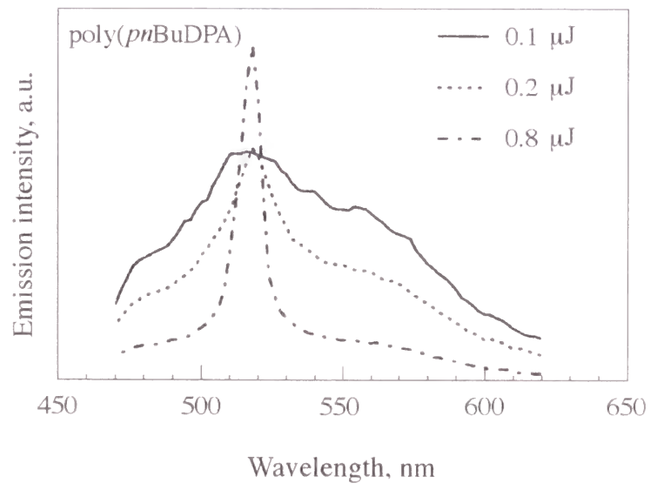

Figure 9. Spectral narrowing of photoluminescence in poly(*pn*BuDPA).

Experimental

Materials. Substituted polyacetylenes such as poly[1-phenyl-2-(*p*-phenoxyphenyl)acetylene] [poly(*p*PhODPA)], poly[l-phenyl-2-(*p*-adamantylphenyl)-acetylene] [poly(*p*AdDPA)], poly[1-phenyl-2-(*p*-*t*-butylphenyl)acetylene] [poly(*pt*BuDPA)], poly[1-phenyl-2-(*p*-*n*-butylphenyl)acetylene] [poly(*pn*BuDPA)], poly[1-phenyl-2-[*m*-(trimethylsilyl)phenyl]acetylene] [poly(*m*Me_3SiDPA)], poly[1-phenyl-2-[*p*-(trimethylsilyl)phenyl]acetylene] [poly(*p*Me_3SiDPA)], poly[1-phenyl-2-[*p*-(triisopropylsilyl)phenyl]acetylene] [poly(*pi*Pr_3SiDPA)], and poly[1-phenyl-2-[*p*-(triphenylsilyl)phenyl]acetylene] [poly(*p*Ph_3SiDPA)], poly(1-phenyl-1-propyne) [poly(PP)], poly(l-phenyl-1-butyne) [poly(PB)], poly(1-phenyl-1-octyne) [poly(PO)], poly [1-(α-naphtyl)-1-propyne] [poly(αNP)], poly[(*o*-trimethylsilylphenyl)acetylene) [poly(*o*Me_3SiPA)], poly[(*o*-trifluoromethylphenyl)acetylene] [poly(*o*CF_3PA)], poly[*o*-(dimethylphenylsilylphenyl)acetylene) [poly(*o*Me_2PhSiPA)], poly[3-(N-indolyl)-1-propyne] [poly(IP)], poly(3-diphenylamino-1-propyne) [poly(DPAP)], poly(1-chloro-2-phenylacetylene) [poly(ClPA)] and poly[1-chloro-2-(β-naphthyl)acetylene] [poly(ClβNA)], the molecular structures of which are shown in Figure 1, were studied.

The synthesis of these polyacetylene derivatives is described elsewhere.[15,16] These polyacetylene derivatives are soluble in common organic solvents such as $CHCl_3$.

Measurements. Absorption and PL spectra of films spin-coated from $CHCl_3$ solution on quartz plates were measured under vacuum using a spectrophotometer (HP8452 or Hitachi 330) and a fluorescence spectrophotometer (Hitachi F-2000), respectively.

Electrochemical measurements such as cyclic voltammetry were carried out utilizing a potentiostat (Hokuto-Denko HA-501) and a programmable function generator (Hokuto-Denko HB-l05) in a dry box filled with argon. A three-electrode electrochemical cell with Ag wire, a sample film on ITO-coated glass and a Pt plate were used as reference electrode, working electrode and counter electrode, respectively. The electrochemical cell was filled with purified acetonitrile containing

dried tetrabutylammonium tetrafluoroborate as a supporting salt. In situ absorption spectrum measurement during electrochemical doping was carried out by putting the electrochemical cell with the sample film on ITO in the sample chamber of a spectrophotometer (Hitachi 330).

For preparation of the EL device, a conducting polymer film was formed on an ITO-coated glass plate by the spin-coating method utilizing $CHCl_3$ solution (0.01 $moll^{-1}$). Then an Mg-In alloy was deposited by vacuum evaporation on the top of the film. Multi-layered devices were prepared by forming second and third conducting polymer films on the first layer by the spin-coating method, followed by the deposition of aluminium by evaporation on them. The active area of this device was approximately 6 mm^2. EL characteristics were studied either under vacuum (at room temperature) or in liquid nitrogen by a method reported previously.[2-9]

For the study of PL spectral narrowing, a laser beam of 355 nm with 100 ps pulse width at 100 Hz repetition rate produced by third-harmonic generation of a Nd-YAG laser was used. The emission spectra were measured utilizing a scanning 0.25 m spectrometer with 2 nm resolution.

References

1) Burroughs, J. H.; Bradley, D. D. C.; Brown, A. R.; Marks, R. N.; Mackey, K.; Friend, R. H.; Burns, P. L.; Holmes, A. B. *Nature* **1990**, *347*, 539.

2) Ohmori, Y.; Uchida, M.; Muro, K.; Yoshino, K. *Jpn. J. Appl. Phys.* **1991**, *30*, L1938.

3) Yoshida, M.; Fujii, A.; Ohmori, Y.; Yoshino, K. *Jpn. J. Appl. Phys.* **1996**, *35*, L397.

4) Hamaguchi, M.; Yoshino, K. *Appl. Phys. Lett.* **1996**, *69*, 143.

5) Yoshida, M.; Fujii, A.; Ohmori, Y.; Yoshino, K. *Appl. Phys. Lett.* **1996**, *69*, 734.

6) Tada, K.; Sawada, H.; Kyokane, J.; Yoshino, K. *Jpn. J. Appl. Phys.* **1995**, *34*, L1083.

7) Tada, K.; Hidayat, R.; Hirohata, M.; Teraguchi, M.; Masuda, T.; Yoshino, K. *Jpn. J. Appl. Phys.* **1996**, *35*, L1138.

8) Hirohata, M.; Tada, K.; Hidayat, R.; Masuda, T.; Yoshino, K. *Jpn. J. Appl. Phys.* **1997**, *36*, L302.

9) Hidayat, R.; Hirohata, M.; Tada, K.; Teraguchi, M.; Masuda, T.; Yoshino, K. *Jpn. J. Appl. Phys.* **1997**, *36*, in press.

10) Heeger, A. J.; Kivelson, S.; Schriefer, J. R.; Su, W. P. *Rev. Mod. Phys.* **1998**, *60*, 781.

11) Yoshino, K.; Hayashi, S.; Inuishi, Y.; Hattori, K.; Watanabe, Y. *Solid State Commun.* **1983**, *46*, 583.

12) Fitchen, D. B. *Synth. Met.* **1984**, *9*, 341.

13) Yoshino, K.; Takahashi, H.; Morita, S.; Kawai, T.; Sugimoto, R. *Jpn. J. Appl. Phys.* **1994**, *33*, L254.

14) Frolov, S.; Ozaki, M.; Gellermann, W.; Vardeny, Z. V.; Yoshino, K. *Jpn. J. Appl. Phys.* **1996**, *35*, L1371.

15) Masuda, T.; Hamano, T.; Tsuchihara, K.; Higashimura, T. *Macromolecules* **1990**, *23*, 1374.

16) Shirakawa, H.; Masuda, T.; Takeda, K. In *The Chemistry of Triple-Bonded Functional Groups (supplement C2)*; Patai, S., Ed.; Wiley: Chichester, 1994; Chapter 17.

List of Publications

Chapter 1

"Polymerization of Diphenylacetylenes Having Very Bulky Silyl Groups and Polymer Properties"

Teraguchi, M.; Masuda, T.

J. Polym. Sci., Part A: Polym. Chem. **1998**, *36*, 2721–2725.

Chapter 2

"Synthesis and Properties of Copolymers from 1-[3,5-Bis(trimethylsilyl)phenyl]-2-phenylacetylene"

Teraguchi, M.; Hachisuka, H; Masuda, T.

J. Macromol. Sci., Pure Appl. Chem. submitted.

Chapter 3

"Synthesis and Properties of Polymers from Disubstituted Acetylenes with Chiral Pinanyl Groups"

Aoki, T.; Kobayashi, Y.; Kaneko, T.; Oikawa, E.; Yamamura, Y.; Fujita, Y.; Teraguchi, M.; Nomura, R.; Masuda, T.

Macromolecules **1999**, *32*, 79–85.

Chapter 4

"Synthesis and Properties of Copolymers from a Diphenylacetylene Having Hexaphenylbenzene Moiety"

Teraguchi, M.; Fechtenkoetter, A; Müllen, K.; Masuda, T.

Polym. Bull. to be submitted.

Chapter 5

"Synthesis and Properties of Polyacetylenes with Adamantyl Groups"

Teraguchi, M.; Masuda. T.

J. Polym. Sci., Part A: Polym. Chem. **1999**, *37*, 4546–4553.

Chapter 6

"Synthesis and Properties of Polyacetylenes Having Azobenzene Pendant Groups"

Teraguchi, M.; Masuda, T.

Macromolecules in press.

Chapter 7

"Gas Permeability and Hydrocarbon Solubility of Poly[1-phenyl-2-[*p*-(triisopropylsilyl)phenyl]acetylene] (PTPSDPA)"

Nagai, K; Toy, L. G.; Freeman, B. D.; Teraguchi, M.; Masuda, T.; Pinnau, I.

J. Polym. Sci., Part B: Polym. Phys. submitted.

Chapter 8

"Local Mobility of Substituted Polyacetylenes Measured by Quasielastic Neutron Scattering and Its Relationship with Gas Permeability"

Kanaya, T.; Teraguchi, M.; Masuda, T.; Kaji, K.

Polymer **1999**, *40*, 7157–7161.

Chapter 9

"Study of High Permeability Polymers by Means of the Spin Probe Technique"

Yampolskii, Y. P.; Motyakin, M. V.; Wasserman, A. M.; Masuda, T.; Teraguchi, M.; Khotimskii, V. S.; Freeman, B. D.

Polymer **1999**, *40*, 1745–1752.

Chapter 10

"Optical Properties and Electroluminescence Characteristics of Polyacetylene Derivatives Dependent on Substituent and Layer Structure"

Yoshino, K.; Hirohata, M.; Hidayat, R.; Tada, K.; Sata, T.; Teraguchi, M.; Masuda, T.; Frolov, S. V.; Shkunov, M.; Vardeny, Z. V.; Hamaguchi, M.

Synth. Met. **1997**, *91*, 283–287.

Publications Not Included in this Thesis

1) "Synthesis and Gas Permeability of Poly(diphenylacetylenes) with Substituents"
Masuda, T.; Teraguchi, M.; Nomura, R.
In *Polymer Membranes for Gas and Vapor Separation : Chemistry and Materials Science*; Freeman, B. D., Pinnau, I., Eds.; ACS Symp. Ser. 733; Am. Chem. Soc.: Washigton, DC, 1999; Chapter 2.

2) "Pure-Gas Permeation and Sorption Properties of Poly[1-phenyl-2-[*p*-(trimethylsilyl)phenyl]acetylene] (PTMSDPA)"
Toy, L. G.; Nagai, K.; Freeman, B. D.; Pinnau, I.; He, Z.; Masuda, T.; Teraguchi, M.
Macromolecules submitted.

3) "Optical Properties and Blue and Green Electoluminescence in Soluble Disubstituted Acetylene Polymers"
Tada, K.; Hidayat, R.; Hirohata, M.; Teraguchi, M.; Masuda, T.; Yoshino, K.
Jpn. J. Appl. Phys. **1996**, *35*, L1138–L1141.

4) "Donor Polymer (PAT6) – Acceptor Polymer (CNPPV) Fractal Network Photo-cells"
Tada, K.; Hosoda, K.; Hirohata, M.; Hidayat, R.; Kawai, T.; Onoda, M.; Teraguchi, M.; Masuda, T.; Zakhidov, A. A.; Yoshino, K.
Synth. Met. **1997**, *85*, 1305–1306.

5) "Effect of Molecular Structure of Substituents on Green Electroluminescence in Disubstituted Acetylene Polymers"
Hidayat, R.; Hirohata, M.; Tada, K.; Teraguchi, M.; Masuda, T.; Yoshino, K.
Jpn. J. Appl. Phys. **1997**, *36*, 3740–3743.

6) "Spectral Narrowing of Emission in Di-substituted Polyacetylene"
Frolov, S. V.; Shkunov, M.; Vardeny, Z. V.; Tada, K.; Hidayat, R.; Hirohata, M.; Teraguchi, M.; Masuda, T.; Yoshino, K.
Jpn. J. Appl. Phys. **1997**, *36*, L1268–L1271.

7) "Photoluminescence and Electroluminescence in Polymer Mixture of Poly(alkylphenylacetylene) and Poly(diphenylacetylene) Derivatives"
Hidayat, R.; Hirohata, M.; Tada, K.; Teraguchi, M.; Masuda, T.; Yoshino, K.
Jpn. J. Appl. Phys. **1998**, *37*, L180–L183.

8) "Microlasers and Micro-LEDs from Disubstituted Polyacetylene"
Frolov, S. V.; Fujii, A.; Chinn, D.; Hirohata, M.; Hidayat, R.; Teraguchi, M.; Masuda, T.; Yoshino, K.; Vardeny, Z. V.
Adv. Mater. **1998**, *10*, 869–872.

9) "Electronic Properties and Electroluminescence of Monosubstituted Polyacetylenes and their Mixtures with Disubstituted Polyacetylene"
Hidayat, R.; Hirohata, M.; Fujii, A.; Teraguchi, M.; Masuda, T.; Yoshino, K.
Jpn. J. Appl. Phys. **1999**, *38*, 931–935.

10) "Excitation Dynamics in Disubstituted Polyacetylene"
Gontia, I.; Frolov, S. V.; Liess, M.; Ehrenfreund, E.; Vardeny, Z. V.; Tada, K.; Kajii, H.; Hidayat, R.; Fujii, A.; Yoshino, K.; Teraguchi, M.; Masuda, T.
Phys. Rev. Lett. **1999**, *82*, 4058–4061.

11) "PL and EL Characteristics of Mixture of Polyacetylene Derivatives and Dynamics of Excitons"
Hidayat, R.; Hirohata, M.; Tatsuhara, S.; Ozaki, M.; Teraguchi, M.; Masuda, T.;

Yoshino, K.
Synth. Met. **1999**, *101*, 210–211.

12) "Photoluminescence and Electroluminescence in Polyacetylene Derivatives"
Yoshino, K.; Hirohata, M.; Hidayat, R.; Kim, D. W.; Tada, K.; Ozaki, M.; Teraguchi, M.; Masuda, T.
Synth. Met. **1999**, *102*, 1159.

13) "Ytterbium(III) Trifluoromethanesulfonate Catalyzed High Pressure Reaction of Epoxides with Indole. An Enantioselective Synthesis of (+)-Diolmycin A2"
Kotsuki, H.; Teraguchi, M.; Shimomoto, N.; Ochi, M.
Tetrahedron Lett. **1996**, *37*, 3727–3730.

14) "High-Pressure Promoted and Silica Gel Catalyzed Aminolysis of Epoxides with Glycine Esters"
Kotsuki, H.; Shimanouchi, T.; Teraguchi, M.; Kataoka, M.; Tatsukawa, A.; Nishizawa, H.
Chemistry Lett. **1994**, 2159–2162.

Acknowledgments

This thesis presents the studies that the author carried out at the Department of Polymer Chemistry, Kyoto University, during the years from 1995 to 1999 under the supervision of Professor Toshio Masuda.

The author would like to express his sincere gratitude to Professor Toshio Masuda for his continuous guidance, valuable suggestions, and encouragement throughout the present investigation. The author is also grateful to Professor Yoshiki Chujo and Professor Shinzaburo Ito for their helpful suggestions.

The author would like to thank Professor Eizo Oikawa and Associate Professor Toshiki Aoki (Department of Chemistry and Chemical Engineering, Niigata University), Professor Klaus Müllen (Max-Planck Institute for Polymer Research), Professor Keisuke Kaji and Associate Professor Toshiji Kanaya (Institute for Chemical Research, Kyoto University), Professor Benny D. Freeman and Dr. Kazukiyo Nagai (Department of Chemical Engineering, North Carolina State University), Professor Yuri P. Yampolskii (A. V. Topchiev Institute of Petrochemical Synthesis, Russian Academy of Sciences), and Professor Katsumi Yoshino (Department of Electronic Engineering, Osaka University) for their collaboration and helpful suggestions in the present works.

The author wishes to express his gratitude to Dr. Yoshihiko Misumi and Dr. Ryoji Nomura for their helpful advice and discussion during this research. Sincere thanks are due to all colleagues in the Masuda laboratory for their discussion, and particularly, to Mr. Yasufumi Yamamura, Yoji Fujita, and Tomoaki Sata for their collaborations in this thesis.

The author acknowledges the support by JSPS Research Fellowships for Young Scientists.

Finally, the author expresses his deep appreciation to his family, especially his parents, Mr. Masaru Teraguchi and Mrs. Miyoko Teraguchi for their constant assistance and kind-hearted encouragement.

Masahiro Teraguchi
Kyoto University
January 2000